MECHANISMS UNDERLYING THE AGE-RELATED CHANGES IN MUSCLE CONTRACTILE PROPERTIES

JORGELINA RAMOS

A thesis submitted in partial fulfilment of the requirements for the degree of Doctor of Philosophy at the Manchester Metropolitan University and the degree of Doctor in Biomedical Sciences at the KU Leuven

School of Healthcare Science. Manchester Metropolitan University.

Manchester, United Kingdom

2016

Director of Studies:

Prof. Hans Deges (School of Healthcare Science, Manchester Metropolitan University)

Co-Supervisors:

Prof. Louise Deldicque (Department of Kinesiology, KU Leuven)

Prof. David Jones (School of Healthcare Science, Manchester Metropolitan University)

Dr. Stephen Lynch (School of Computing, Mathematics and Digital Technology, Manchester Metropolitan University)

Contents

List of Figures

List of tables

Abstract

Changes in isometric fore and power output in old age have been extensively studied for but less attention has been paid to eccentric contractions where, paradoxically, there are suggestions that eccentric strength is maintained with ageing. Decreased isometric force and relatively increased eccentric strength are feature of permeabilised single fibres developed in the presence of high inorganic phosphate (Pi) and it is possible that there may be a connection between the changes in contractile function seen with ageing and the actions of Pi. The work described in this thesis involved mouse soleus fibres and had two major aims. The first was to understand more about the nature of the response to stretch and the role of Pi, especially concerning the rate of stress relaxation which may provide information about cross bridge kinetics. The second aim was to study to what extent changes in cross bridge function account for the age related changes in contractile characteristics. In the first study, three features of the force response to stretch, peak force at the end of the ramp stretch, the stress relaxation and the residual force enhancement were observed in young mouse single fibres at different velocities of stretch. Stress relaxation was analysed as a double exponential decay with a constant component, force enhancement (FE). The speed of the fast exponential component increased with speed of stretch and the proportions of the fast component (A2) relative to the slow component (A1) also increased with speed of stretch. FE was independent of speed. Addition of Pi slowed stress relaxation and increased the proportion of the slow component. One explanation is that the slow component represents the detachment of attached cross bridge states that generate little or no force while the fast component is due to detachment of cross bridges in a high force state. FE is probably due to stretching of a series compliance such as titin.

The response to stretch varied with age in complex ways. In mice aged 3, 10 and 18-month-old there were small but non-significant increases in the force sustained during stretch relative to the isometric force together with a similar stress relaxation. However, with 32-month-old fibres the stress relaxation was faster than seen with young fibres consistent with an increase in the proportion of the fast A2 cross bridge intermediate state. Adding Pi to the oldest fibres changed the proportions of A1 and A2 to those seen in young fibres in the absence of Pi.

The results largely contradict previous reports of the relative preservation of eccentric force with age, which may be due to simple change in fibre type composition of whole muscles, but do indicate possible changes in cross bridge kinetics affecting the transition from low to high force states.

CHAPTER 1

General Introduction

1. General Introduction

1.1 Muscle structure

Volitional movement is one of the defining features that separates animals from plants and in vertebrates it is the skeletal muscles that are responsible for producing force and mechanical work enabling them to move, stabilize or adjust posture and ventilate their lungs. The cell unit of striated muscle is a *muscle fibre*, which is unusual being a multinucleate cell formed by the fusion of mononuclear myoblasts during embryonic development. Each muscle fibre contains myofibrils running more or less the entire length of the fibre, and are formed of a series of *sarcomeres*, elements connected in series that give striated muscles their characteristic pattern. Each sarcomere extends from one *Z line* to the next and these lines appear under the microscope as dark lines in the centre of the lighter *I band*, actin not overlapped by myosin (Gans, 1982; Zatsiorsky & Prilutsky, 2012). An example of a single fibre seen under the microscope (40x) is shown in Figure 1.1.

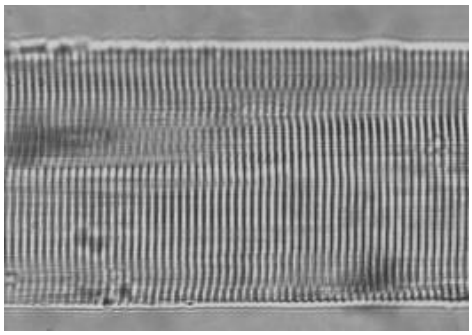

Figure 1.1 *Photomicrograph of a skinned single soleus fibre from a male mouse in relaxing solution.*

1.1.1 Contractile and structural proteins

As shown in Figure 1.2, a sarcomere is composed of thick (red) and thin (black) filaments oriented along the axis of the fibre and arrayed in parallel. The thin filaments from one sarcomere join those from the next sarcomere at the *Z lines,* while in the middle of the sarcomere and forming the A band, the thick filaments join to each other at the centre at the *M line* (Matthews, 2013).

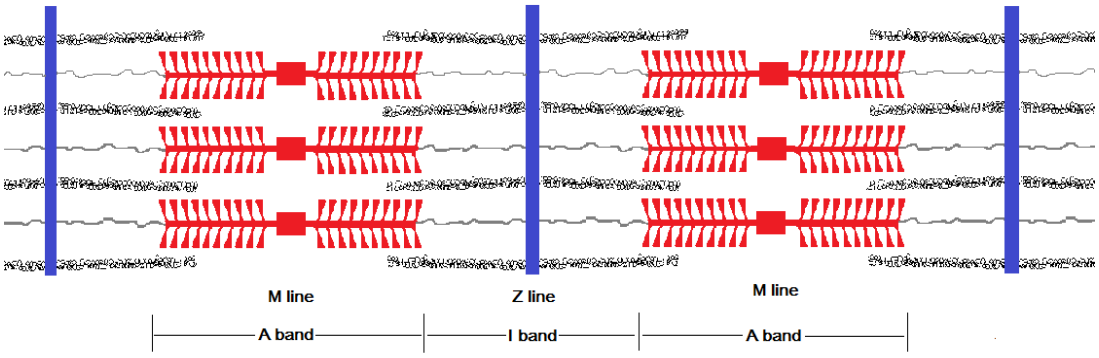

Figure 1.2 *Schematic representation of thin and thick filaments, lines and bands layout in a relaxed muscle, as explained in the text. Red: myosin; dotted grey: actin; curled grey line: titin.*

The thick filaments consist of approximately 300 molecules of the protein *myosin*. Two major parts can be defined within the myosin molecule; a globular 'head' and a fibrous 'tail'. The thin filament is composed of the protein *actin*, a globular protein that polymerizes to form long chains. On the thin filaments are *troponin* and *tropomyosin,* which are responsible for regulating the interaction between actin and myosin. In addition there are a number of other proteins which help maintain the structure of the sarcomere. The largest protein within the sarcomere (and possibly the largest protein known to exist) is *titin*. This is a highly elastic filament which connects the myosin filaments to the *Z lines* (See Figure 1.2). Apart from providing longitudinal stability to the sarcomere as a structural protein, titin gives rise to the resting tension when the muscle is passively stretched (Maruyama et al., 1977; Wang et al., 1979; Jones et al., 2004).

1.1.2 Mechanism of muscle contraction

The force a muscle can generate is proportional to the filament overlap. The interaction between actin and myosin filaments shortens the muscle and the mechanism of this muscle change of length is explained by the sliding filament theory (Huxley & Niedergerke, 1954; Huxley & Hanson, 1954). What is actually happening is that the myosin head binds to a specific binding site on the actin filament, forming a *cross bridge.* A rotation of the head and a swinging action of the neck region stretch the compliant portion of the neck (S2) and thereby pulls on the actin filament, producing force (Huxley, 1969). Figure 1.3 illustrates the changes in the sarcomeres while the muscle is shortened during a contraction.

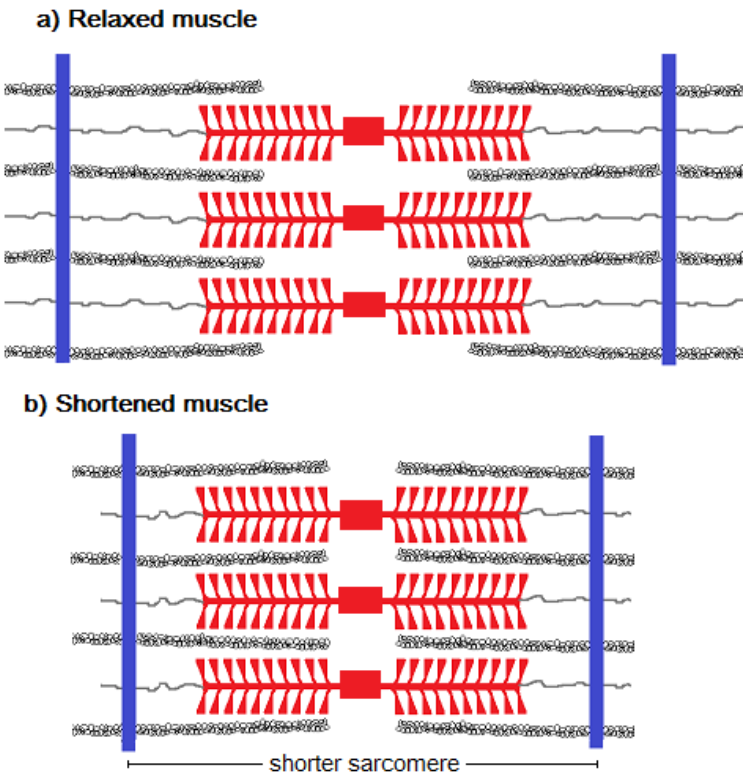

Figure 1.3 *Schematic representation of cross bridge action while the muscle is subjected to a shortening contraction. Notice the shorter sarcomere in b) without a change in the length of the actin and myosin filaments. The width of the A band is unaffected, and as a result of the increased actin-myosin overlap the I band is shortened.*

1.2 Muscle force

Three types of muscle contractions can be distinguished:

- where the length of the muscle does not change: *isometric contraction*
- where the muscle shortens: *concentric or shortening contraction*
- where the muscle lengthens: *eccentric or lengthening contraction (sometimes called plyometric contraction)*

Regardless of the type of contraction, the extent of activation depends on the binding of Ca^{2+} ions to troponin which by interacting with tropomyosin, exposes binding sites of the actin filaments and thus determines the maximum number of myosin cross bridges, and thus the force, which can be generated.

1.2.1 Isometric contraction

As this type of contraction is achieved by maintaining a constant muscle length, the myosin and actin biding sites remain relatively in the same position and it is believed

that around 80% of cross bridges are attached during a maximal isometric contraction (*Fo)*. Since the tension is known to be a function of the number of sarcomeres working in parallel, i.e. the cross-sectional area (CSA) of the fibre/muscle, the larger the cross-sectional area the higher the isometric force produced (Wickiewicz et al., 1983; Jones et al., 2004). Specific force, *Po,* is the maximal force normalized to the cross-sectional area of the muscle or muscle fibre. The *Po,* also called specific tension, is an index of the intrinsic muscle strength. For human soleus muscle, for example, the specific tension *in vivo* was found to be 15 $\pm$ 1.2 (N/cm^2) while *in vitro* it was around 14 $\pm$ 0.2 (N/cm^2) (Maganaris et al., 2001; Widrick et al., 1997). In rats, the figures for single fibres of the soleus are between 9.5 $\pm$ 0.5 and 15 $\pm$ 0.3 (N/cm^2) (Thompson & Brown, 1999; Widrick, 2002; Debold et al., 2006; Degens et al, 1998, 2010). For mice, the *Po* of whole soleus muscle has been reported to be between 12.7 $\pm$ 0.5 and 22.4 $\pm$ 1.4 (N/cm^2) (Brooks & Faulkner, 1988; Selsby, 2010; James et al., 1994; Moran et al., 2005; Leijendekker & Elzinga, 1990), which is similar to that seen in rats and humans. Only one study by González et al. in 2000 reported the specific force on mouse soleus single fibres to be ~40 (N/cm^2), which seems much higher than values seen in whole muscle. It thus appears that the specific tension does not differ much, if at all, between species.

1.2.2 Shortening contraction

The interaction between the thin and thick filaments generates force and depending on whether this force is more or less than the load, the muscle will either shorten or lengthen.

1.2.2.1 Force-velocity relationship during shortening

The relationship between force and speed of shortening is a common experience of daily life: it is common knowledge that we can lift lighter objects faster than heavy ones, so that with increasing loads the speed of shortening decreases. This relationship between force and velocity was described by Hill in 1938 and is given by

$$v(P+a)=b(Po-P),$$

where *P* is force during shortening (or the load), *Po* the isometric force, *v* is the shortening velocity and *a* and *b* are constants. The relation described is a hyperbola with asymptotes at *P=-a* and *v=-b,* where *P* is lower than *Po*. When *P=0, v=Vmax,* which is the maximum velocity of shortening. Besides, some other relations can be determined

$$aVmax=bPo,$$

or,

$$a/Po=b/Vmax,$$

where the ratios *a/Po* and *b/Vmax* have no dimensions. *a/Po* represents the *curvature* of the force-velocity relationship and as this ratio increases, the hyperbola flattens (Hill, 1938; Katz, 1939). To obtain force-velocity curves from a certain muscle (or muscle fibre), the experimental approach has been to specify one of the parameters of the experiment, force or velocity (or change of length over time), as the input and to use the not specified as the output. The parameter used as input, is varied systematically from trial to trial and both, the force and velocity are measured and plotted to obtain the force-velocity curve (Winters, 1990). To obtain the rest of parameters of the equation, the data points are fitted to the Hill equation by a non-linear least squares regression.

1.2.3 Lengthening contraction

An eccentric or lengthening contraction occurs when a muscle is active and forcibly stretched, i.e. the load on the muscle is greater than the isometric force. Compared to isometric and shortening contractions, the kinetics of cross bridge action during eccentric contractions has received little attention. Although the word contraction implies shortening and this is how muscle actions are usually thought of, the generation of force while being lengthened is a common and fundamental function of muscle. Such lengthening, or eccentric, contractions are present in many movements of daily life such us lowering a weight from a shelf, sitting down in a chair or while absorbing energy when stepping down or landing from a jump. In these situations the force an active muscle sustains can be considerably higher than the isometric force (Cavagna, 1993; De Ruiter et al., 2000; Roig et al., 2010).

1.2.3.1. Peak force

The increment in muscle force as a result of a step or ramp stretch has been reported to be more than 1.8 times greater than the isometric force (Sugi, 1972; Lombardi & Piazzesi, 1990; Linari et al., 2003; Brooks et al., 1994b; Getz et al., 1998). These values have been measured at the end of a ramp or step stretch at different velocities, where the force reaches a 'peak' or *Fpeak.* Once the stretch ends and length is held constant, the force decays to a new force level that is higher than the preceding isometric force. According to the literature, *Fpeak* is dependent on the velocity of length change (Flitney & Hirst, 1978; Bagni et al., 2005). If *Fpeak* normalized to *Fo* is plotted against the stretch speed, a force-velocity relationship can be determined for the lengthening

contractions and added to a Hill's force-velocity curve by setting the lengthening speed with negative values (Linari et al., 2003; Krylow & Sandercock, 1997). It is important to note, however, that the lengthening data cannot be fitted by the Hill equation.

1.2.3.2. Stress relaxation

Information about the state of cross bridge kinetics may be obtained by following the transition from one state to another; e.g. from stretch to maintaining length at the end of a stretch. As commented in the previous paragraph, at the end of a ramp or step stretch, the force decreases. This is sometimes called stress relaxation and it has been shown that it consists of both a fast and a slow phase decreasing exponentially (Colomo et al., 1989), where the rate of relaxation increases with increasing stretch speed (Cavagna, 1993). Precisely what determines the amplitude or contribution of these two phases to the stress relaxation remains to be determined and will be examined in the following chapters.

1.2.3.3. Force enhancement

Once the ramp stretch finishes, the force starts to decay to a steady value. This new force the decay tends to has been observed to be greater than the isometric force developed before the stretch, or than the isometric force that would be expected at the new longer length (Abbott & Aubert, 1952; De Ruiter et al., 2000; Rassier et al., 2003). This characteristic of the force response to a lengthening contraction is another poorly understood feature and will be addressed in the subsequent chapters.

1.3 Inorganic phosphate

Force generation in skeletal muscle has been shown to be closely related to the release of inorganic phosphate (Pi) during the cyclic interaction of the myosin cross bridge with actin (Osterman & Arner, 1995). Briefly, Figure 1.4 represents a scheme with a number of intermediate states in the hydrolysis of MgATP and the interaction between the contractile proteins, myosin and actin.

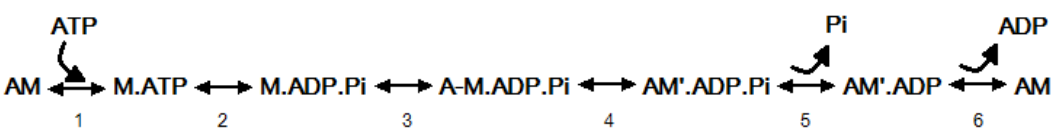

***Figure 1.4**. Cross bridge ATPase cycle.*

The reaction pathway starts with the binding of MgATP (substrate) to the myosin head, followed by a detachment of actin and myosin (Step 1). The hydrolysis of ATP takes place while it is bound to the myosin head (Step 2) and actin and myosin, with bound hydrolysis products, interact to form a weakly bound state (Step 3) that isomerizes to form a strongly bound AM'.ADP.Pi cross bridge (Step 4). This last cross bridge is already able to produce force before the release of Pi (Step 5), while the AM'.ADP state after the release also produces force. The ADP is finally released (Step 6) and the cycle starts again (Kawai & Halvorson, 1991; Tesi et al., 2002; Caremani et al., 2008).

1.3.1 Effects of Pi on contractile properties

Inorganic phosphate has been shown to depress the isometric force in skinned muscle fibres; 20 (mM) Pi reduced the isometric tension level to 30% of the control value (Kentish, 1986; Iwamoto, 1995). The addition of Pi has been found not only to reduce the isometric force but also to increase the kinetics of cross bridge interactions so that the rate constant of isometric force development increases with increasing [Pi] (Caremani et al., 2008). Although not fully understood, it is likely that the decrease in *Fo* with increased [Pi] is due to an increased proportion of cross bridges being trapped in a low-force intermediate state, just before the release of Pi from the actomyosin complex (Step 4 in Figure 1.4), and this could have implications for the force generated, or sustained, during movement, either shortening or lengthening. Pi concentrations between 12 (mM) and 20 (mM) did not affect maximum shortening velocity, *Vmax* (Cooke et al., 1985; Osterman et al., 1995), implying that the low-force cross bridges have no trouble dissociating during rapid shortening. However, addition of 15 (mM) Pi has been found to increase the eccentric force at different velocities of lengthening (Stienen et al., 1992). If there is an increase in the proportion of cross bridges in a low-force state it is likely that they will resist force when stretched in much the same way as cross bridges in other attached states. The consequence being that the force sustained during stretch will be greater than expected from the isometric strength which is largely the result of cross bridges which are attached in the high-force state. The kinetics of the cross bridges in presence of Pi during isometric and shortening contractions has been of appreciable interest among researchers. What is still not well stablished is the role of Pi during the stress relaxation after a step or ramp stretch and whether the presence of Pi affects the kinetics of cross bridges while and after an eccentric contraction.

1.4 Ageing

Human ageing is a multidimensional process of psychological, social and physiological change. It may be argued that many of the problems originate with the physical changes (Kjaer et al., 2009) so that with age there is an increasing difficulty in performing activities of daily living, in maintaining postural balance and in recovering from impending falls (Degens & McPhee, 2013). These problems may themselves have multiple causes such as loss of proprioception, of balance and neural control but it is loss of muscle mass and function that may ultimately cause the transition from an independent to a dependent lifestyle (Degens, 2007). Decrease of the muscle cross-sectional area (Trappe et al., 2003), loss of strength (Rutherford & Jones, 1992) and slowing of movement are prominent features of old age in humans (D'Antona et al., 2003). Although a loss of muscle mass is the most visible consequence of ageing, there is good evidence that there are also significant changes in the contractile properties of muscle fibres, such as a slower cross bridge kinetics (Larsson et al., 1997b; Miller et al., 2013) and loss of force generating capacity (Canepari et al., 2010; Morse et al., 2005), both processes contributing to the impairment of muscle performance in old age.

1.4.1 Effects of ageing on contractile properties

During the past, nearly, 200 years, investigators have studied the changes in different muscles with age, but the basic observation of Quetelet (1835) remains that between 30 and 80 years of age, muscle strength decreases 30-40% (Brooks & Faulkner, 1994a). This loss of muscle strength is associated with a loss in muscle mass, although the loss of mass is generally found to be somewhat less than that of force so older people have a lower force per cross-sectional area, or specific tension (Goodpaster et al., 2006). Cross-sectional area of the quadriceps was 25% smaller in old men than in young (Young et al., 1985) while CSA of the gastrocnemius lateralis (GL) was 17% smaller in elderly men compared to the young men (Morse et al., 2005). When measurements were made on single fibres, force per CSA (i.e., *Po*) was found to be reduced in older men in both type I and type IIA fibres identified by their myosin heavy chain (MyHC) isoform (Frontera et al., 2000). This observation is consistent with other experiments (Larsson et al., 1979; 1997a; Ochala et al., 2007). To some extent these changes are also seen in disuse (D'Antona et al., 2007) and this suggests that the intrinsic ability of muscle fibres to generate force is affected not only by ageing, but may also depend on the level of physical activity of the elderly population. The decrease in specific tension can be due to a decreased myosin concentration in older

fibres (D'Antona et al., 2003), to a lower number of strongly bound actin-myosin cross bridges during maximal activation and/or a reduced force-generating capacity per cross bridge (Ochala et al., 2007). Similar results have been found in muscle and skinned single fibres of rats and mice. The maximal isometric force in mice was around 23% lower in old soleus muscle tested *in vitro* and single fibres compared to young muscles and muscle fibres (Moran et al, 2005; Brooks & Faulkner, 1988). In rats, the maximal isometric force was around 50% less in old than young soleus fibres (Thompson & Brown, 1999). Atrophy of the soleus fibres was reported in aged rats compared to young (Brown & Hasser, 1996; Thompson & Brown, 1999). The specific force assessed in mice was also lower in older muscle compared with young (Phillips et al., 1991; Moran et al., 2005) and this loss of strength was also present at single fibres level (Gonzalez et al., 2000; Chan & Head, 2010).

Maximum shortening velocity of muscle fibres has been reported to be slower in elderly men compared to young subjects (Larsson et al., 1997a; Canepari et al., 2010; Ochala et al., 2007). This was also seen in rat single fibres (Degens et al., 1998), although a previous study in mouse single fibres reported no significant differences between age-groups (Brooks & Faulkner, 1988). What is particularly interesting in the context of the muscle changes with ageing is the fact that while specific isometric force, and presumably the force during shortening, is reduced with age, the force sustained during lengthening has been reported to be relatively well maintained (Vandervoort et al., 1990; Phillips et al., 1991). However, there is one study with a large sample size reporting no significant preservation of eccentric torque in older adults (Lindle et al., 1997). One possible reason for the increased force generated by older muscle during stretch is that they have increased levels of intracellular Pi, but studies with aged mouse muscle have not shown increased levels of inorganic phosphate (Phillips et al., 1993). It is also possible that older muscle may have different sensitivity to Pi so that a normal Pi that has no effect on young muscle may adversely affect the function of older muscle. It becomes interesting then to assess how ageing affects, or not, the force as a result of an eccentric contraction in mice single fibres, since the study ran by Phillips et al. in 1991 was conducted on whole mouse muscle, as well as that conducted by Brooks & Faulkner in 1988. This assessment would show whether what was shown in whole muscle is reflected or not at a single fibre level. In addition, the presence of Pi during eccentric contractions could reveal whether the increased concentration of phosphate affects in similar or different ways the young and old muscle.

Investigating the response of ageing muscle to stretch, with and without the addition of Pi, is most unlikely to be of any practical benefit. It will not improve mobility or combat obesity in old people but it might highlight age-related changes in cross bridge kinetics

and specific proteins, such as myosin which, in turn, could throw light on the process of cellular ageing.

1.5 Hysteresis in muscle

Since the first use of the term *hysteresis* by Ewing, in his classical theory of magnetic hysteresis in the 19th century, the phenomenon has been found in many fields. Starting from magnetism, optics and material sciences, the concept of hysteresis has captured the attention of biologists to study memory-dependent dynamic systems within its framework (Noori, 2013). The first biological model involving hysteresis studied mathematically, was a model for bacterial growth patterns (Hoppensteadt et al., 1980) and since then, there have been many different biological models exhibiting hysteresis cycles. One of the simplest hysteresis cycles from the biological field is the one determined by the melting and setting temperatures of the agar gel. As hysteresis is the time-based dependence of a system's output that is based on past and present outputs, in the example of the agar gel the liquid or solid state will depend on the past state of the gel, apart from the value of the actual temperature. Although hysteresis cycles of tendon force change with elongation have been reported (Magnusson et al., 2013), there are no studies about the presence of kiss-and-go hysteretic cycles in muscle force response to shortening and lengthening contractions.

1.6 Outline of the chapters

The overall aim of this thesis was to compare the force-velocity properties during shortening and lengthening contractions of isolated and permeabilised single muscle fibres taken from young and old mice, and how these are affected by inorganic phosphate to understand the changes in cross bridge function that may explain the differences in function between young and old. In the first experimental chapter (Chapter 2) the force response to eccentric contractions is characterised by three features: the peak force exerted at the end of a stretch ramp; the stress relaxation once the stretch finishes and the difference in force after the decay finishes with the isometric force value before the stretch. These features will be evaluated at different lengthening speeds. In Chapter 3, the effects of different concentrations of inorganic phosphate on the contractile properties as well as on the features of the force discussed in Chapter 2 while the muscle is stretching at different velocities are reported. In Chapter 4, the contractile properties of skinned soleus single fibres obtained from mice of different ages that comprise the whole life span, are assessed during isometric, shortening and lengthening contractions. The focus of the chapter is to observe whether the eccentric

force in old muscle is better maintained than that of isometric and shortening actions and how ageing affects the cross bridge kinetics when the muscle is stretched. Chapter 5 examines the effect of Pi on the contractile properties of muscle fibres from mice of different ages. The aim of this study was to observe whether the older muscle has a different sensitivity to the presence of Pi than the young samples. In the appendix A section a work done on fibres from 18-month-old mice to study the presence of hysteresis cycles in muscle is reported. Therefore, fibres were subjected to a periodic stimulus consisting of shortening and lengthening contractions, i.e. change of muscle length, along different frequencies and the force response to that stimuli was recorded. When plotting the force response vs. the change of length, the curve described hysteresis cycles that have not been reported before in muscle fibres.

In the last chapter (Chapter 6) the data will be discussed in the context of the current literature and some suggestions for future research are given.
Finally, in Appendix B is presented a table stating the characteristics of mice used in the experiments as well as the number of single fibres of each mouse used in each chapter.

References

Abbott, B. C., & Aubert, X. M. (1952). The force exerted by active striated muscle during and after change of length. *Journal of Physiology*, *117*, 77–86.

Bagni, M. A., Cecchi, G., & Colombini, B. (2005). Crossbridge properties investigated by fast ramp stretching of activated frog muscle fibres. *The Journal of Physiology*, *565*(Pt 1), 261–8.

Brooks, S. V., & Faulkner, J. A. (1988). Contractile properties of skeletal muscle from young, adult and aged mice. *Journal of Physiology*, *404*, 71–82.

Brooks, S. V., & Faulkner, J. A. (1994a). Skeletal muscle weakness in old age: underlying mechanisms. *Medicine and Science in Sports and Exercise*, *4*, 432–439.

Brooks, S. V., & Faulkner, J. A. (1994b). Isometric, shortening and lengthening contractions of muscle fiber segments from adult and old mice. *The American Journal of Physiology*, *267*, C507–13.

Brown, M., & Hasser, E. M. (1996). Complexity of age-related change in skeletal muscle. *The Journals of Gerontology. Series A, Biological Sciences and Medical Sciences*, *51*(2), B117–23.

Canepari, M., Pellegrino, M. A., D'Antona, G., & Bottinelli, R. (2010). Single muscle fiber properties in aging and disuse. *Scandinavian Journal of Medicine and Science in Sports*, *20*(1), 10–19.

Caremani, M., Dantzig, J., Goldman, Y. E., Lombardi, V., & Linari, M. (2008). Effect of inorganic phosphate on the force and number of myosin cross-bridges during the isometric contraction of permeabilized muscle fibers from rabbit psoas. *Biophysical Journal*, *95*(12), 5798–808.

Cavagna, G. (1993). Effect of temperature and velocity of stretching on stress relaxation of contracting frog muscle fibres. *Journal of Physiology*, *462*, 161–173.

Chan, S., & Head, S. I. (2010). Age- and Gender-Related Changes in Contractile Properties of Non-Atrophied EDL Muscle. *PloS One*, *5*(8), 20–22.

Colomo, F., Lombardi, V., Menchetti, G., & Piazzesi, G. (1989). The recovery of isometric tension after steady lengthening in tetanized fibres isolated from frog muscle. *Journal of Physiology*, *415*, 130P.

Cooke, R., & Pate, E. (1985). The effects of ADP and phosphate on the contraction of muscle fibers. *Biophysical Journal*, *48*(5), 789–798.

D'Antona, G., Pellegrino, M. A., Adami, R., Rossi, R., Carlizzi, C. N., Canepari, M., … Bottinelli, R. (2003). The effect of ageing and immobilization on structure and function of human skeletal muscle fibres. *The Journal of Physiology*, *552*(Pt 2), 499–511.

D'Antona, G., Pellegrino, M. A., Carlizzi, C. N., & Bottinelli, R. (2007). Deterioration of contractile properties of muscle fibres in elderly subjects is modulated by the level of physical activity. *European Journal of Applied Physiology*, *100*(5), 603–611.

De Ruiter, C. J., Didden, W. J., Jones, D. A., & Haan, A. D. (2000). The force-velocity relationship of human adductor pollicis muscle during stretch and the effects of fatigue. *The Journal of Physiology*, *526 Pt 3*, 671–81.

Debold, E. P., Romatowski, J., & Fitts, R. H. (2006). The depressive effect of Pi on the force-pCa relationship in skinned single muscle fibers is temperature dependent. *American Journal of Physiology. Cell Physiology*, *290*(4), C1041–C1050.

Degens, H., Yu, F., Li, X., & Larsson, L. (1998). Effects of age and gender on shortening velocity and myosin isoforms in single rat muscle fibres. *Acta Physiologica Scandinavica*, *163*, 33–40.

Degens, H. (2007). Age-related skeletal muscle dysfunction: Causes and mechanisms. *Journal of Musculoskeletal Neuronal Interactions*, *7*(3), 246–252.

Degens, H., Bosutti, A., Gilliver, S. F., Slevin, M., Van Heijst, A., & Wüst, R. C. I. (2010). Changes in contractile properties of skinned single rat soleus and diaphragm fibres after chronic hypoxia. *European Journal of Physiology*, *460*(5), 863–873.

Degens, H., & Mcphee, J. S. (2014). *Muscle wasting, dysfunction and inflammaging. Inflammation, Advancing Age and Nutrition*. Elsevier Inc.

Flitney, F. W., & Hirst, D. G. (1978). Cross-bridge detachment and sarcomere "give" during stretch of active frog's muscle. *The Journal of Physiology*, *276*, 449–465.

Frontera, W. R., Suh, D., Krivickas, L. S., Hughes, V. A., Goldstein, R., & Roubenoff, R. (2000). Skeletal muscle fiber quality in older men and women. *American Journal of Physiology. Cell Physiology*, *279*(3), C611–8.

Gans, C. (1982). Fiber architecture and muscle function. *Exercise & Sport Sciences Reviews*, *10*(1), 160–207.

Getz, E. B., Cooke, R., & Lehman, S. L. (1998). Phase transition in force during ramp stretches of skeletal muscle. *Biophysical Journal*, *75*(6), 2971–2983.

González, E., Messi, M. L., & Delbono, O. (2000). The specific force of single intact extensor digitorum longus and soleus mouse muscle fibers declines with aging. *Journal of Membrane Biology*, *178*(3), 175–183.

Goodpaster, B. H., Park, S. W., Harris, T. B., Kritchevsky, S. B., Nevitt, M., Schwartz, A. V, (2006). The Loss of Skeletal Muscle Strength, Mass , and Quality in Older Adults : The Health , Aging and Body Composition Study. *Journal of Gerontology*, *61*(10), 1059–1064.

Hill, A. V. (1938). The heat of shortening and the dynamic constants of muscle. *Proceedings of the Royal Society of London*, 136–195.

Hoppensteadt, F. C., Jäger, W., & Pöppe, C. (1984). A hysteresis model for bacterial growth patterns. In W. Jäger & J. D. Murray (Eds.), *Modelling of Patterns in Space and Time* (pp. 123–134). Berlin, Heidelberg: Springer Berlin Heidelberg.

Huxley, A. F., & Niedergerke, R. (1954). Structural changes in muscle during contraction; interference microscopy of living muscle fibres. *Nature*, *173*(4412), 971–973.

Huxley, H., & Hanson, J. (1954). Changes in the Cross-Striations of Muscle during Contraction and Stretch and their Structural interpretation. *Nature*, *173*, 973–976.

Huxley, H. E. (1969). The Mechanism of Muscular Contraction. *Science*, *164*(3886), 1356–1366.

Iwamoto, H. (1995). Strain sensitivity and turnover rate of low force cross-bridges in contracting skeletal muscle fibers in the presence of phosphate. *Biophysical Journal*, *68*(1), 243–50.

James, R. S., Altringham, J. D., & Goldspink, D. F. (1995). The mechanical properties of fast and slow skeletal muscles of the mouse in relation to their locomotory function. *The Journal of Experimental Biology*, *198*(Pt 2), 491–502.

Jones, D. A., Round, J. M., & de Haan, A. (2004). *Skeletal Muscle from Molecules to Movement: A Textbook of Muscle Physiology for Sport, Exercise, Physiotherapy and Medicine*. Churchill Livingstone.

Katz, B. (1939). The relation between force and speed in muscular contraction. *Journal of Physiology*, *96*, 45–64.

Kawai, M., & Halvorson, H. R. (1991). Two step mechanism of phosphate release and the mechanism of force generation in chemically skinned fibers of rabbit psoas muscle. *Biophysical Journal*, *59*(February), 329–342.

Kentish, J. C. (1986). The effects of inorganic phosphate and creatine on force production in skinned muscles from rat ventricule. *Journal of Physiology*, *370*, 585–604.

Kjaer, M., & Jespersen, J. G. (2009). The battle to keep or lose skeletal muscle with ageing. *The Journal of Physiology*, *587*(Pt 1), 1–2.

Krylow, A. M., & Sandercock, T. G. (1997). Dynamic force responses of muscle involving eccentric contraction. *Journal of Biomechanics*, *30*(1), 27–33.

Larsson, L., Grimby, G., & Karlsson, J. (1979). Muscle strength and speed of movement in relation to age and muscle morphology. *Journal of Applied Physiology: Respiratory, Environmental and Exercise Physiology*, *46*(3), 451–456.

Larsson, L., Li, X., & Frontera, W. R. (1997a). Effects of aging on shortening velocity and myosin isoform composition in single human skeletal muscle cells. *The American Journal of Physiology*, *272*(2 Pt 1), C638–49.

Larsson, L., Li, X., Yu, F., & Degens, H. (1997b). Age-related changes in contractile properties and expression of myosin isoforms in single skeletal muscle cells. *Muscle & Nerve. Supplement*, S74–8.

Leijendekker, W. J., & Elzinga, G. (1990). Metabolic recovery of mouse extensor digitorum longus and soleus muscle. *European Journal of Physiology*, *416*(1), 22–27.

Linari, M., Bottinelli, R., Pellegrino, M. A., Reconditi, M., Reggiani, C., & Lombardi, V. (2003). The mechanism of the force response to stretch in human skinned muscle fibres with different myosin isoforms. *The Journal of Physiology*, *554*(Pt 2), 335–52.

Lindle, R. S., Metter, E. J., Lynch, N. A., Fleg, J. L., Fozard, J. L., Tobin, J., … Hurley, B. F. (1997). Age and gender comparisons of muscle strength in 654 women and men aged 20-93 yr. *Journal of Applied Physiology (Bethesda, Md. : 1985)*, *83*(5), 1581–7.

Lombardi, V., & Piazzesi, G. (1990). The contractile response during steady lengthening of stimulated frog muscle fibres. *Journal of Physiology*, *431*, 141–171.

Maganaris, C. N., Baltzopoulos, V., Ball, D., & Sargeant, a J. (2001). In vivo specific tension of human skeletal muscle. *Journal of Applied Physiology (Bethesda, Md. : 1985)*, *90*(3), 865–872.

Magnusson, S. P., Narici, M. V, Maganaris, C. N., & Kjaer, M. (2008). Human tendon behaviour and adaptation, in vivo, *Journal of Physiology*, 586, 71–81.

Maruyama, K., Kimura, S., & Ohashi, K. (1977). Connectin, an elastic protein of muscle. *Journal of Biochemistry*, *82*(2), 317–337.

Matthews, G. G. (2013). *Cellular Physiology of Nerve and Muscle*. Wiley.

Miller, M. S., Bedrin, N. G., Callahan, D. M., Previs, M. J., Jennings, M. E., Ades, P. A, … Toth, M. J. (2013). Age-related slowing of myosin actin cross-bridge kinetics is

sex specific and predicts decrements in whole skeletal muscle performance in humans. *Journal of Applied Physiology (Bethesda, Md. : 1985)*, *115*(7), 1004–14.

Moran, A. L., Warren, G. L., & Lowe, D. A. (2005). Soleus and EDL muscle contractility across the lifespan of female C57BL/6 mice. *Experimental Gerontology*, *40*(12), 966–975.

Morse, C. I., Thom, J. M., Reeves, N. D., Birch, K. M., & Narici, M. V. (2005). In vivo physiological cross-sectional area and specific force are reduced in the gastrocnemius of elderly men. *Journal of Applied Physiology (Bethesda, Md. : 1985)*, *99*(3), 1050–5.

Noori, H. R. (2013). *Hysteresis Phenomena in Biology*. Springer Berlin Heidelberg.

Ochala, J., Frontera, W. R., Dorer, D. J., Van Hoecke, J., & Krivickas, L. S. (2007). Single skeletal muscle fiber elastic and contractile characteristics in young and older men. *The Journals of Gerontology. Series A, Biological Sciences and Medical Sciences*, *62*(4), 375–81.

Osterman, A., & Arner, A. (1995). Effects of inorganic phosphate on cross-bridge kinetics at different activation levels in skinned guinea-pig smooth muscle. *The Journal of Physiology*, *484 (Pt 2*(1995), 369–83.

Phillips, S. K., Bruce, S. A., & Woledge, R. C. (1991). In mice, muscle weakness due to age is absent during stretching. *Journal of Physiology*, *437*, 63–70.

Phillips, S. K., Wiseman, R. W., Woledge, R. C., & Kushmerick, M. J. (1993). Neither phosphorus metabolite levels nor myosin isoforms can explain the weakness in aged mouse muscle. *Journal of Physiology*, *463*, 157–167.

Quetelet, A. (1835). *Sur l'homme et le développement de ses facultés, ou Essai de physique sociale - Tome I*. Paris, Bachelier.

Rassier, D. E., Herzog, W., Wakeling, J., & Syme, D. A.. (2003). Stretch-induced, steady-state force enhancement in single skeletal muscle fibers exceeds the isometric force at optimum fiber length. *Journal of Biomechanics*, *36*(9), 1309–1316.

Rutherford, O. M., & Jones, D. A. (1992). The relationship of muscle and bone loss and activity levels with age in women. *Age and Ageing*, *21*(4), 286–93.

Selsby, J. T. (2011). Increased catalase expression improves muscle function in mdx mice. *Experimental Physiology*, *96*, 194–202.

Stienen, G. J., Versteeg, P. G., Papp, Z., & Elzinga, G. (1992). Mechanical properties of skinned rabbit psoas and soleus muscle fibres during lengthening : effects of phosphate and Ca^{2+}. *Journal of Physiology*, *451*, 503–523.

Sugi, H. (1972). Tension changes during and after stretch in frog muscle fibres. *Journal of Physiology*, 237–253.

Tesi, C., Colomo, F., Piroddi, N., & Poggesi, C. (2002). Characterization of the cross-bridge force-generating step using inorganic phosphate and BDM in myofibrils from rabbit skeletal muscles. *The Journal of Physiology*, *541*(Pt 1), 187–99.

Thompson, L. V, & Brown, M. (1999). Age-related changes in contractile properties of single skeletal fibers from the soleus muscle. *Journal of Applied Physiology*, *86*, 881–886.

Trappe, S., Gallagher, P., Harber, M., Carrithers, J., Fluckey, J., & Trappe, T. (2003). Single muscle fibre contractile properties in young and old men and women. *The Journal of Physiology*, *552*(Pt 1), 47–58.

Vandervoort, A. A., Kramer, J. F., & Wharram, E. R. (1990). Eccentric knee strength of elderly females. *Journal of Gerontology*, *45*(4), B125–8.

Wang, K., McClure, J., & Tu, A. (1979). Titin: major myofibrillar components of striated muscle. *Proceedings of the National Academy of Sciences*, *76*(8), 3698–3702.

Wickiewicz, T. L., Roy, R. R., Powell, P. L., & Edgerton, V. R. (1983). Muscle architecture of the human lower limb. *Clinical Orthopaedics and Related Research*, (179), 275–283.

Widrick, J. J., Romatowski, J. G., Bain, J. L., Trappe, S. W., Trappe, T. a, Thompson, J. L., … Fitts, R. H. (1997). Effect of 17 days of bed rest on peak isometric force and unloaded shortening velocity of human soleus fibers. *The American Journal of Physiology*, *273*(5 Pt 1), C1690–9.

Widrick, J. J. (2002). Effect of P-i on unloaded shortening velocity of slow and fast mammalian muscle fibers. *Amer.J.Physiol Cell Physiol*, *282*(4), C647–C653.

Winters, J. M. (1990). Hill-based muscle models: a systems engineering perspective. *Multiple Muscle Systems*, 69–93.

Young, A., Stokes, M., & Crowne, M. (1985). The size and strength of the quadriceps muscles of old and young men. *Clinical Physiology*.

Zatsiorsky V. M. & Prilutsky B. I. (2012). *Biomechanics of skeletal muscles.* Human Kinetics.

CHAPTER 2

The response of single muscle fibres to stretch

2.1 Abstract

Many daily life activities require the skeletal muscles to exert eccentric contractions apart from the well-known isometric or concentric contractions. The study of the contractile properties while the muscles are active and forcibly stretched is important to gain a better understanding of the muscle function. The aim of the work described in this chapter was to evaluate the characteristics of the force response to stretch and how different velocities of lengthening affect those characteristics. Single and permeabilised soleus fibres from seven 10-month-old mice were used in this study. Each fibre was submerged in activating solution and once their length, isometric force (*Fo*) and cross-sectional area were determined, they were subjected to four sequences of four isotonic steps in order to obtain the force-velocity curve. They were then subjected to 5% isovelocity ramp-and-hold stretches at 0.0625 (fl/s), 0.25 (fl/s) and 1 (fl/s) at 15ºC. The peak force (*Fpeak*) at the end of the ramp, the stress relaxation following the *Fpeak* and the steady force at the end of the decay were observed at all velocities. The Fpeak was found to be higher than the isometric force before the stretch, being around 200% of *Fo* and increasing with the velocity of stretch. Meanwhile, the decay of force or stress relaxation (SR), was fitted to a double exponential, thus obtaining two rate constants kd1 and kd2 for slow and fast exponential terms, respectively. In addition, the contributions of each exponential, A1 for the slow and A2 for the fast term, were determined. The kd1 showed values between 3.5 and 7 (s^{-1}) and was weakly affected by stretching speed. On the contrary, kd2 was increased significantly with the velocity of stretch with values between 20 and 80 (s^{-1}). The contributions A1 and A2 varied, with higher proportions of A2 at higher speed of stretch, leading to faster stress relaxation. Force enhancement, the force remaining after the end of stretch was 15-19% higher than the isometric force before the stretch at all velocities and was independent of the speed of lengthening. In conclusion, two different populations of cross bridges, one with a slow rate of attachment-detachment (kd1) and another one with a high rate of turnover and a fast rate constant (kd2) contributed to the SR. The independency of force enhancement to the cross bridge kinetics suggests that the residual force is a result of stretching titin filaments.

2.2 Introduction

The contractile properties of skeletal muscle are generally described in terms of isometric strength, maximum velocity of shortening (Vmax) and the curvature of the force-velocity relationship (a/Po in the Hill equation). However, during daily life many activities such as landing from a jump, sitting down on a chair, walking down the stairs

or lowering a weight from a shelf, require eccentric contractions and a description of the eccentric force-velocity relationship is also providing important information of muscle function. A muscle acts eccentrically when it is forcibly stretched while active. The first characteristic of eccentric contractions is that the force a muscle can sustain during such contractions (peak force, *Fpeak*), or active stretch, can be around twice the value of the isometric force (*Fo*) (Katz, 1939; Sugi, 1972; Edman et al., 1982; Linari et al., 2003; Bagni et al., 2005) and even greater (Getz et al., 1998). Secondly, if the active muscle is held isometric at the new longer length achieved after the stretch, the force decreases with a time course that consists of both fast and slow phases that are well approximated by the sum of two exponential terms (Colomo et al., 1989). Cavagna (1993) referred to this phenomenon as “stress relaxation”. Values reported for the fast rate constant range from around 100-150 (s^{-1}) for rat flexor hallucis brevis fibres at 20ºC (Pinniger et al. 2006), 200 (s^{-1}) for rabbit psoas fibres at 10ºC (Getz et al. 1998) and ~250 (s^{-1}) for frog tibialis anterior fibres at 14ºC (Cavagna, 1993). In all cases, the slow rate constant ranged between 1-10 (s^{-1}). The stress relaxation has been reported to be faster with increasing speed of stretch (Cavagna, 1993), but it is not known why this should be or what determines the amplitude of the two phases. There is a third interesting characteristic of the force response to a stretch, termed residual force enhancement, where the force level after an appropriate period of stress relaxation, is greater than the isometric level before the stretch or the isometric force generated if the muscle is activated at the new longer length (De Ruiter et al., 2000; Rassier et al., 2003; Power et al., 2012). This residual force enhancement has been reported to appear only when the sarcomere length is above 2.2 µm (Edman et al., 1978). The aim of the present study was to assess the way in which the three characteristics of eccentrically contracting mouse soleus muscle fibres (peak force, rate of stretch relaxation and force enhancement) depend on the velocity of stretch as a prelude to further studies of the changes which may occur with ageing.

2.3 Materials and Methods

2.3.1 Muscle samples

Soleus muscles were dissected from three 10-month-old adult female gtf2ird (knock-out mice, assumed this had no effect on muscle function) and four 10-month-old adult female wild-type mice. The animals were humanely killed using approved schedule 1 methods (cervical dislocation) for another research study approved by the local Animal Ethics Research Committee of the University of Manchester. This is in accord with the generally accepted guideline of reducing animal numbers to a minimum in biomedical

research. The right soleus muscle was excised from each animal and immersed in glycerol/relax solution (see Solutions below) at 4°C for 24 hrs. It was then treated with increasing concentrations of sucrose in relax solution (Frontera and Larsson, 1997; Degens et al., 2010), which acts as an effective cryoprotectant, preventing damage of the contractile machinery of fibres. After sucrose-treatment, the muscles were frozen in liquid nitrogen and stored at -80°C for later use.

2.3.2 Solutions

The composition of the solutions have been described previously (Larsson and Moss, 1993; Gilliver et al., 2009; Degens et al., 2010). The relaxing solution contained (mM): MgATP, 4.5; free Mg^{2+}, 1; imidazole, 10; EGTA, 2 and KCl, 100 and the pH was adjusted to 7.0 using KOH. The glycerol/relax was the same as relaxing solution containing 50% (*v/v*) glycerol. The pCa (-log[free Ca^{2+}]) of the activating solution was 4.5 and contained: MgATP, 5.3; free Mg^{2+}, 1; imidazole, 20; EGTA, 7; creatine phosphate, 19.6; KCl, 64 with pH 7.0. The ionic strength of both relaxing and activating solution was adjusted to 180 mM with KCl.

2.3.3 Preparation of single fibres

The methods for preparing single fibres and determining their contractile properties have been described previously (Degens et al., 2010; Gilliver et al, 2010; 2011). Briefly, the sample was taken from the -80°C storage, thawed and treated with decreasing concentrations of sucrose and stored in glycerol/relax at -20°C for use within a month. At the day of use a small bundle was cut from the muscle and immersed in relaxing solution containing 1% Triton X-100 for 20 minutes to permeabilise the membranes and sarcoplasmic reticulum. Then fibres were teased from the bundle, mounted in a permeabilised-fibre test system (400 Aurora Scientific Inc. Ontario, Canada) and tied with nylon thread to insect pins attached to the force transducer (Aurora, 403) and the lever arm (Aurora, 312C). The sarcomere length (*sl*) was set at 2.6 µm and checked along the length of the fibre. Fibre length (*Lo*) was determined to the nearest 0.01 mm and were between 1.4 and 2.7 mm long. These procedures were carried out with the fibre in relaxing solution. Fibre diameter was measured at three places along the length of the fibre while submerged in relaxing solution and the cross-sectional area calculated assuming a circular circumference of the fibre. All experiments were carried out at 15°C.

2.3.4 Concentric contractions

To maximally activate the fibres they were transferred from the relax solution to the activating solution (4.5 pCa). When isometric force had reached a plateau, the fibre was subjected to four sequences of four isotonic shortening steps (Degens et al., 2010; Gilliver et al., 2010, 2011; Botinelli et al, 1996). The fibre was stretched back to its original length after each sequence while in activating solution. This sequence (Figure 2.1) was repeated four times at different percentages of isometric force. These measurements were used to determine the Force-Velocity relationship for the concentric contractions.

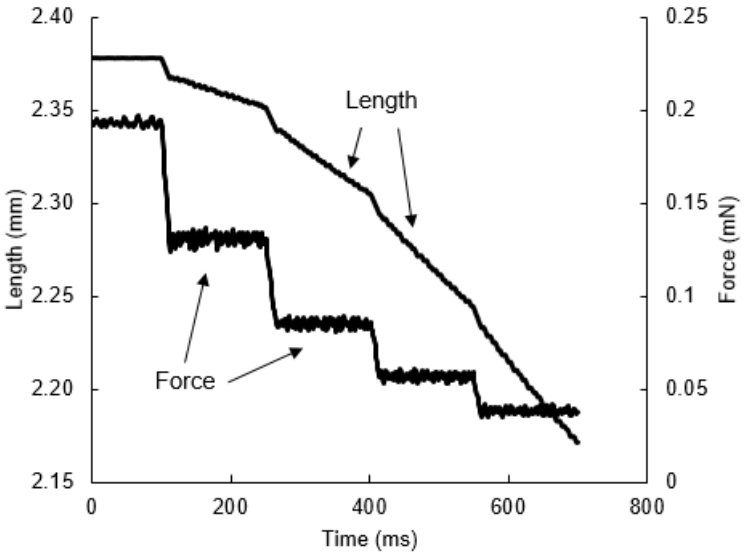

Figure 2.1: *Sequence of four isotonic shortening steps. Each step is set at a different percentage of isometric force. Curves of force and length vs time.*

2.3.5 Eccentric contractions

After the four sequences of isotonic shortening steps, the fibre was returned to relaxing solution. If *Fo* had not decreased by more than 10% and sarcomere length not more than 0.1 µm, the fibres were transferred again to the activating solution and after force reached a plateau subjected to isovelocity stretches of 5% *Lo* at three different velocities: 0.0625 fibre length per second (fl/s), 0.25 (fl/s) and 1 (fl/s). Between each stretch, the fibre was held at the new length for 1 second, then shortened back to *Lo* and once the three stretches were completed, transferred back to the relaxing solution. An example of a mouse soleus fibre stretched at slow, medium and fast speeds is shown in Figure 2.2b with peak force, stress relaxation and force enhancement indicated. The isovelocity ramps at three speeds are shown in Figure 2.2a.

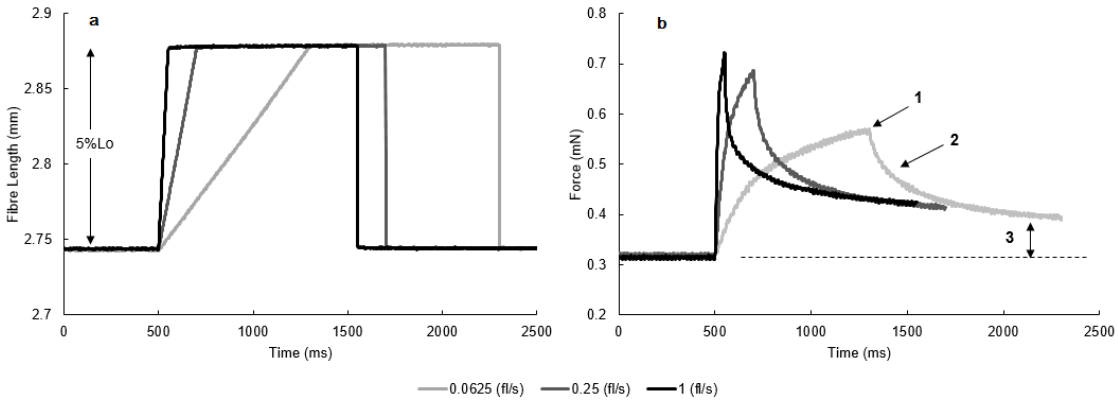

Figure 2.2a: *Fibre length vs time curve showing the 5% Lo lengthening ramp at three speeds used as the input.* ***b:*** *Single fibre stretched at different speeds with the three main characteristics of the force response indicated: (1) peak force, (2) decay or stress relaxation and (3) force enhancement.*

As shown in figure 2.2b, in the present study the force enhancement was defined as the difference in force before and after the stretch and subsequent stress relaxation. The actual force value was different from that indicated in figure 2.2b, and was given as the constant C in the fitted double exponential curve using non-linear least squares regression, that best represented the stress relaxation (SOLVER, Microsoft Excel). Through this fitting routine, the rate constants for stress relaxation were also determined.

All fibres in this and subsequent chapters were tested at a *sl* = 2.6 µm and shortening and lengthening contractions within the same range of 5% of Lo. For isotonic shortening the length change of the muscle fibre depended on the speed of the fibre whereas for the isovelocity lengthening, the length changes were all at the same range.

2.3.6 Statistics

Data are presented as mean ± standard error (SE). Differences between groups were determined by a repeated-measures ANOVA with as within factor velocity of stretch (3 levels). Effects were considered significant at $p<0.05$. If significant effects were found a *post hoc* t-test with Bonferroni correction was used to locate the significant differences between groups.

2.4 Results

There were no significant differences between genotype, as illustrated in Table 2.1, and therefore all data are further presented as the average of all seven mice combined. The mean values and SE of isometric force, cross-sectional area (CSA) and force per

CSA (specific force, *Po*) for the single fibres used in this study (number of different single fibres, n=61) are shown below in table 2.2. In this experiment, 5 fibres were rejected according to the exclusion criteria.

	Gtf2ird1(n fibres=28)	**Wild type** (n fibres=33)
Fo (mN)	0.31±0.18	0.29±0.17
CSA (μm^2)	2168±75	2311±64
Po (N/cm^2)	14.2±0.4	13.7±0.6
Vmax (Fl/s)	0.49±0.01	0.5±0.02
a/Po	0.24±0.01	0.23±0.01

Table 2.1: *means and SE of the maximum isometric force (Fo), cross-sectional area (CSA), force per CSA (Po), Vmax and a/Po for the different genotypes of mice. No significant differences were found.*

Fo (mN)	0.3±0.2
CSA (μm^2)	2240±82
Po (N/cm^2)	13.9±0.7
Vmax (Fl/s)	0.5±0.03
a/Po	0.23±0.01

Table 2.2: *means and SE of the maximum isometric force (Fo), cross-sectional area (CSA), force per CSA (Po), Vmax and a/Po. (Number of different single fibres, n=61)*

2.4.1 Shortening contractions

Figure 2.3 shows the average force-velocity relationship obtained as mean of 61 different fibres. This curve was fitted to the Hill equation with mean values of Vmax and a/Po as given in table 2.2.

2.4.2 Eccentric contractions

The force at the end of the stretch, i.e. peak force (*Fpeak*), the rate of 'stress relaxation' and the force enhancement were determined for each of the three stretching velocities. As shown in Figure 2.2b for the 0.0625 (fl/s) case, the force response to an isovelocity ramp stretch consisted of a fast rise in force followed by a slower rise until reaching the peak force. The decay following the stretch, or stress relaxation, was fitted by a double exponential and here the important feature to observe were the two rate constants from the exponential decays. The force enhancement (*FE*) after the stretch was given as the ratio *Fafter/Fo*. A typical example of the responses of a single fibre to stretches at three different velocities is shown in figure 2.2b.

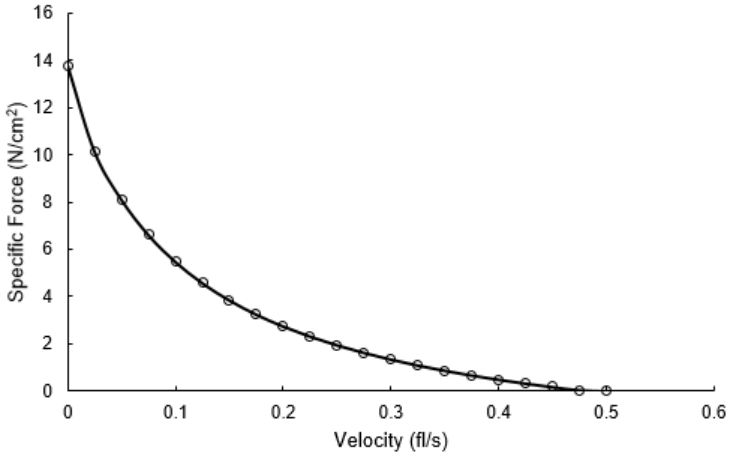

Figure 2.3: *mean force-velocity relationship in terms of the Hill equation (P+a)(V+b)=(Po+a)b. Mean values of a, Po and Vmax from n=61 single fibres were used to calculate force values for given velocity values.*

2.4.2.1 Peak Force

In figure 2.2b, the *Fpeak* increased with the speed of stretch. The mean values for 61 (at 0.0625 fl/s), 61 (at 0.25 fl/s) and 58 (at 1 fl/s) single fibres are given in Figure 2.4. It can be seen that the *Fpeak* increases with the speed of the stretch (*p<0.01*) and plateaus at higher velocities.

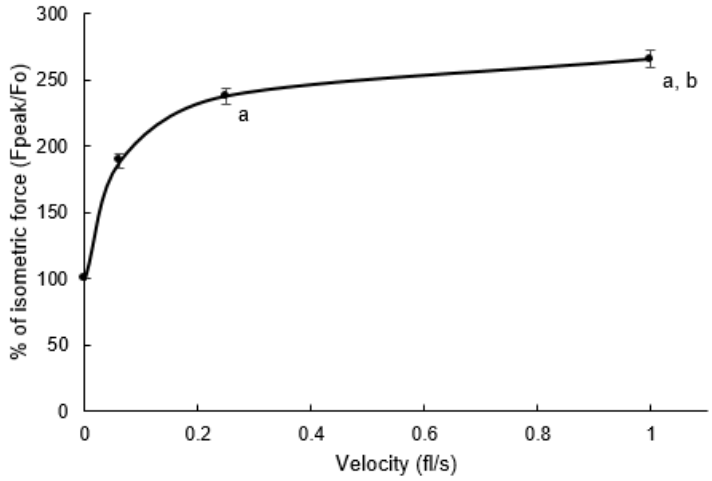

Figure 2.4*: Values of force sustained at three different velocities of stretching (Means and SE) compared to the isometric force (value at 0 (fl/s)). a: significantly different from 0.0625 (fl/s); b: significantly different from 0.25 (fl/s). (n=61 single fibres)*

2.4.2.2 Stress relaxation

The second interesting feature was the stress relaxation immediately after the stretching ramp. This decay was initially fitted to a single exponential but at each of the three velocities of stretch better results were obtained when the curves were fitted to a

double exponential (Figure 2.5a). The function representing the double exponential could be defined as:

$$F = A1*e^{-kd1*t}+A2*e^{-kd2*t} + C, \quad (1)$$

and five parameters determined, a slow and fast rate constants called kd1 and kd2, respectively; A1 the contribution of the slow component and A2 the contribution of the fast component. Both components are shown in Figure 2.5b. C is the solution of the equation and the value to which both components trend at $t \rightarrow \infty$.

The slow component of stress relaxation was slower at 0.0625 (fl/s) than at faster stretches *(p<0.05)*. However, it did not differ significantly between the fast (1 fl/s) and the medium (0.25 fl/s) speed stretches (Figure 2.6, left). The fast component (kd2, Figure 2.6, right) did show a progressive increase with increasing speed of stretch *(p<0.001)*.

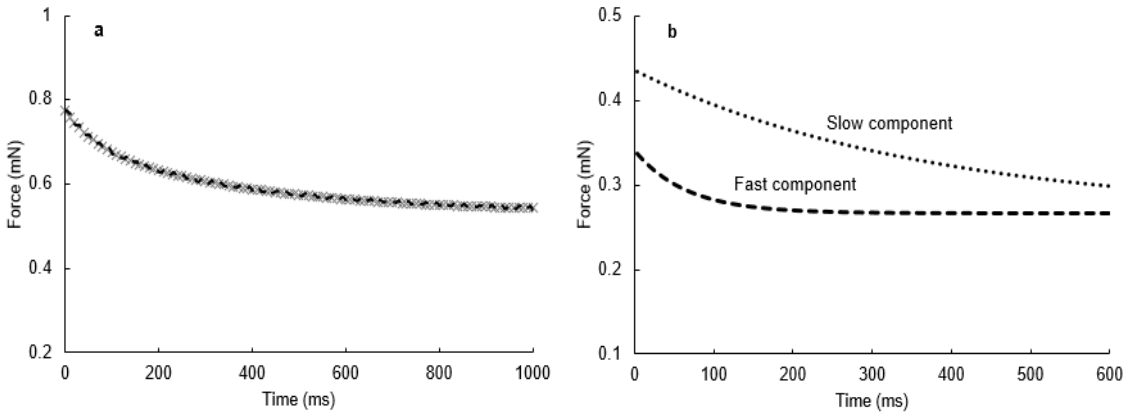

Figure 2.5: (a) *example of stress relaxation after a fibre stretch at 0.0625 (fl/s), fitted to a double exponential. The dashed line is the data curve and the x symbols represent the fitted curve. (b) Slow and fast components of the double exponential fitted to the force data in a)*

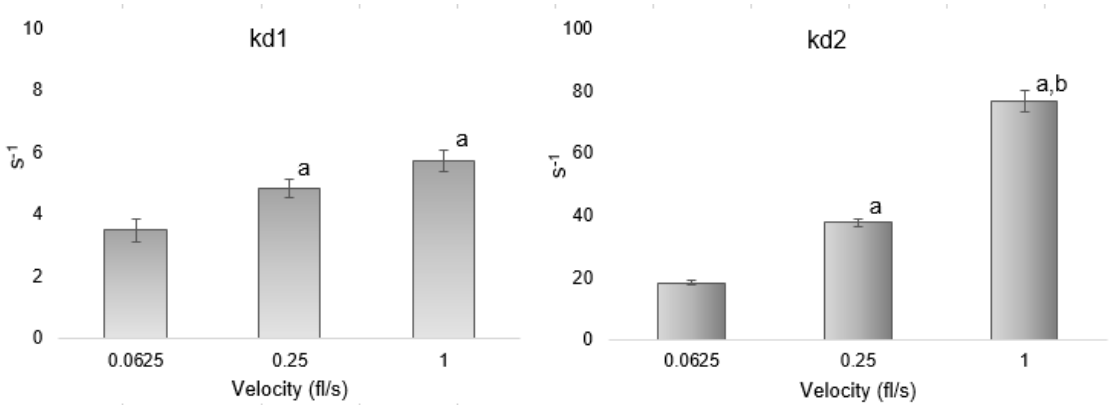

Figure 2.6: *Means ± SE of the exponential rate constants, slow (kd1) and fast (kd2). a: significantly different (p<0.05) from 0.0625 (fl/s). b: significantly different (p<0.001) from 0.25 (fl/s). (n=61 single fibres)*

The proportions of the slow and fast components for the stress relaxation were called A1 and A2, respectively. As shown in table 2.2, the proportion of the slow component of the stress relaxation decreased with the increasing speed of lengthening while the proportion of the fast component increased.

Proportions of	A1 (%)	A2 (%)
0.0625 (fl/s)	60 ± 2*	40 ± 2*
0.25 (fl/s)	57 ± 1*	43 ± 1*
1 (fl/s)	47 ± 1	53 ± 1

Table 2.2: *proportions of the slow, A1, and fast, A2, rate constants of the stress relaxation, at the three different stretching speeds (Mean ± SE). * Significantly different from 1 (fl/s). (n=61 single fibres)*

2.4.2.3 Force Enhancement

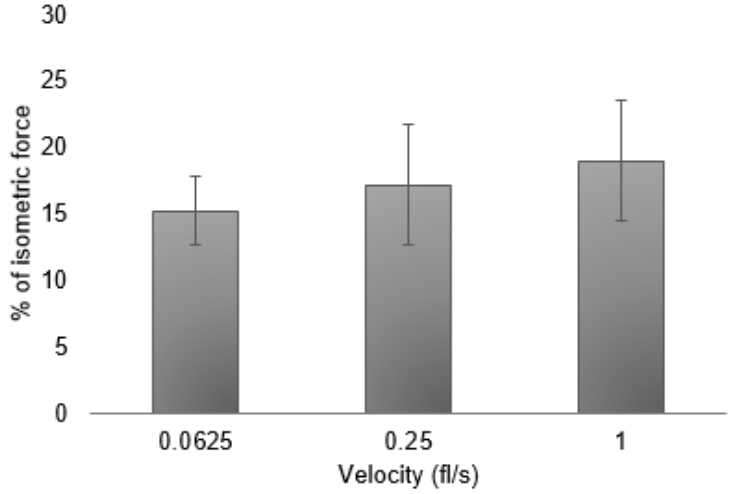

Figure 2.7: *means and SE of the % of force enhancement obtained for three speeds of stretching. (n=61 single fibres)*

There were no significant differences in the force enhancement expressed as a percentage of *Fo* at the different velocities of stretch (figure 2.7). Therefore, the FE is independent of the velocity of stretch over the range tested in this study.

2.5 Discussion

Muscles can sustain considerably larger forces when stretched whilst activated than during an isometric contraction (Katz, 1939; Sugi, 1972; Edman et al., 1982; Linari et al., 2003; Bagni et al., 2005), but the effects of different velocities of stretch on the stress relaxation phase and on force enhancement have received less attention. The study of these aspects of the force response may provide information about the kinetic

properties of the contractile apparatus. Such information is relevant, as there are instances, such as ageing and fatigued muscles, where the decrease in force during stretch is proportionally less than the age- or fatigue-induced decrement in isometric force (Cavagna, 1993; De Ruiter et al., 2000; Roig et al., 2010). In this study it was found that while the peak forces and the rate of stress relaxation increase with increasing stretch velocity (see Figures 2.4 and 2.6), the residual force enhancement is not significantly affected by the rate of the stretch (Figure 2.7). This suggests that the force enhancement after a stretch is independent of the action of cross bridges, while stress relaxation is a feature of cross bridge kinetics. The specific forces of single permeabilised fibres from adult mice of 13.9 $\pm$ 0.7 (N/cm^2), as well as the curvature *a/Po* of the force-velocity relationship, are within the range reported in previous studies for specific force (Brooks & Faulkner, 1988; Phillips et al., 1993) and *a/Po* (Brooks & Faulkner, 1988).

2.5.1 The force response during stretch

In activated fibres, the force rise during an isovelocity ramp stretch consisted of two phases: an initial fast increase in force, followed by a slower rise until the end of the stretch where it reaches a maximum, or peak force. The two phases are more evident in the example at 0.0625 (fl/s) from Figure 2.2b. The initial steep slope is likely a consequence from deformation of all attached cross bridges while the following reduction in the slope might be explained by a forcible detachment of some of the cross bridges and continuing deformation of the attached bridges (Getz et al., 1998; Pinniger et al., 2006). An alternative view suggests that during stretch, deformation of the attached cross bridge causes the second non-attached myosin head to come into a position where it can attach to actin (Fusi et al., 2010; Brunello et al., 2007). In this model, the additional force is almost entirely explained by the force generated by the second head. These observations, however, are based on relatively short and rapid stretches and it is not clear what happens when the double headed attachment is stretched beyond the normal range of cross bridge action and, whether with one or two heads, must detach. The Lombardi & Piazzesi (1990) and Bickham et al (2011) models of cross bridge action that consider only single head attachment predict that to sustain a force during a prolonged stretch it is necessary for detached cross bridges to re-attach very rapidly. It is possible that the initial rapid rise in force at the start of the stretch could be a consequence of attachment of the second myosin head but the subsequent behaviour during a prolonged stretch could involve rapid detachment and reattachment without the release of Pi. One feature of the stretch response that is not explained by the Lombardi & Piazzesi (1990) and Bickham et al. (2011) models is the continued rise in force during the second phase of the stretch (Figure 2.2b). It is

possible that this rise is associated with the phenomenon of force enhancement, the nature of which is not clear but is frequently suggested to be arising from stretching non-cross bridge structures such as titin (Pinniger et al., 2006; Edman & Tsuchiya, 1996; Noble, 1992). The behaviour during stretch of this structure has been suggested to be similar to a Hookian spring (De Ruiter et al., 2000). However, this does not explain the second phase rise in force that has been calculated to be around 38% of the total increment (*Fpeak-Fo*) and that is more than the 15% FE shown in Figure 2.7.

2.5.2 Peak force at the end of a stretch

The dependence of the peak force on the stretch velocity of activated muscle fibres is not predicted by the Hill force-velocity equation and there is no unique equation to describe it as is the case for shortening (Cole et al., 1996; Krylow and Sandercock, 1997). The peak force values experimentally observed here are more than double the isometric force before the stretch and are in general agreement with those values reported previously by stretching a variety of muscle preparations (Sugi, 1972; Getz et al., 1998; Bagni et al., 2005).

The data shown in Figure 2.4 suggests that the peak force reaches a plateau at a stretch velocity of around 1 (fl/s). These data are difficult to compare directly with other reports since a variety of preparations and temperatures have been used. However, they are very similar to those of Stienen et al (1992) who also found the force to plateau at stretches around 1 (fl/s) for rabbit muscle fibres at 15^{o}C. Linari et al (2003), working with human fibres at 12^{o}C, reported peak force to plateau at slower velocities, around 0.25 (fl/s). Phillips et al (1991) reported the peak force to be maximal at around 2 (fl/s) for whole mouse soleus muscles maintained at room temperature while Sugi (1972) found the peak force to plateau at around 8 (fl/s) working with frog semitendinosus muscle also at room temperature. While the shape of the peak force vs velocity of stretch relationship may vary between studies, they all agree that the force response is velocity dependent.

2.5.3 Stress Relaxation

Whilst there has been considerable interest concerning the increase in force during stretch there has been only a few studies concentrating on the decay of force after the end of stretch. Colomo et al. (1989) and Cavagna (1993) both found the stress relaxation to be a complex curve that is best described by the sum of two exponential terms. Colomo et al. (1989) worked with frog tibialis anterior muscle fibres at 4^{o}C and Cavagna et al. (1993) used semitendinosus frog muscle at 14^{o}C. Both studies found that the rate of the fast component increased with increasing rates of stretch from 50 (s^{-1}) to

250 (s^{-1}), while the slow component was independent of the velocity of the stretch and was about 2.5 (s^{-1}) in the first study and about 5 (s^{-1}) in the second study. Pinniger et al. (2006), evaluated the stress relaxation of rat flexor hallucis brevis muscle fibres at 20^{o}C and also obtained varying fast (25 s^{-1} to around 85 s^{-1}) and relatively slow (~5 s^{-1}) rate constants when stretching the fibres with velocities ranging from 0.1 to 1 (fl/s). These values are comparable to the results presented in Figures 2.6, where the fast component mean values are between 20 (s^{-1}) and ~80 (s^{-1}) when the velocity of stretch increased from 0.0625 (fl/s) to 1 (fl/s). All the studies agree that the fast component of the double exponential increases with increasing stretch velocity. Cavagna et al (1993) suggested that the slow component of stress relaxation was due to a non-enzymatic process and this raises the possibility that the slow component represents the decay of force enhancement over time. This is unlikely, however, since the analysis of the stress relaxation curves involves the force decaying to an elevated baseline value that is the force enhancement. Therefore, the decay in peak force following a stretch consists of three components; a fast component, a slow component and then a very slow component corresponding to the decrease in force enhancement. Here an alternative to the suggestion by Cavagna is proposed. When an active single fibre is stretched, two cross bridge populations could be considered. During a stretch one population of cross bridges will remain within the normal range of attachment. Once the stretch ramp finishes, they would detach with a slow rate constant (or kd1). The second population of cross bridges would be carried beyond that normal range of attachment, where the myosin neck would be stretched more than usual producing a higher force. These cross bridges would be forcibly and rapidly detached and re-attached during stretch and this population would increase with an increase in the stretch velocity, i.e. dependent on the stretch velocity. Such cross bridges would have a high rate of turnover and a fast rate constant (kd2) at the end of the stretch. Depending on the velocity of stretch, the size of each population would change: while the stretch is slow the term A1 would be larger than A2, as shown in table 2.1; this means that the first population of cross bridges with slow rate constant, kd1, would be larger. When the stretch velocity increases, the second population would become larger, given by A2 > A1. This alternative would then explain the velocity dependence of the peak force as well as the dependence of the fast relaxation term kd2. This model of cross bridge action during stretch implies that the additional force is the result of strained, rather than an increased number of, attached cross bridges. Such an explanation is consistent with the report of Colombini et al. (2007) that 15% of the additional force is attributable to additional cross bridges, while the major portion of the additional force (85%) was attributed to strained cross bridges. Lombardi & Piazzesi (1990) and, more recently, Bickham et al. (2011), have developed kinetic

models that also show that the additional force during stretch is due to strained cross bridges. A feature of these models is the prediction of an unusual second detached state called D2. It is proposed that when the intermediate AM.ADP.Pi is strained it can rapidly dissociate and that the D2 state, M.ADP.Pi, can reattach very rapidly. Apart from providing a good fit to the observed force response to stretch, this model also explains why, during stretch, there is a much reduced ATP turnover since the D2 state continuously cycles without releasing Pi (Bickham et al, 2011). The suggestion made above, of two cross bridge states, is broadly consistent with the Lombardi & Piazzesi (1990) and Bickham et al (2011) models.

2.5.4 Residual force enhancement

Force enhancement, sometimes known as “stretch activation” has been well documented, first by Abbott & Aubert (1952) and numerous authors since (De Ruiter et al., 2000; Rassier et al., 2003; Power et al., 2012). After reaching the peak force at the end of the stretch, the force decayed to a level that was greater than the isometric force before the stretch. The force enhancement is dependent on the length of the stretch (Edman et al., 1982; Koppes et al., 2013), but, as shown in Figure 2.7, independent of the velocity of stretch. There is little agreement as to the cause of the residual force enhancement phenomenon. Linari et al (2000) have presented data to show that following a stretch the orientation of the myosin heads does not return to the resting state for some time and argue that this represents an increased number of attached cross bridges remaining long after the steady lengthening has finished. On the other hand, Herzog (2014) suggested that force enhancement is the result of stretching titin filaments, which become stiff because of calcium activation, providing a passive compliant element that would provide the length dependent aspect of force enhancement and would not obviously be affected by the velocity of stretch. The current observation that the FE is independent of velocity of stretch is consistent with this view. The response to stretch has been shown to be affected by fatigue (de Ruiter et al., 2000) and it is possible that the increased intracellular [Pi] during fatigue may alter the relative proportions of cross bridge states and thereby the response to stretch. The next chapter will address the question on how the addition of inorganic phosphate affects the characteristics of the eccentric contractions.

Conclusion

The study has showed that skinned single fibres behave much the same as other muscle preparations during and after a ramp stretch. The results obtained in this chapter constitute a set of basic values to compare further with phosphate and ageing effects.

References

Abbott, B. C., & Aubert, X. M. (1952). The force exerted by active striated muscle during and after change of length. *Journal of Physiology,* 117, 77–86.

Bagni, M. A., Cecchi, G., & Colombini, B. (2005). Crossbridge properties investigated by fast ramp stretching of activated frog muscle fibres. *The Journal of Physiology*, *565*(Pt 1), 261–8.

Bickham, D. C., West, T. G., Webb, M. R., Woledge, R. C., Curtin, N. A., & Ferenczi, M. A. (2011). Millisecond-scale biochemical response to change in strain. Biophysical Journal, 101(10), 2445–54.

Brunello, E., Reconditi, M., Elangovan, R., Linari, M., Sun, Y.-B., Narayanan, T., Lombardi, V. (2007). Skeletal muscle resists stretch by rapid binding of the second motor domain of myosin to actin. Proceedings of the National Academy of Sciences of the United States of America, 104(50), 20114–20119.

Cavagna, G. (1993). Effect of temperature and velocity of stretching on stress relaxation of contracting frog muscle fibres. *Journal of Physiology*, *462*, 161–173.

Cole, G. K., Van Den Bogert, A. J., Herzog, W., & Gerritsen, K. G. M. (1996). Modelling of force production in skeletal muscle undergoing stretch. *Journal of Biomechanics*, 29(8), 1091–1104.

Colombini, B., Nocella, M., Benelli, G., Cecchi, G., & Bagni, M. A. (2007). Crossbridge properties during force enhancement by slow stretching in single intact frog muscle fibres. The Journal of Physiology, 585(Pt 2), 607–615.

Colomo, F., Lombardi, V., Menchetti, G., & Piazzesi, G. (1989). The recovery of isometric tension after steady lengthening in tetanized fibres isolated from frog muscle. *Journal of Physiology,* 415, 130P.

De Ruiter, C. J., Didden, W. J., Jones, D. A., & Haan, a D. (2000). The force-velocity relationship of human adductor pollicis muscle during stretch and the effects of fatigue. *The Journal of Physiology*, *526 Pt 3*, 671–81.

Degens, H., Bosutti, A., Gilliver, S., Slevin, M., van Heijst, A., Wust, R. (2010). Changes in contractile properties of skinned single rat soleus and diaphragm fibres after chronic hypoxia. *European Journal of Physiology,* 460, 863-873.

Edman, K. a, Elzinga, G., & Noble, M. I. (1982). Residual force enhancement after stretch of contracting frog single muscle fibers. *The Journal of General Physiology*, *80*(5), 769–784.

Frontera, W. R., & Larsson, L. (1997). Contractile studies of single human skeletal muscle fibers: A comparison of different muscles, permeabilization procedures, and storage techniques. *Muscle and Nerve*, *20*(8), 948–952.

Fusi, L., Reconditi, M., Linari, M., Brunello, E., Elangovan, R., Lombardi, V., & Piazzesi, G. (2010). The mechanism of the resistance to stretch of isometrically contracting single muscle fibres. The Journal of Physiology, 588(Pt 3), 495–510.

Getz, E. B., Cooke, R., & Lehman, S. L. (1998). Phase transition in force during ramp stretches of skeletal muscle. *Biophysical Journal*, *75*(6), 2971–2983.

Gilliver, S. F., Degens, H., Rittweger, J., Sargeant, a J., & Jones, D. a. (2009). Variation in the determinants of power of chemically skinned human muscle fibres. *Experimental Physiology*, *94*(10), 1070–8.

Gilliver, S. F., Jones, D. a, Rittweger, J., & Degens, H. (2010). Effects of oxidation on the power of chemically skinned rat soleus fibres. *Journal of Musculoskeletal & Neuronal Interactions*, *10*(4), 267–73.

Gilliver, S. F., Degens, H., Rittweger, J., & Jones, D. A. (2010). Effects of submaximal activation on the determinants of power of chemically skinned rat soleus fibres. *Experimental Physiology*, *96*(2), 171–8.

Herzog, W. (2014). The role of titin in eccentric muscle contraction. *The Journal of Experimental Biology*, *217*(Pt 16), 2825–33. doi:10.1242/jeb.099127

Katz, B. (1939). The relation between force and speed in muscular contraction. *Journal of Physiology*, *96*, 45–64.

Koppes, R. A., Herzog, W., & Corr, D. T. (2013). Force enhancement in lengthening contractions of cat soleus muscle in situ: transient and steady-state aspects. *Physiological Reports*, *1*(2), e00017.

Krylow, A. M., & Sandercock, T. G. (1997). Dynamic force responses of muscle involving eccentric contraction. Journal of Biomechanics, 30(1), 27–33.

Larsson, L., & Moss, R. L. (1993). Maximum velocity of shortening in relation to myosin isoform composition in single fibres from human skeletal muscles. *Journal of Physiology*, *472*, 595–614.

Linari, M., Bottinelli, R., Pellegrino, M. A., Reconditi, M., Reggiani, C., & Lombardi, V. (2003). The mechanism of the force response to stretch in human skinned muscle fibres with different myosin isoforms. *The Journal of Physiology*, *554*(Pt 2), 335–52.

Linari, M., Lucii, L., Reconditi, M., Casoni, M. E. V., Amenitsch, H., Bernstorff, S., Lombardi, V. (2000). A combined mechanical and X-ray diffraction study of stretch potentiation in single frog muscle fibres. *Journal of Physiology*, 526, 589-596.

Lombardi, V., & Piazzesi, G. (1990). The contractile response during steady lengthening of stimulated frog muscle fibres. Journal of Physiology, 431, 141–171.

Mantovani, M., Heglund, N. C., & Cavagna, G. a. (2001). Energy transfer during stress relaxation of contracting frog muscle fibres. *The Journal of Physiology*, *537*(Pt 3), 923–39.

Noble, M. I. (1992). Enhancement of mechanical performance of striated muscle by stretch during contraction. *Experimental Physiology*, *77*(4), 539–552.

Phillips, S. K., Bruce, S. A., & Woledge, R. C. (1991). In mice, muscle weakness due to age is absent during stretching. *Journal of Physiology*, *437*, 63–70.

Pinniger, G. J., Ranatunga, K. W., & Offer, G. W. (2006). Crossbridge and non-crossbridge contributions to tension in lengthening rat muscle: force-induced reversal of the power stroke. *The Journal of Physiology*, *573*(Pt 3), 627–43.

Rassier, D. E., Herzog, W., Wakeling, J., & Syme, D. A. (2003). Stretch-induced, steady-state force enhancement in single skeletal muscle fibers exceeds the isometric force at optimum fiber length. *Journal of Biomechanics*, *36*(9), 1309–1316.

Stienen, G. J., Versteeg, P. G., Papp, Z., & Elzinga, G. (1992). Mechanical properties of skinned rabbit psoas and soleus muscle fibres during lengthening : effects of phosphate and Ca^{2+}. *Journal of Physiology*, *451*, 503–523.

Sugi, B. Y. H., & Tsuchiya, T. (1981). Enhancement of mechanical performance in frog muscle fibres after quick increases in load. *Journal of Physiology*, 239–252.

Sugi, H. (1972). Tension changes during and after stretch in frog muscle fibres. *Journal of Physiology*, 237–253.

CHAPTER 3

Effects of inorganic phosphate on the force response of skinned soleus mouse muscle fibres to a ramp stretch

3.1 Abstract

The force exerted by skeletal muscles is the result of the interaction of myosin and actin filaments, which requires the hydrolysis of ATP in ADP and inorganic phosphate (Pi). It has been shown that addition of Pi reduces isometric force but not the force when a muscle is stretched. Analysis of stress relaxation may provide information about changes in cross bridge kinetics that underlie this behaviour. Single fibres from four female 10 months-old mouse soleus were used in this study. They were subjected to isometric and shortening contractions in order to determine the isometric force (*Fo*), cross-sectional area (CSA), maximum velocity of shortening (Vmax), specific force (*Po*) and curvature of the force-velocity curve (a/Po). Then, they were subjected to stretches at 0.0625 (fl/s), 025 (fl/s) and 1 (fl/s) in activating solution with either no added Pi, or the addition of 5 or 15 (mM) Pi. *Fo* and *Po* were reduced with increasing [Pi], while Vmax was not affected by the presence of phosphate. During the eccentric contractions, the peak force at the end of the ramp was decreased in presence of phosphate. However, when normalized to the preceding *Fo* the ratio *Fpeak/Fo* increased with increasing [Pi] up to four-fold at 15 (mM) Pi. Stress relaxation was fitted to a double exponential by keeping the variables kd1 and kd2 constant for a given speed of stretch in order to determine how the contributions A1 and A2 would vary with added Pu. With increasing Pi, there was an increase in A1 and consequent decrease in A2 so that the SR was slower the higher the [Pi]. As discussed in the previous chapter, A1 has been associated to a low-force producing state and A2 to a high-force producing state. The shift in the proportion of A1 suggests a larger proportion of cross bridges in a low force state when phosphate is added. Finally, the force enhancement was not affected by different [Pi].

3.2 Introduction

The study of cross bridge kinetics while the muscle is actively stretched has received less attention than the kinetics of shortening, even though eccentric or lengthening contractions of the muscle and the force produced during these contractions are as fundamental to muscle function as are those of shortening contractions. At the end of a ramp stretch, the force sustained by the active muscle starts to decrease. It has been shown that this decline in force, called ‘stress relaxation’, consists of both a slow and a fast phase. The proportions of the fast phase have been reported to increase with increasing lengthening velocity (Cavagna, 1993; Chapter 2).

The production of force is the result of the cyclic interaction between myosin and actin with hydrolysis of ATP releasing ADP and inorganic phosphate (Pi). A Pi concentration

of 30 mM in skinned single muscle fibres has been shown to depress the isometric force, *Fo,* to ~30% of the control value (Kentish, 1986; Iwamoto, 1995). The cross bridge ATPase cycle has been extensively studied and it is generally thought that force production occurs before the Pi release in the reaction pathway (Dantzig et al., 1992, Tesi et al., 2000, Caremani et al., 2008) since even high levels of Pi do not completely abolish force.

There are two main theories as to how additional Pi reduces force. One view is that the cross bridge intermediate states before the release of Pi (see section 1.3) generate less force than those following the release of Pi. In this situation, force would be reduced to a greater extent than fibre stiffness, assuming that all attached cross bridges either in a high- or low-force state contribute equally to muscle stiffness, and we might expect the force sustained during a ramp stretch relative to isometric force to be greater in the presence than absence of Pi (Stienen et al. 1992). The alternative view of the response to stretch, based on careful measurements of stiffness which differentiate between the contribution of the cross bridges and that of the thick and thin filaments, is that the additional force is due to attachment of the second myosin head. In these circumstances it is expected that there is no difference between the changes in stiffness of the myosin cross bridges and force during stretch (Caremani et al., 2008). In contrast to the effects on lengthening contractions, previous studies have shown that Pi concentrations between 12 mM and 20 mM did not affect the maximum shortening velocity, (Cooke & Pate, 1985; Osterman & Arner, 1995). The addition of 15 mM Pi has been shown to increase the eccentric force as a proportion of the isometric force at different velocities of lengthening (Stienen et al., 1992). However, that study concentrated on the force development and peak force and did not examine the subsequent stress relaxation phase or comment on the residual force enhancement. The kinetics of stress relaxation may provide some insight into the nature of the cross bridge states that exist during the ramp stretch, as discussed in chapter 2. The addition of Pi may give additional information on the contribution of the low and high force states of cross-bridges to the peak forces during stretch and cross bridge kinetics during stress relaxation. Consequently, the objective of the study described in this chapter was to observe the effects of different concentrations of inorganic phosphate on the stress relaxation and force enhancement after a ramp stretch. More specifically, to test the proposition that with increasing [Pi] there is a change in the proportions A1 and A2 and that these proportions could be related to the AM'.ADP.Pi and AM'.ADP states, respectively, before and after the release of Pi in the cross bridge ATPase cycle.

3.3 Materials and methods

3.3.1 Mouse muscle

The muscle samples were obtained from two female 10-month-old gtf2ird mice and two female 10-month-old wild type mice, as explained in Chapter 2.

3.3.2 Solutions

The solutions were as described in Chapter 2 (Degens et al., 1998; Degens & Larsson, 2007). Activating solutions containing 5 (mM) or 15 (mM) of inorganic phosphate (P_i) were made up by adding KH_2PO_4 and reducing the KCl to maintain the ionic strength.

3.3.3 Preparation of single fibres

The procedures for preparing single fibres have been described in Chapter 2 and elsewhere (Larsson & Moss, 1993; Degens & Larsson, 2007; Gilliver et al., 2010).

3.3.4 Contractile properties

The fibre was transferred from the relaxing solution to the activating solution (pCa 4.5) with either no added Pi or to 5 (mM) or 15 (mM) added Pi in random order to prevent any recursive effect on the measurements. Once a plateau of isometric force (*Fo*) was reached, the fibre was subjected to four sequences of four isotonic shortening steps, as described before (Degens et al., 2010; Gilliver et al., 2010). In each sequence, the muscle force was maintained at four predetermined different percentages of the maximal isometric force for 150 (ms). The predetermined percentages of *Fo* were different in each sequence. Between sequences, the fibre was stretched back to its original length while still in activating solution. These shortening steps (Figure 3.1) provided 16 data points that were used to fit to the Hill equation, *(P+a)(V+b)=(Po+a)b*.

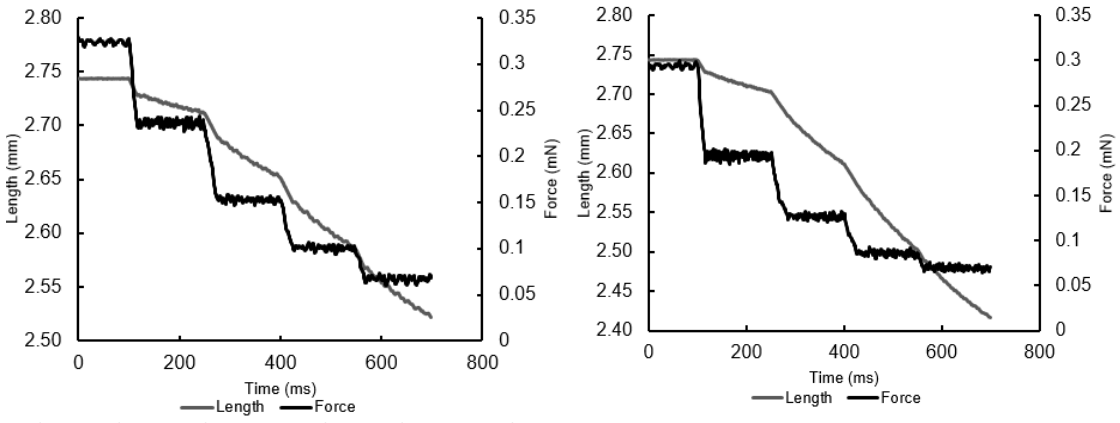

Figure 3.1*: Curves of force and length vs time for the same fibre in activating solution (left) and with addition of 5mM Pi (right). The figure shows a sequence of four isotonic shortening steps.*

Once the four sequences of four isotonic shortening steps finished, the fibres were subjected to isovelocity stretches of 5% *Lo* at 0.0625 (fl/s), 0.25 (fl/s) and 1 (fl/s), in that order. After the ramp stretch, the fibre was held at the new length for at least 1 second and then shortened back to its initial length. This was repeated in 0 (no added), 5 and 15 mM Pi. An example of the force responses to different stretch velocities is shown in Figure 3.2.

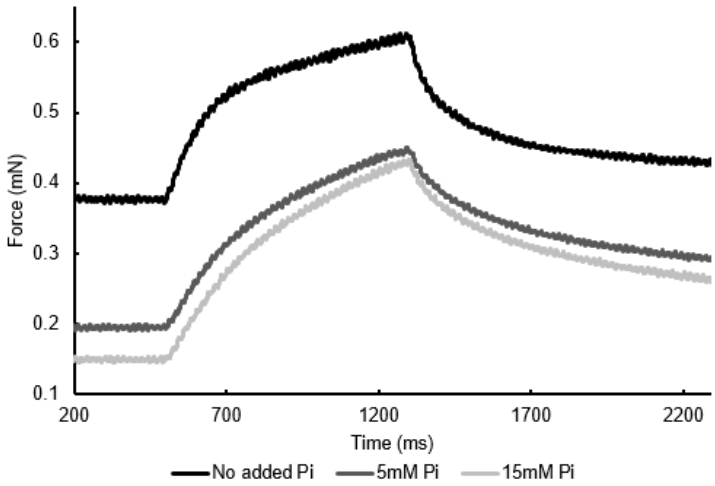

Figure 3.2: T*races of force vs time for a 5% Lo lengthening ramp and hold at 0.0625 (fl/s). The curves belong to the same fibre stretched in three different concentrations of Pi.*

3.3.5 Data analysis and statistics

The force and length data from the shortening steps were analysed by fitting least squares linear regressions to the last 100 (ms) of each step, generating a value of the shortening velocity for a given force. These data points were then fitted to the Hill equation using a non-linear least squares regression (Solver, Microsoft Excel) to obtain the force velocity curve by getting the best fit of the Hill constant values *a* and *b*. The maximum velocity of shortening was expressed as fibre length per second *(fl/s)* while the force as force per cross-sectional area, *Po,* (N/cm^2). Data were rejected if the isometric force dropped more than 10% during the course of the experiments, the sarcomere length had changed by more than 0.1 µm or had become heterogeneous (defined by observation after contraction) and/or if $R^2 < 0.96$ when data were fitted to the Hill equation. The force data from the end of the stretch, corresponding to the stress relaxation, was fitted to a double exponential function using non-linear least squares regression (Solver, Microsoft Excel),

$$F = A1*e^{-kd1*t}+A2*e^{-kd2*t} + C \quad (1)$$

Thus, two rate constants of stress relaxation, kd1 and kd2, were obtained at each velocity of stretch together with values for A1 and A2. C is the residual force at some theoretical infinite time after the end of stress relaxation and the sum of the components A1, A2 and C gives the peak force *(Fpeak)* at the end of stretch and the beginning of stress relaxation. The difference between the starting isometric force and C constitutes the residual force enhancement (*FE*). Values in the results section are presented as mean and standard error (SE). The means were evaluated by a repeated-measures ANOVA, with as within factors stretch velocity (3 levels) and [Pi] (3 levels). If significant main effects were found, Bonferroni-corrected post-hoc tests were performed to locate the differences between groups. Effects and differences were considered significant at $p<0.05$.

3.4 Results

3.4.1 Shortening contractions

The main results of the concentric contractions in different concentrations of inorganic phosphate are shown in Table 3.1. The maximum isometric force and specific force decreased with increasing Pi ($p<0.05$) (Table 1 and Figure 3.3). The number of fibres rejected under rejection criteria was 3.

	Fo (mN)	**Vmax (Fl/s)**	**a/Po**
0 mM Pi	0.32±0.03	0.50±0.04	0.23±0.01
5 mM Pi	0.18±0.02[a]	0.46±0.03	0.28±0.02
15 mM Pi	0.13±0.01[a,b]	0.39±0.03	0.26±0.02

Table 3.1*: means and SE of the maximum isometric force (Fo), maximum velocity of shortening (Vmax) and curvature of the force-velocity relationship (a/Po). a: significantly different from no added Pi. b: significantly different from 5mm [Pi]. Number of single fibres tested, n=36.*

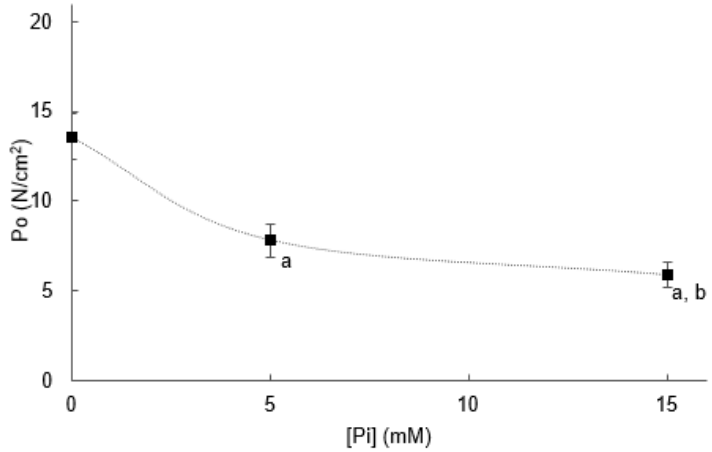

Figure 3.3: *Means and SE of the specific force at three different [Pi]. a: significantly different from no added Pi. b: significantly different from 5mm [Pi]. (Number of fibres tested n=36)*

3.4.2 Eccentric contractions

The fibres were subjected to isovelocity ramp stretches in three different concentrations of Pi at three different lengthening speeds. The peak force (*Fpeak*), the rate of the stress relaxation and the force enhancement (*FE*) after the stretch were studied.

3.4.2.1 Peak force

The force at the end of the stretch, or *Fpeak***,** was determined for three different solutions: activating solution (4.5 pCa) with no addition of phosphate, activating solution with 5 (mM) Pi and activating solution with 15 (mM) Pi and are shown in Figure 3.4.

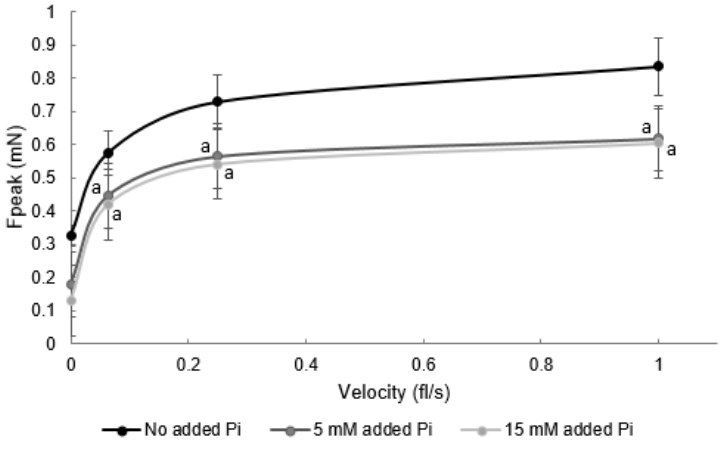

Figure 3.4: *Means and SE of the absolute peak force (Fpeak) values for different [Pi] at three speeds of stretch. a: significantly different from no added Pi. (Fibres tested, n=36)*

The *Fpeak* normalized to the isometric force, *Fpeak/Fo*, was increased with increasing phosphate concentration (Figure 3.5; $p<0.05$).

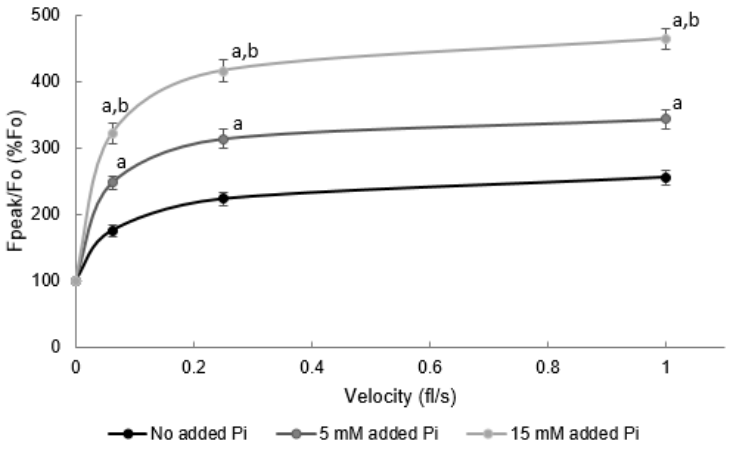

Figure 3.5: *Means and SE of the peak force (Fpeak) as percentage of the isometric force before the stretch in three different [Pi] at three different velocities of stretch. a: significantly different from no [Pi]. b: significantly different from 5 mM [Pi]. (Fibres tested, n=36)*

There were significant differences in *Fo* between the three different [Pi] (p<0.05; Table 3.1). It is also evident that the increase in force above *Fo* (*Fpeak-Fo*) was relatively constant in the different activating solutions and consequently, the increase in *Fpeak/Fo* observed with increasing concentration of inorganic phosphate was a result primarily of the decrease in *Fo* rather than an increase in *Fpeak*.

3.4.2.2 Stress relaxation

At the end of the isovelocity ramp stretch, force decays to a value that is slightly higher than the isometric force before the stretch (force enhancement). This decay, or 'stress relaxation', was fitted to a double exponential as this provided a better fit than to a single exponential. In Figures 3.6a, b and c, stress relaxation at each speed of stretch is shown for 0 (mM) Pi, 5 (mM) Pi and 15 (mM) Pi, as an average of all the fibres tested. The force is normalized to the *Fpeak-Fo* value of each phosphate concentration.

The stress relaxation curves showed a slower relaxation with increasing phosphate concentration. As can be seen in the curves of Figure 3.7a, b and c, this was true for each of the lengthening speeds.

To quantify the changes in shape of the stress relaxation curves, the data were fitted to a double exponential function. Figure 3.7 shows examples of real data and curve fitting of the stress relaxation of one single fibre for each lengthening speed. The data were fitted to the double exponential function in two ways. In Figures 3.7a, c and e data were fitted allowing changes in all variables, kd1, kd2, A1, A2 and C. Excellent fits were obtained and the values for the variables are given in Table 3.2. In the second case, shown in Figures 3.7b, d and f, the rate constants kd1 and kd2 were kept the same as those determined in the absence of Pi and only A1, A2 and C were allowed to vary

when fitting the data obtained with 5 and 15 (mM) added Pi. This also gave excellent fits to the data (r^2>0.96) and the proportions of A1 and A2 making up the difference between *Fpeak* and C are given in Figure 3.8 for different speeds of stretch and with and without added Pi.

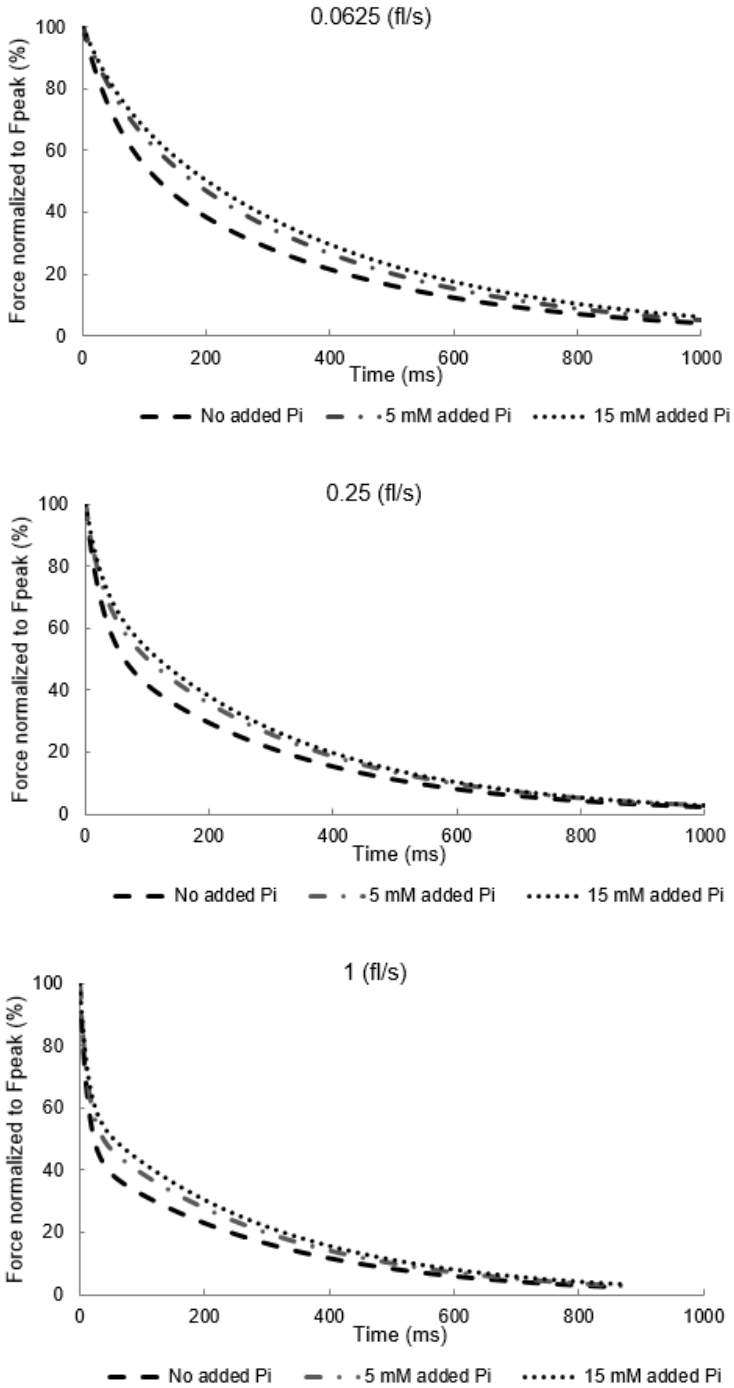

***Figure 3.6**: Stress relaxation as average of all fibres in different [Pi] at three speeds of stretch. The stress relaxation is normalized to % of the increase above Fo. (Fibres tested, n=36)*

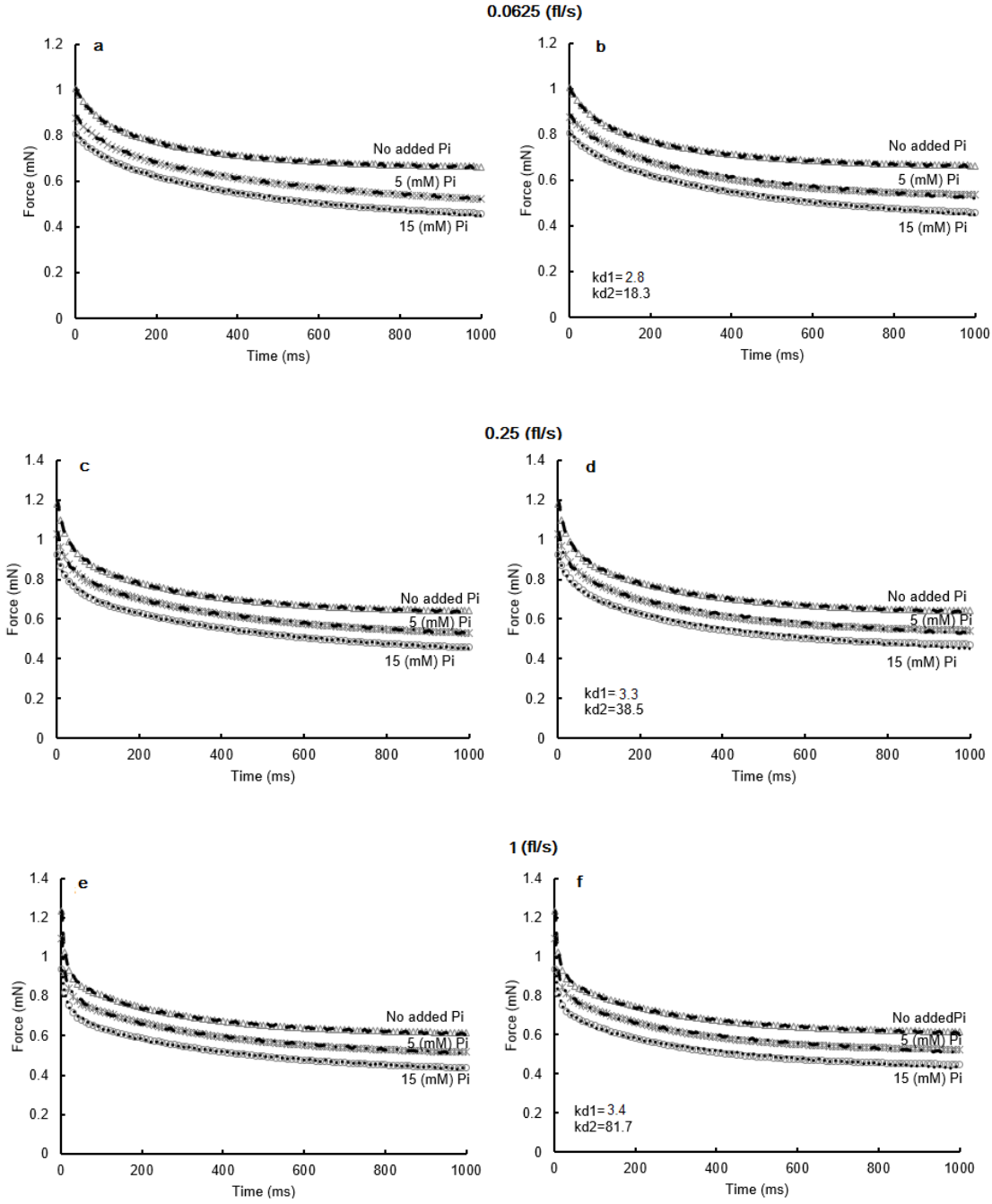

Figure 3.7: *Real data (black dashed lines) and curve fitting (grey symbols) stress relaxation. On the left column, all variables were allowed to vary for different [Pi] and stretch velocities. On the right column, kd1 and kd2 were kept constant by software for all [Pi]. (Fibres tested, n=36)*

0.0625 (fl/s)	**Kd1 (s^{-1})**	**Kd2 (s^{-1})**	**A1 (%)**	**A2 (%)**	**C (mN)**
No added Pi	3.5±0.9	21.9±3.3	66	34	0.38±0.1
5 (mM) added Pi	1.9±0.6	15.5±3.1	71	29	0.26±0.07
15 (mM) added Pi	1.6±0.5	13.2±3	84	16	0.21±0.06
0.25 (fl/s)					
No added Pi	3.5±1.5	36.9±4.5	56	44	0.39±0.12
5 (mM) added Pi	2.5±1.5	34.7±4.2	62	38	0.26±0.09
15 (mM) added Pi	2.1±1.2	33.8±4.1	65	35	0.21±0.07
1 (fl/s)					
No added Pi	3.7±2	89.4±6.4	46	54	0.39±0.13
5 (mM) added Pi	2.9±1.8	79.7±6.1	50	50	0.26±0.1
15 (mM) added Pi	2.6±1.6	63.9±5.3	55	45	0.21±0.1

Table 3.2: *Means and SE of the five stress relaxation variables, at three different velocities of stretch. These have been calculated allowing all variables to vary as explained in previous paragraph and belong to the curves showed in Figures 3.8a, c and e. (Fibres tested, n=36)*

As the speed of stretch increased the proportion of the faster A2 component increased whereas the effect of adding Pi was to increase the proportion of the slow A1 component.

3.4.2.3 Force enhancement

FE was here calculated, in absolute terms, as the difference between the force value C and the isometric force *Fo*, immediately before the beginning of the stretch. FE amounted to approximately 10% *Fo* of the fibre activated in the absence of added Pi and there was a tendency for FE to be slightly larger in the presence of Pi although this was not significant. There was no effect of stretch velocity on the absolute values of FE either in the presence or absence of added Pi.

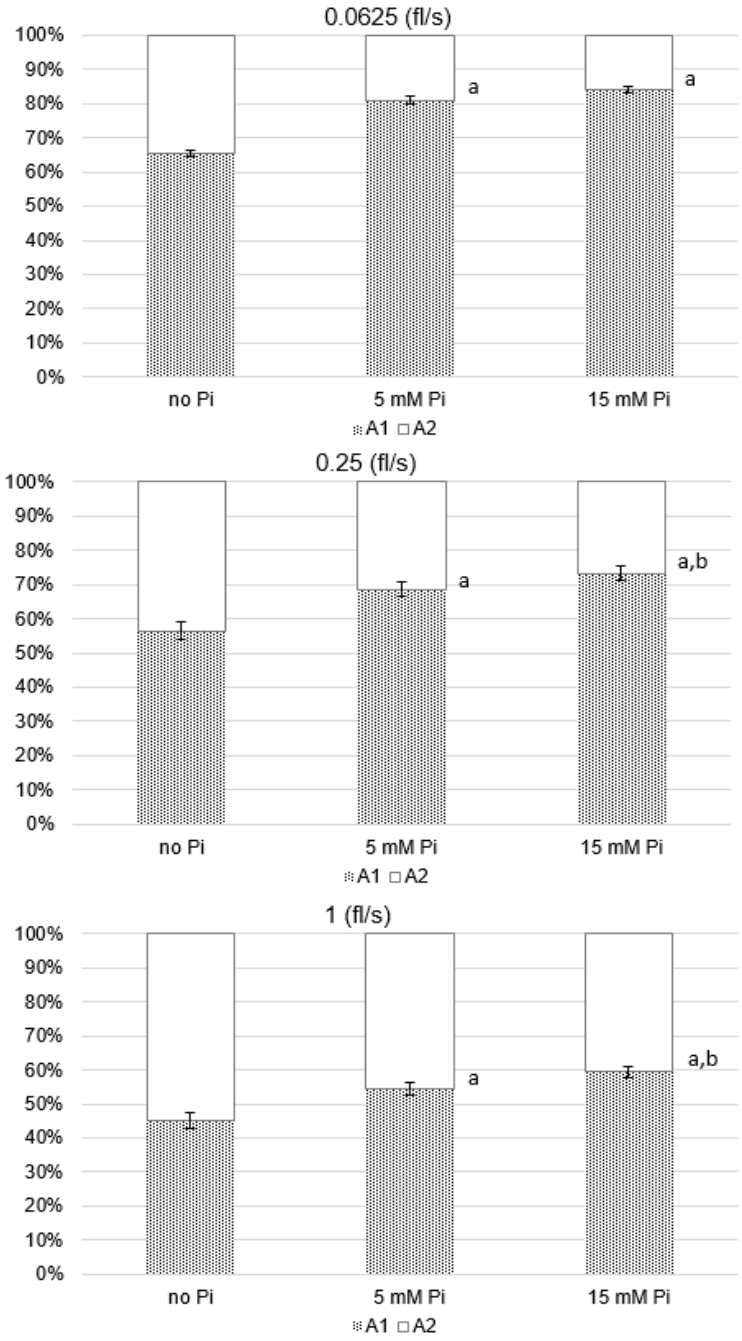

Figure 3.8: *means and SE of the proportions of the slow component (A1) and the fast component (A2) of the stress relaxation for different [Pi] at different stretch velocities. Values of A1 and A2 were determined using values of kd1 and kd2 given in Figures 3.8b, d and f. a: significantly different from no Pi. b: significantly different from 5 mM [Pi]. (Fibres tested, n=36)*

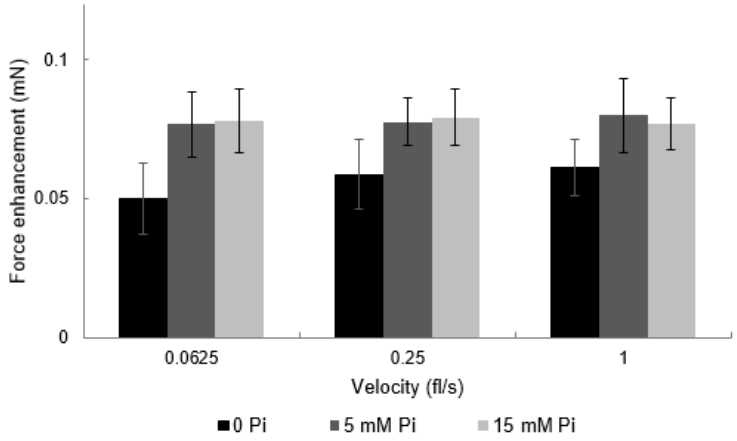

Figure 3.9: *Absolute mean values and SE of force enhancement at the end of the stress relaxation for different phosphate concentrations at three stretching speeds. (Fibres tested, n=36)*

3.5 Discussion

The effects of different concentrations of inorganic phosphate on shortening and, more specifically, lengthening contractions have been investigated in the present study. The isometric force was reduced with increasing [Pi], while the maximum velocity of shortening was not affected by different [Pi] as reported previously (Caremani et al., 2008; Widrick 2002; Osterman & Arner, 1995). The specific force, *Po*, was reduced by 43% in 5 mM added Pi and by 57% in 15 mM Pi. These reductions are similar to the percentages reported by Tesi et al. (2000), although even greater reductions have been reported in 30 mM Pi (Debold et al., 2006). Whether the reduction in force is due to an increase in the proportion of low force cross bridges (Stienen et al., 1992) or a reduction in the total number of cross bridges (Caremani et al., 2008) remains to be determined. During the eccentric contractions in the absence of added Pi, the activated fibres developed a peak force of more than double *Fo* when stretched at the highest velocity. As the isometric force was decreased with increasing [Pi], the value of *Fpeak/Fo* was increased for increasing [Pi] for all the three stretching speeds assessed in this study so that in the presence of 15 (mM) added Pi, *Fpeak* was approximately 400% *Fo*. These results are consistent with a study on rabbit psoas fibres by Iwamoto, in 1995.

At the end of the lengthening ramp force decayed in a double exponential fashion, as shown in Figure 3.6. The slow constant kd1 was independent of the velocity of stretch while the fast component, kd2, increased as the velocity of stretch increased (see values in Figures 3.7b, d and f and Table 3.2). The range of values of kd1 and kd2 observed in the present study are similar to previous observations (Colomo et al., 1989;

Cavagna, 1993). These authors reported the range of kd2 to be between 50 s^{-1} and 250 s^{-1}, while the range of the slow component, kd1, was between 2.5 s^{-1} and 5 s^{-1}. Pinniger et al. (2006) reported values of kd1 of ~5 s^{-1} and a range of kd2 from 25 s^{-1} to ~85 s^{-1} for rat fibres stretched at velocities, from 0.1 (fl/s) to 1 (fl/s), which are lengthening speeds similar to those used in this study. There is no unique solution to fitting a double exponential function with five variables, so all that can be shown, at best, is that certain combinations of variables result in a good fit with the experimental data. The aim of this study was to test the proposition that with increasing [Pi] there is an increase in the proportion of low force cross bridges (presumably AM'.ADP.Pi) and that the low force cross bridges dissociate slowly during stress relaxation and constitute the A1 population while high force cross bridges (presumably AM'.ADP) detach rapidly and constitute the A2 population. See Figure 3.10 where the A1 and A2 proportions are associated with a low- and high-force states, respectively.

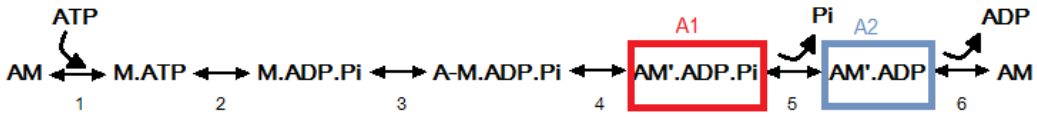

Figure 3.10: *Cross bridge ATPase cycle showing the association between proportion of cross bridges A1 and A2 with two different cross bridge force states.*

Consequently, the data were analysed first by obtaining the best fit to data obtained in the absence of added Pi by allowing all five variables to change (Figures 3.7a, c and e). Next, the data obtained in the presence of Pi was fitted using the same values of kd1 and kd2 as in the absence of added Pi, and allowing only values of A1 and A2 to change. The fit obtained in the latter way was very good (Figures 3.7b, d and f) and the data are therefore consistent with the notion that A1 and A2 represent populations of cross bridges in low and high force states and, as suggested by Stienen et al. (1992), the proportions are shifted towards the low force (A1) state by the presence of added Pi. The weakness of this argument is that kd1 does not vary significantly with velocity of stretch as would be expected for strain dependent detachment of cross bridges and there remains the possibility that the slow component may not be a function of cross bridges but some series compliance, as suggested by Cavagna (1993). Cavagna came to this conclusion based on different responses of the fast and slow components of stress relaxation to changes in temperature and it would be useful to know how kd1 and kd2 respond to changes in temperature. Caremani et al. (2008) suggested that there is no low-force cross bridge state and that the additional force seen during stretch

is due to an increase in the binding of the second myosin head. It is, however, difficult to see how this could account for the very high increases of force obtained during stretch in the presence of Pi. If the additional force during stretch is due to the attachment of a second myosin head then the increase in force above isometric will be a maximum of 100%, which is the case in the absence of Pi. However, in the presence of Pi the force can increase by 200% (Fig 3.5) which is not consistent with the double head theory. The other possibility is that the additional force during stretch is, at least in part, due to stretching titin as suggested by Herzog (2014). However, if FE represents the action of titin, then titin is unlikely to play any significant role in the different stretch responses seen during different stretch velocities and Pi concentrations since FE was largely independent of differences in both velocity and [Pi] (Figure 3.9).

Conclusion

In the absence of phosphate, there is a proportion of slow and fast components of the stress relaxation. When Pi is present, the decay becomes slower and the contribution of the slow component, A1, is increased with increasing phosphate. Therefore, it might be that cross bridges (A1 and A2) populations are reflecting two different force-producing states. Changes in the proportions of these cross bridges in response to Pi could contribute to Pi-induced decrease in isometric force, yet maintained peak force during a stretch. This is consistent with chapter 2 that considers the phases of stress relaxation as two separated cross bridge populations.

References

Bottinelli, R., Canepari, M., Pellegrino, M. A., & Reggiani, C. (1996). Force-velocity properties of human skeletal muscle fibres: myosin heavy chain isoform and temperature dependence. *The Journal of Physiology*, *495 Pt 2*, 573–86.

Caremani, M., Dantzig, J., Goldman, Y. E., Lombardi, V., & Linari, M. (2008). Effect of inorganic phosphate on the force and number of myosin cross-bridges during the isometric contraction of permeabilized muscle fibers from rabbit psoas. *Biophysical Journal*, *95*(12), 5798–808.

Cavagna, G. (1993). Effect of temperature and velocity of streching on stress relaxation of contracting frog muscle fibres. *Journal of Physiology*, *462*, 161–173.

Colomo, F., Lombardi, V., Menchetti, G., & Piazzesi, G. (1989). The recovery of isometric tension after steady lengthening in tetanized fibres isolated from frog muscle. *Journal of Physiology*, *415*, 130P.

Cooke, R., & Pate, E. (1985). The effects of ADP and phosphate on the contraction of muscle fibers. *Biophysical Journal*, *48*(5), 789–98. doi:10.1016/S0006-3495(85)83837-6

Dantzig, J. A., Goldman, Y. E., Millar, N. C., Latckis, J., & Homsher, E. (1992). Reversal of the cross-bridge force-generating transition by photogeneration of phosphate in rabbit psoas muscle fibres. *Journal of Physiology*, *451*, 247–278.

Debold, E. P., Romatowski, J., & Fitts, R. H. (2006). The depressive effect of Pi on the force-pCa relationship in skinned single muscle fibers is temperature dependent. *American Journal of Physiology. Cell Physiology*, *290*(4), C1041–C1050. doi:10.1152/ajpcell.00342.2005

Degens, H., Yu, F., Li, X., & Larsson, L. (1998). Effects of age and gender on shortening velocity and myosin isoforms in single rat muscle fibres. *Acta Physiologica Scandinavica*, *163*, 33–40.

Degens, H., & Larsson, L. (2007). Application of skinned single muscle fibres to determine myofilament function in ageing and disease. *Journal of Musculoskeletal & Neuronal Interactions*, *7*(1), 56–61.

Edman, K. A., Elzinga, G., & Noble, M. I. (1978). Enhancement of mechanical performance by stretch during tetanic contractions of vertebrate skeletal muscle fibres. *The Journal of Physiology*, *281*, 139–155.

Gilliver, S. F., Jones, D. A., Rittweger, J., & Degens, H. (2010). Effects of oxidation on the power of chemically skinned rat soleus fibres. *Journal of Musculoskeletal & Neuronal Interactions*, *10*(4), 267–73.

Herzog, W. (2014). The role of titin in eccentric muscle contraction. *The Journal of Experimental Biology*, *217*(Pt 16), 2825–33. http://doi.org/10.1242/jeb.099127

Iwamoto, H. (1995). Strain sensitivity and turnover rate of low force cross-bridges in contracting skeletal muscle fibers in the presence of phosphate. *Biophysical Journal*, *68*(1), 243–50. doi:10.1016/S0006-3495(95)80180-3

Kentish, J. C. (1986). The effects of inorganic phosphate and creatine on force production in skinned muscles from rat ventricule. *Journal of Physiology*, *370*, 585–604.

Larsson, L., & Moss, R. L. (1993). Maximum velocity of shortening in relation to myosin isoform composition in single fibres from human skeletal muscles. *Journal of Physiology*, *472*, 595–614.

Osterman, A. & Arner, A. (1995). Effects of inorganic phosphate on cross-bridge kinetics at different activation levels in skinned guinea-pig smooth muscle. *The Journal of Physiology*, *484*, 369–83.

Pinniger, G. J., Ranatunga, K. W., & Offer, G. W. (2006). Crossbridge and non-crossbridge contributions to tension in lengthening rat muscle: force-induced reversal of the power stroke. *The Journal of Physiology*, *573*(Pt 3), 627–43. doi:10.1113/jphysiol.2005.095448

Stienen, G. J., Versteeg, P. G., Papp, Z., & Elzinga, G. (1992). Mechanical properties of skinned rabbit psoas and soleus muscle fibres during lengthening : effects of phosphate and Ca^{2+}. *Journal of Physiology*, *451*, 503–523.

Tesi, C., Colomo, F., Nencini, S., Piroddi, N., & Poggesi, C. (2000). The effect of inorganic phosphate on force generation in single myofibrils from rabbit skeletal muscle. *Biophysical Journal*, *78*(6), 3081–3092.

Widrick, J. J. (2002). Effect of P-i on unloaded shortening velocity of slow and fast mammalian muscle fibers. *American Journal of Physiology- Cell Physiology*, *282*(4), C647–C653.

CHAPTER 4

Effects of ageing on the force response of skinned soleus mouse fibres after a ramp stretch

4.1 Abstract

Loss of skeletal muscle mass, loss of strength and slowing of movement are amongst the well-known features of old muscle and, thus, of ageing. However, the reduced strength found in old muscle of different species during isometric and shortening contractions has been reported to not decrease in such extent during eccentric contractions, but to be well maintained. Although the effects of ageing have been extensively studied on isometric and shortening actions, there is very little concerning the stress relaxation and the residual force enhancement after the decay of force. Therefore, the aim of the chapter is to determine how the stress relaxation and the residual force after the stretch are affected by ageing. Four different age-groups of soleus single fibres of mice were studied, 3, 10, 18 and 32-month-old and subjected to isometric contractions and shortening isotonic steps to determine the force-velocity relationship. Afterwards, the fibres were stretched at three different speeds and the stress relaxation fitted to a double exponential using the rate constants kd1 and kd2, obtained from the 10-month-old fibres, to look for changes in the proportions A1 and A2 of the different age groups. Between the 3, 10 and 18-month-old fibres the CSA and isometric strength increased with maturation of the muscle, with no significant changes for the specific strength between these three groups. On the other hand, the oldest muscle showed reductions in both isometric and specific force. The maximum velocity of shortening was also significantly reduced for the oldest fibres. In contrast to reported evidence, the force at the end of the stretch did not appear to be maintained in the old muscle, and was even slightly, but not significantly reduced when compared to the three younger groups. Stress relaxation was found to be faster in the oldest fibres with a larger proportion of A2. If A2 is associated with a high force state it would suggest that there are changes in the kinetics determining the equilibria between the various cross bridge states favouring force generation state (A2) in older muscles which might be reversed by the addition of Pi.

4.2 Introduction

Sarcopenia, the age-associated loss of skeletal muscle mass, is a major factor in the decline of strength with ageing (Chan & Head 2010; Goodpaster et al., 2006) but there are also changes in the quality of the muscle such as reductions in the specific tension and contractile speed, although this is less well documented (Thompson & Brown 1999; Degens et al., 1998; Larsson et al., 1997a). In contrast to investigations involving isometric and shortening contractions, there is very little published literature concerning the effects of ageing on lengthening contractions although the published evidence

suggests that the force sustained during stretch is better maintained with age than is the isometric or shortening force. These data come from observations of human muscle (Hortobágyi et al., 1995; Ochala et al. 2006) and isolated intact mouse fibres (Brooks & Faulkner, 1994b). The work of Phillips et al. (1991) concentrated on the differences between young and old muscle preparations in the peak force after stretch and found that this was relatively well maintained in comparison with isometric force. The authors did not, however, report any data concerning stress relaxation or FE. As described in the previous Chapters, analysis of stress relaxation may give some insight into the proportions of cross bridges attached in different intermediate states, so that, for instance in the presence of added Pi, the greater proportion of the A1 state may account for the reduced isometric tension yet sustain a normal force during stretch. The purpose of the work described in this chapter was, therefore, to extend this study to stress relaxation which may give some insight into differences in cross bridge kinetics with ageing. It was hypothesised that a greater force during stretch relative to isometric in older muscle fibres would be associated with a greater proportion of cross bridges in the A1 state.

4.3 Materials and methods

4.3.1 Muscle samples

Soleus muscles were obtained from three 3-month-old (young male adult) C57BL6, three 10-month-old (female adult) gtf2ird and two 10-month-old (female adult) wild type, five 18-month-old (middle-age male adult) gtf2ird and two 32-month-old (male old) C57BL6 mice. The animals were humanely killed using approved schedule 1 methods (cervical dislocation) for other purposes in a research study approved by the local Animal Ethics Research Committee of the University of Manchester. This is in accord with the generally accepted guideline of reducing animal numbers to a minimum in biomedical research. The soleus muscle was excised from each animal and immersed in glycerol/relax solution (see Solutions below) at 4°C for 24 hrs. It was then treated with increasing concentrations of sucrose in relax solution (Larsson et al., 1997b; Degens et al., 2010), which acts as an effective cryoprotectant, preventing damage of the contractile function of fibres. After sucrose-treatment, the muscles were frozen in liquid nitrogen and stored at -80°C for later use.

4.3.2 Solutions

The composition of the solutions have been described previously (Larsson and Moss, 1993; Gilliver et al., 2009; Degens et al., 2010). The relaxing solution contained (mM):

MgATP, 4.5; free Mg^{2+}, 1; imidazole, 10; EGTA, 2 and KCl, 100 and the pH was adjusted to 7.0 using KOH. The Glycerol/relax was the same as relaxing solution containing 50% (*v/v*) glycerol. The pCa (-log[free Ca^{2+}]) of the activating solution was 4.5 and contained: MgATP, 5.3; free Mg^{2+}, 1; imidazole, 20; EGTA, 7; creatine phosphate, 19.6; KCl, 64 with pH 7.0.

4.3.3 Preparation of single fibres

The preparation of single fibres to determine their contractile properties have been described previously (Degens et al., 2010; Gilliver et al., 2010; 2011, and in previous chapters). Briefly, the muscle sample was taken from the -80°C storage, thawed and treated with decreasing concentrations of sucrose and stored in glycerol/relax at -20°C for use within a month. At the day of use a small bundle was cut from the muscle and immersed in relaxing solution containing 1% Triton X-100 for 20 minutes to permeabilise the membranes and sarcoplasmic reticulum, while the rest of the sample was kept at -20°C for later use. Once the bundle was permeabilised, fibres were teased from it, mounted in a permeabilised-fibre test system (400 Aurora Scientific Inc. Ontario, Canada) and tied with nylon thread to insect pins attached to the force transducer (Aurora, 403) at one end and the lever arm (Aurora, 312C) at the other end. The sarcomere length (*sl*) was set at 2.6 µm and checked along the length of the fibre. Fibre length (*lo*) was then determined and checked at regular intervals thereafter. These procedures were carried out with the fibre in relaxing solution. Fibre diameter was measured at three places along the length of the fibre while submerged in relaxing solution and the cross-sectional area calculated assuming a circular circumference of the fibre. The fibres varied in length between 1.6 and 3.1 mm, measured to the nearest 0.01 mm. All experiments were carried out at 15°C.

4.3.4 Concentric contractions

To maximally activate the fibres they were transferred from the relax solution to the activating solution (4.5 pCa). When isometric force (*Fo*) had reached a plateau, the fibre was subjected to four sequences of four isotonic shortening steps (Degens et al., 2010; Gilliver et al., 2010, 2011; Bottinelli et al., 1996). The fibre was stretched back to its original length after each sequence while in activating solution. This sequence was repeated four times at different percentages of isometric force. This resulted in 16 data points for each fibre that were fitted to the Hill equation $(P+a)(V+b)=(Po+a)b$. Using a non-linear least squares regression (Solver, Microsoft Excel) to obtain the best fit values for the Hill constants *a* and *b*, and therefore, the force-velocity relationship. The maximum velocity of shortening was obtained as fibre length per second *(Fl/s)* while the force was expressed as force per cross-sectional area (N/cm^2).

4.3.5 Eccentric contractions

After the four sequences of isotonic shortening steps, the fibre was returned to relaxing solution. If *Fo* had not decreased by more than 10% and sarcomere length not more than 0.1 µm, the fibres were transferred again to the activating solution and after force reached a plateau, they were subjected to isovelocity stretches of 5% of *Lo* at three different velocities: 0.0625 (fl/s), 0.25 (fl/s) and 1 (fl/s). Between each stretch, the fibre was held at the new length for 1 second, then shortened back to *Lo* and once the three stretches were completed, transferred back to the relaxing solution.

4.3.6 Statistics

Data are presented as mean ± standard error (SE). The differences between age-groups were statistically different when the value of *p,* determined by a repeated measurements ANOVA test, was below 0.05. As data presented here are clustered in four groups, a *post hoc* test was needed to determine between which age groups differences were significant. For this purpose, a Bonferroni test was used.

4.4 Results

4.4.1 Contractile properties during isometric and shortening contractions

The contractile properties described in this section were compared between four different age-groups: 3, 10, 18 and 32-month-old. Figures 4.1a, b and c show the means and SE for the isometric force (*Fo)*, cross-sectional area (CSA) and absolute power (*P*) of the single fibres, respectively. A total of 124 single fibres were tested (see legend in Figure 4.1 for details). Under rejection criteria, 8 fibres were rejected (two 3-month-old fibres, two 10-month-old fibres, one 18-month-old and two 32-month-old fibres).

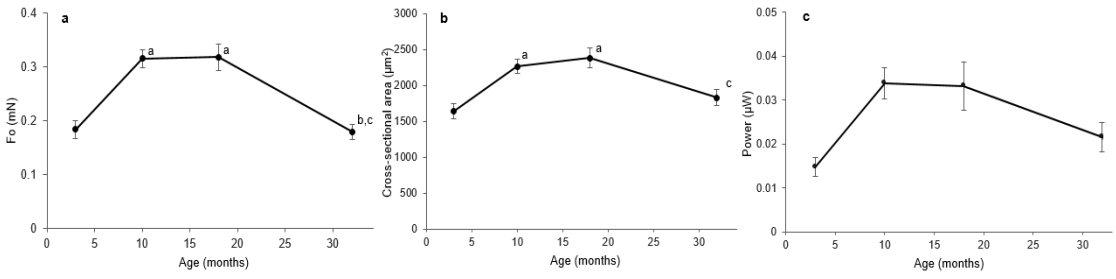

Figure 4.1a: *Means and SE of the isometric force (Fo) for four different age-groups.* ***4.1b:*** *means and Se of the cross-sectional area for each age.* ***4.1c:*** *Absolute power means and SE for all studied ages. a: significantly different from 3 month-old; b: significantly different from 10 month-old; c: significantly different*

from 18 month-old. n, number of single fibres tested in each age-group, 3 months n=32; 10 months n=34; 18 months n=32; 32 months n=26.

The differences observed in *Fo* and CSA between ages were a result of two stages along the lifespan of mice studied here. The first rise in force and CSA from 3 months to 10 and 18 months was mainly due to maturation effects. Then, there is a visible decay in both variables attributable to ageing. The peak power (Figure 4.1c) did not show significant differences but followed the maturation and ageing stages as indicated by arrows in Figure 4.2b below. Meanwhile, in Figure 4.2a the absolute force-velocity relationship is shown for different age-groups.

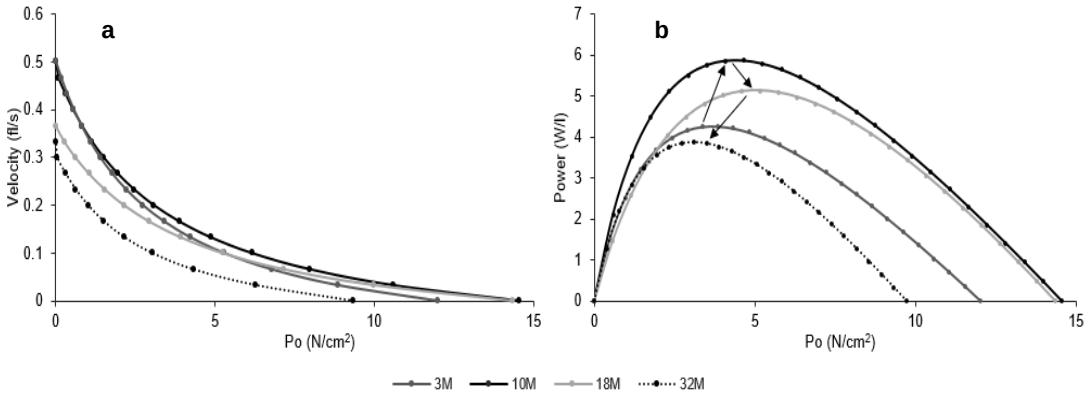

Figure 4.2a: *mean force-velocity (F-V) and* ***4.2b*** *power curves obtained for the four age-groups. The arrows pointing up and down show the maturational and ageing changes, respectively.*

In figure 4.3 are presented the mean values and SE for the contractile properties during the shortening contractions: (a) maximum velocity of shortening, (b) curvature of the force-velocity relationship, (c) specific force and (d) power per volume.

There was a significant decrease in maximum shortening velocity for 32-month-old group compared to the 3- and 10-month-old groups and a reduction of more than 30% in specific force was determined for the oldest group (32 months) compared to the 10- and 18-month-old fibres. As both the *Fo* and CSA increased between 3 and 10/18 months, *Po* did not show significant changes during maturation stage. Besides, the curvature of the force-velocity was not changed with age nor the power peak showed significant changes.

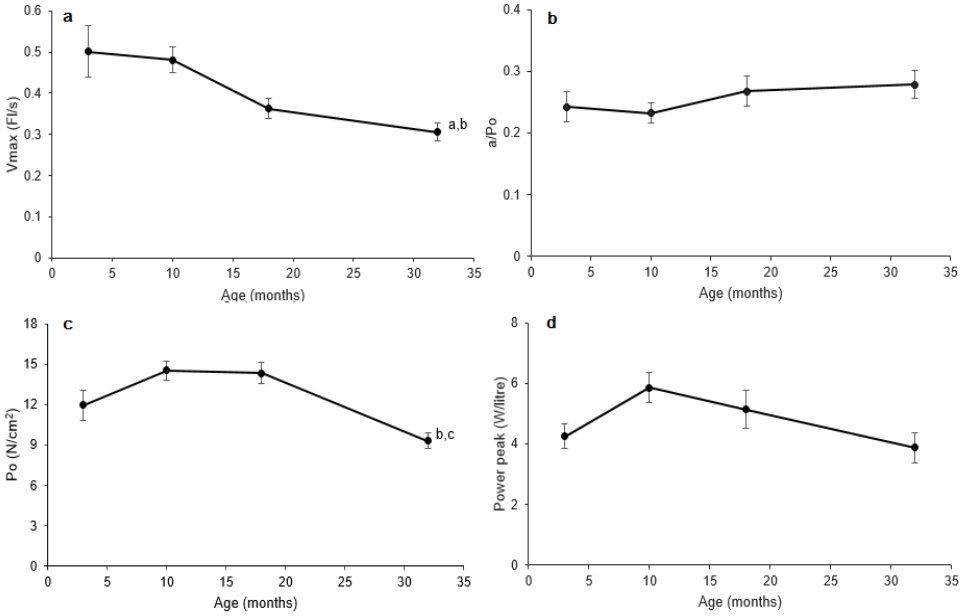

***Figure 4.3**: Means and SE values of: **(a)** maximum shortening velocity (Vmax); **(b)** curvature of the force-velocity relationship, a/Po; **(c)** specific force, Po and **(d)** normalized power. a: significantly different from 3-month-old; b: significantly different from 10-month-old; c: significantly different from 18-month-old.*

4.4.2 Lengthening contractions

Figure 4.4 shows traces of typical force curves where the peak force (*Fpeak*), and the stress relaxation (SR) are indicated. This example reflects the behaviour of the muscle when it is stretched at a speed of 0.25 (fl/s). It should be noted that all the fibres reported in the following section were subjected to three different speeds of lengthening, 0.0625 (fl/s); 0.25 (fl/s) and 1 (fl/s).

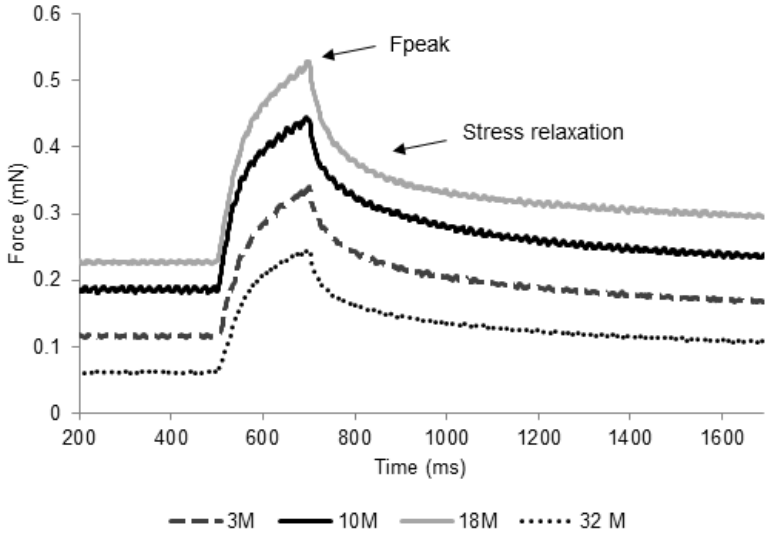

***Figure 4.4:** example of the force response to a 5% ramp stretch at 0. 25 (fl/s) from four fibres from different age-groups. Similar curves were obtained at 0.0625 and 1 (fl/s).*

The data curve from the end of the stretch until the end of the protocol was fitted to a double exponential using a non-linear least squares regression (Solver, Microsoft Excel). Thus, two rates of SR together with their proportional contribution, and a constant value for force enhancement (FE) were obtained, each belonging to an exponential function, at every stretch velocity.

4.4.2.1 Peak Force

The force reached at the end of the length ramp was defined as *Fpeak*. The means of the absolute *Fpeak* values at the different lengthening speeds for each age-group are shown below in Figure 4.5. *Fpeak* at all velocities increased with increasing age up to 18 months but the lowest values were obtained with fibres from then 32 month-old mice. Normalizing the *Fpeak* to the isometric force before the stretch in Figure 4.6 shows that the main reason for the increased *Fpeak/Fo* rate was related to the differences in isometric force. There was a tendency for the peak force normalized to the mean isometric force to increase with age between 3 and 18 months although this was not significant. There was then a drop at 32 months, although, again, this was not significant. There were no significant differences when the *Fpeak/Fo* relationship was compared throughout the age-groups at the three stretching speeds, however, it can be noticed a slight increase in this ratio from 3-month-old to 18-month-old samples and then a little decrease for the oldest group.

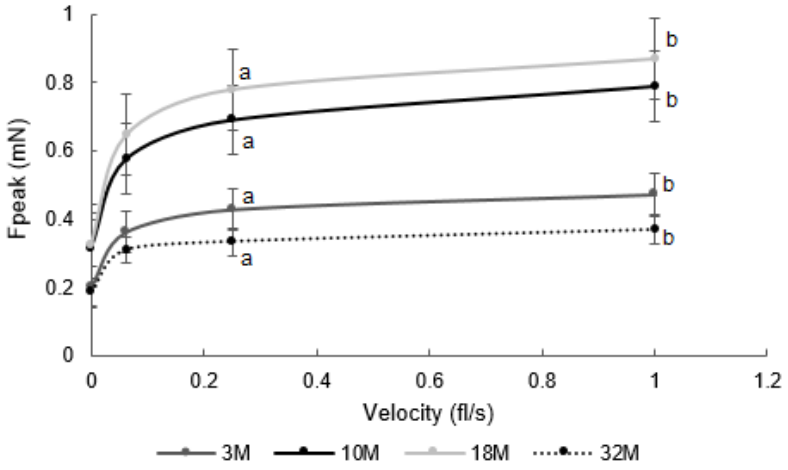

Figure 4.5: *Absolute mean and SE values of peak force (Fpeak) for different age-groups at three velocities of stretch, shown together with the isometric force. a: different from 0.0625 (fl/s). b: different from 0.0625 (fl/s) and 0.25 (fl/s). (n, number of single fibres tested in each age-group, 3 months n=32; 10 months n=34; 18 months n=32; 32 months n=26).*

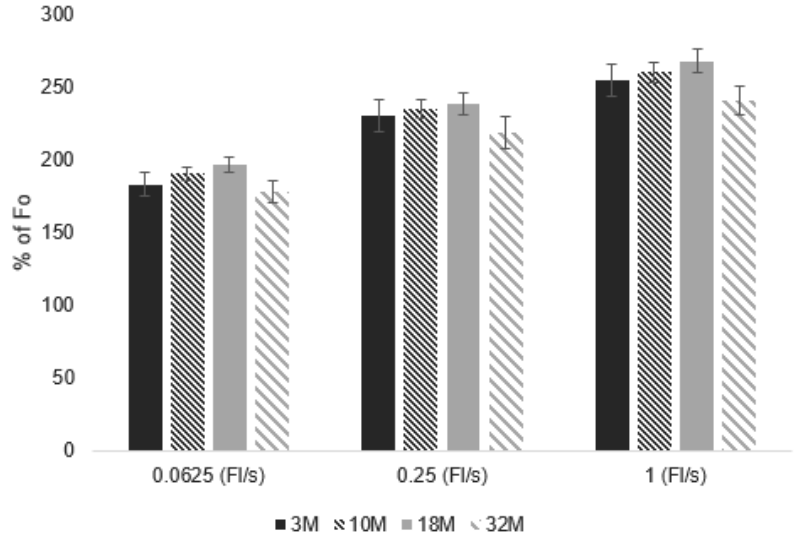

***Figure 4.6**: Mean and SE values of the peak force at the end of the stretch normalized as a % of Fo for different age groups stretched at different speeds. (n, number of single fibres tested in each age-group, 3 months n=32; 10 months n=34; 18 months n=32; 32 months n=26).*

4.4.2.2 Stress relaxation

Once the stretch ramp finished the stress relaxation was fitted to a double exponential and thus, two rate constants named kd1, the slower, and kd2 (faster) were obtained. In line with the method used to analyse the effects of added Pi on stress relaxation (Chapter 3), values for kd1 and kd2 were determined for each velocity with 10-month-old fibres (Table 2.1) and these values used to analyse data from the other age-groups, allowing values for A1, A2 and C to vary.

	0.0625 Fl/s	**0.25 Fl/s**	**1 Fl/s**
kd1	3.3±0.6	4.8±0.4	5.5±0.6
kd2	18.2±1	38.6±1.4[a]	78.2±2.6[a,b]

***Table 4.1:** values of the rate constants from 10 month fibres used to determine the contributions of each exponential to the total stress relaxation. a= significantly different from 0.0625 (fl/s). b= significantly different from 0.25 (fl/s). (n, number of single fibres tested in each age-group, 3 months n=32; 10 months n=34; 18 months n=32; 32 months n=26).*

Figure 4.7 contains traces of the stress relaxation showing how four fibres of different age groups fitted the double exponential (R^2>0.96) with the same kd1 and kd2. Then, in Figure 4.8 the traces from the previous figure are normalized and superimposed to show how the SR behaves at each age.

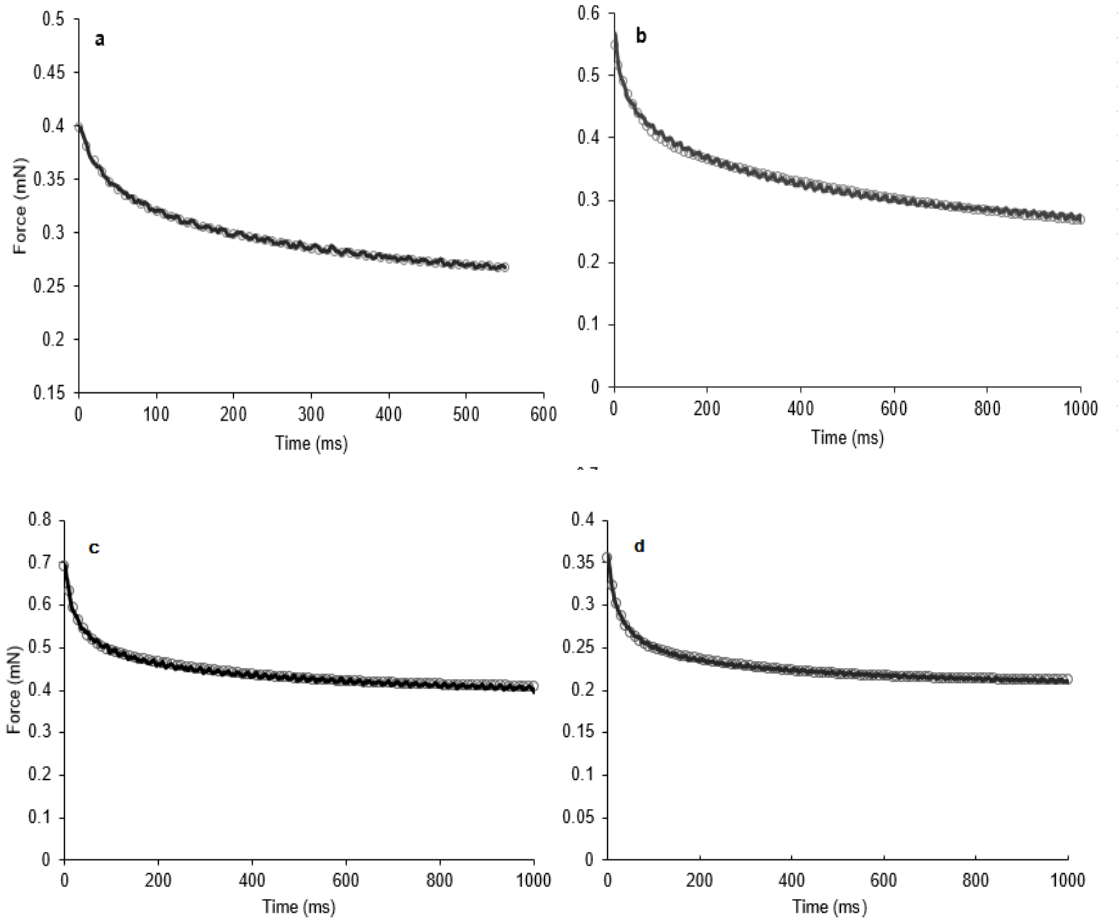

Figure 4.7: *traces of four different fibres showing the fit to the same rate constants kd1=4.8 and kd2=38.6. (a) 3-month-old fibre, (b) 10-month-old fibre, (c) 18-month-old fibre and (d) 32-month-old fibre. The data curve is in black and the fitting curve is represented by grey circles.*

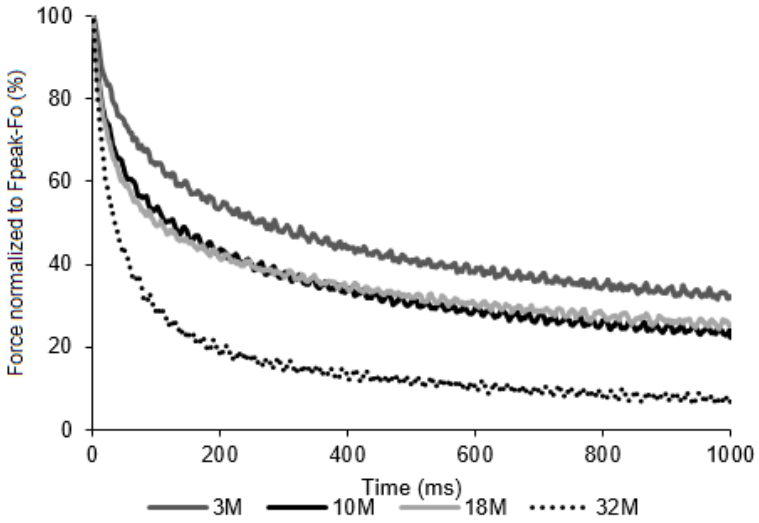

Figure 4.8: *Traces of Figure 4.7 superimposed and normalized to the total force above Fo, Fpeak-Fo. The stress relaxation is faster the older the fibre. This example is at the medium stretching speed, 0.25 (fl/s). Similar curves were obtained at the other speeds of stretch.*

The contributions of the slow (A1) and faster component (A2) were determined for each speed of stretch and each age group. These data are shown in Figure 4.9.

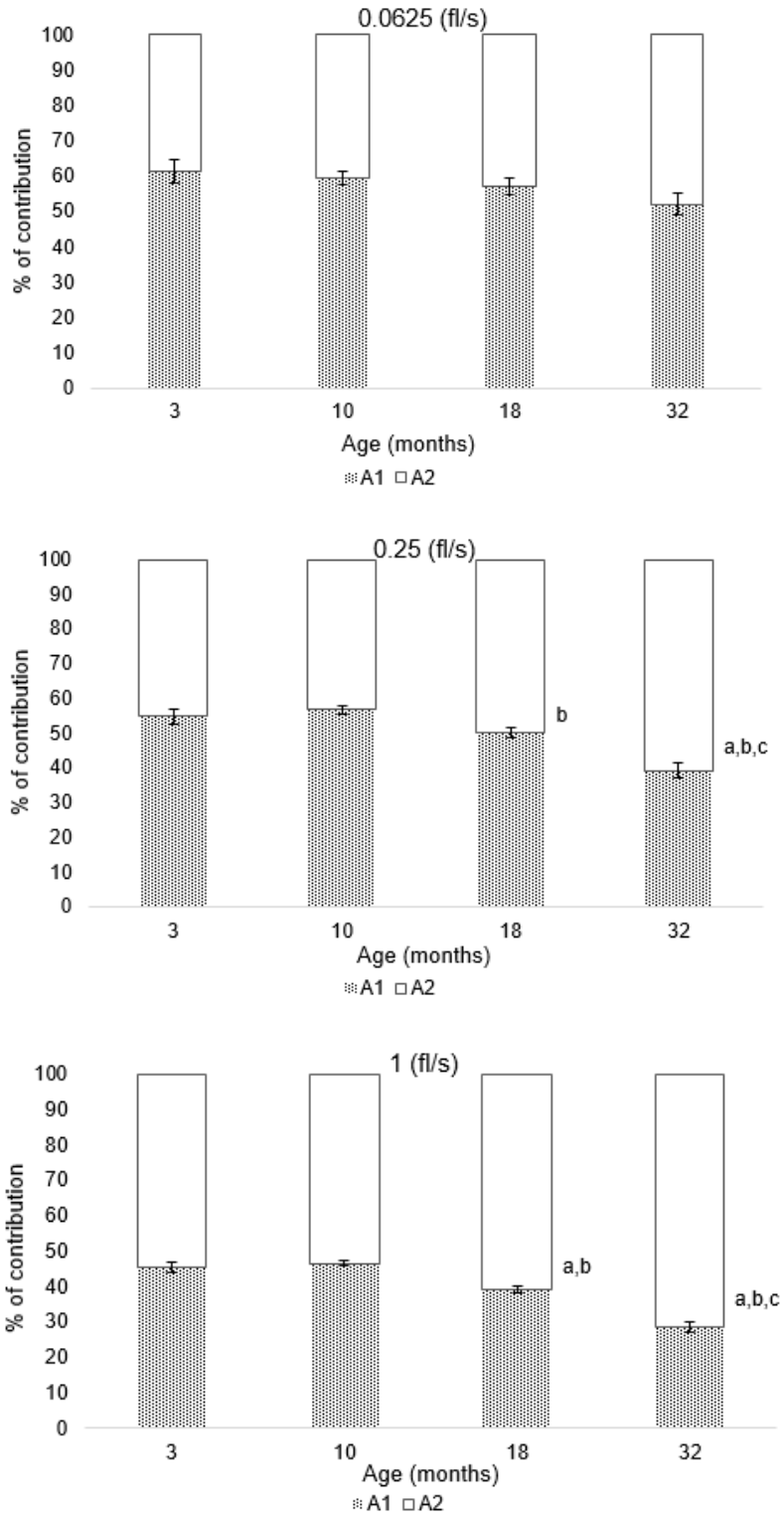

Figure 4.9: *Means and SE of A1 and A2 for the different age-groups at three different speeds of stretching. a: significantly different from 3-month-old; b: significantly different from 10-month-old; c: significantly different from 18-month-old. (n, number of single fibres tested in each age-group, 3 months n=32; 10 months n=34; 18 months n=32; 32 months n=26).*

At the two highest speeds of stretch there was a significantly larger proportion of the fast A2 component for the oldest age groups, 18 and 32 months.

4.4.2.3 Residual force enhancement

Towards the end of the stress relaxation, the fibres tended to a steady force that was in all cases higher than isometric strength before the stretch. The difference between these two forces is here called residual force enhancement and was studied in all four muscle ages at different speeds of stretch. The mean values and SE of the force enhancement as a percentage of *Fo* is presented in Figure 4.10.

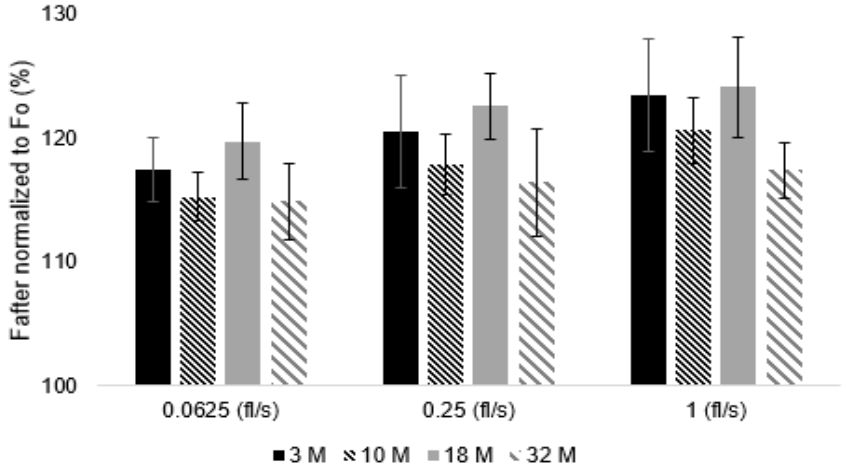

Figure 4.10*: Means and SE of the force enhancement as a percentage of isometric force before the stretch, for different muscle ages (3-, 10-, 18- and 32-month-old) at different stretch speeds as indicated in the graph. (n, number of single fibres tested in each age-group, 3 months n=32; 10 months n=34; 18 months n=32; 32 months n=26).*

4.5 Discussion

The contractile properties during shortening and lengthening of single muscle fibres have been studied for four different age groups of mice: 3-, 10-, 18- and 32-month-old, these representing the average lifespan of mice. While the effects of ageing during shortening or concentric contractions have been widely investigated, there is little information about the effects of ageing on the kinetics of crossbridges during lengthening contractions.

4.5.1 Shortening contractions

During the shortening contractions the maximal isometric force, *Fo*, the maximum velocity of shortening, *Vmax*, the force-velocity curve and the power have been observed in single fibres of different age. The measurement of the cross-sectional area

of the muscle fibre gives the force generating capacity of the muscle, assuming that the contractile material is equally dense within the fibre. The difference in CSA between the 3- and 10-/18-month-old are consistent with growth, or maturational, changes and are similar to those reported for single fibres of plantaris muscle from 5- and 13-month-old rats (Degens et al., 1993a) and of extensor digitorum longus (EDL) muscle from 2-/6- and 20-/22-month-old mice (Chan & Head, 2010). Meanwhile, a decrease of ~23% of muscle fibre cross-sectional area was found between the 18- and 32-month-old groups and is comparable to that found by Thompson & Brown (1999) with rat soleus fibres of 12- and 37-month-old and also by Brown & Hasser (1996) in the same type of fibres from 12- and 36-month-old. The increase in maximal isometric force observed during the maturational stage (Degens et al., 1993b, 1995) is comparable with the increase in the size of muscle fibres (see Figures 4.1a and b). Therefore, no significant increase in the specific force was found between the three younger groups, as shown in Figure 4.3c. On the other hand, the reduction on *Po* observed in the oldest muscle was larger than reported in previous studies in mice (Brooks & Faulkner, 1988, 1994a, 1996; Phillips et al., 1991, 1993; Chan & Head, 2010) although most of the discrepancy can be attributed to different age groups used in the various studies. However, the reduction reported here in *Po* is consistent with that observed in rat soleus by Thompson & Brown (1999), rat plantaris by Degens & Always (2003) and rat soleus, EDL and plantaris muscles by Brown & Hasser in 1996. Besides, in human muscle fibres, such decrease has also been reported (Frontera et al., 2000; Ochala et al., 2007). Single fibre shortening velocity is thought to reflect the maximum speed of actin and myosin interaction and correlates with the myofibrillar ATPase activity or myosin heavy composition (MHC) isoform (Degens & Larsson, 2007). The lower Vmax in older fibres is consistent with previous studies where Vmax was found to be affected by ageing in human, mouse and rat muscle (Ochala et al, 2007; Larsson et al. 1997b; Brooks & Faulkner, 1994b; Degens et al. 1998; D'antona et al. 2003). This age-related slowing of Vmax observed in this study may be related to additional slow and fast MHC isoforms, other thick and thin filament proteins, differences in filament lattice spacing (Larsson et al. 1997b) and/or post-translational modifications such as glycation (Hook et al. 2001).

4.5.2 Lengthening contractions

Phillips et al. (1991) have reported that relatively high forces are generated when older isolated skeletal muscle preparations were subjected to lengthening contractions, but the effects of ageing on the crossbridge kinetics during the stress relaxation have not been investigated and may provide valuable information about the contractile apparatus itself.

The peak forces' development of around 200% of the isometric force reported here when the fibres were stretched at the 0.25 and 1 (Fl/s) are comparable to the magnitude of forces that has been observed by other researchers during eccentric contractions of single fibres (Lombardi & Piazzesi 1990, Stienen et al. 1992, Linari et al. 2003). While the shape of the relationship between *Fpeak* and velocity of stretch may vary between studies they all agree that there is a velocity dependent component of the force response, as shown in Figure 4.5. There is a common belief that, compared to young, the eccentric force of old muscle is better preserved than the concentric or isometric forces. However, this is not supported by the results presented here in Figure 4.6, where the Fpeak/Fo relationship does not differ significantly between the different age-groups, meaning that the eccentric as well as the isometric force are diminished to a similar extent when comparing the different age-groups. Roig et al. in 2010 reviewed the contradictory evidence for the preservation of the eccentric force in older adults, based on the study of Lindle et al. in 1997, and concluded that the preservation may be due to changes in either or both active and passive elements. The studies that have investigated the force response to eccentric contractions in different age-groups comprise either human (Vandervoort et al. 1990; Hortobágyi et al. 1995; Lindle et al. 1997; Power et al. 2012), or mouse muscle samples (Phillips et al. 1991; Brooks & Faulkner, 1994b; Chan & Head, 2010) all using different age-groups, preparations, procedures and temperatures to obtain the force response to eccentric contractions. The work reported by Phillips et al. in 1991 is the most similar, in terms of variables, to the work presented here. However, the temperature used in that study differs from that used here (25^{o}C compared with 15^{o}C) and Phillips reported neither differences in *Fo* or CSA with age. Therefore, the different temperature as well as the choice of age-groups may play a role in these results. In all studies using intact preparations there will be a mix of fibre types, even in the soleus muscle, and it is known that with age there is an increased proportion of fibres expressing slow myosin. Linari & Bottinelli have shown that slow human fibre types have greater *Fpeak/Fo* than fast fibres, therefore an increase in the proportion of slow fibres in aged muscle could explain the observations made on whole muscle preparations. Nevertheless, in the present work it was found that *Vmax* declined with age which suggests an increase in the expression of slow myosin, yet there was no increase in *Fpeak/Fo*. The other possibility is that the observations in whole muscle may reflect the stretching of parallel compliant elements and it is known that older muscle contains a greater proportion of connective tissue. This effect could be detected by stretching at different speeds or lengths but this was not carried out in the experiments of Phillips.

Ochala et al. in 2006, studied the stretch phenomenon in single fibres but although they claim to show an enhanced stretch response in older fibres, their results show quite clearly no difference in the *Fpeak/Fo* ratio for the response to a step increase in length. Brooks & Faulkner (1994b) also looked at single fibres and reported a 30% increase in stretch force in 27 months compared to 12 months fibres, but these were EDL not soleus muscle as used in the present study. The only other study to have considered stress relaxation was that of frog fibres by Cavagna (1993). The SR was found to be a complex curve that could best be described when fitted to a double exponential function. In his study, at 14^{o}C which is similar to the temperature used in the present study, the rate constant for the fast component varied from just under 200 (s^{-1}) at the slowest velocity of 0.25 (fl/s) to approximately 300 (s^{-1}) at 2 (fl/s). The slow component had a rate constant of 5 or 10 (s^{-1}), depending on how it was calculated, but it was independent of the velocity of stretch. This is consistent with the results shown here and in previous chapters, where the rate constant of the slow component, *kd1,* did not vary significantly with the speed of stretching while the fast component rate, *kd2,* is reported to change significantly with the different lengthening speeds. In the present analysis, the rate constants, derived from the fibres at 10 months were used in the fitting of data from other age-groups, thereby deriving values for the proportional contributions of A1 and A2 to stress relaxation. As seen in the example of Figure 4.8, the older the fibre, the faster was the SR. This is reflected later in Figure 4.9, where the mean value of the fast component contribution, A2, was increased significantly with age at the speeds of 0.25 and 1 (fl/s). This new observation, that the stress relaxation is faster the older the muscle, becomes more obvious the faster the speed of the stretch. If the idea of two crossbridges populations are considered here, the higher contribution of the fast decay component would mean that, with ageing, the populations of A1 and A2 are shifted towards a larger number of crossbridges with a faster rate constant. In the previous chapter, A1 and A2 were tentatively associated with different cross bridge intermediates, A1 being a state before the release of Pi and A2 after Pi release. The present results suggest, therefore, that in the oldest muscle there is a shift in the equilibrium between these two states and that the rate of Pi release is faster than occurs in younger muscle. If this is the case then adding Pi would be expected to reverse this trend and make the oldest muscle behave more like young muscle in its response to stretch. This is investigated in the following chapter. The residual force enhancement was study at different lengthening speeds for all four age-groups and no differences were found with age. The oldest group showed a slight lower average value than the rest of the groups, however, it was not significantly decreased.

Conclusion

Maturational and ageing changes in muscle properties have been observed throughout four different age-groups. *Fo*, CSA, *Po* and *Vmax* have either increased or decreased according to the stage of maturation or ageing in which the muscle fibres were. The rate *Fpeak/Fo* did not vary significantly with age during eccentric contractions as has been reported previously (Phillips et al., 1991). However, a slight decrease was found for the oldest group as reported in humans (Lindle et al. 1997) that is in contrast with studies done in mice (Phillips et al. 1991; Brooks & Faulkner, 1994b) and women (Hortobágyi et al. 1985). Selection of age-groups would be a question here, as one of the basis of this study was to investigate the mechanism of the larger stretch response in older muscle. The finding that the stress relaxation is faster in the oldest fibres, suggests that with ageing a there is a shift in the proportions of cross bridges towards intermediates after the release of Pi.

References

Bottinelli, R., Canepari, M., Pellegrino, M. A, & Reggiani, C. (1996). Force-velocity properties of human skeletal muscle fibres: myosin heavy chain isoform and temperature dependence. *The Journal of Physiology*, 495 (Pt 2, 573–86)

Brooks, S. & Faulkner, J. A. (1988). Contractile properties of skeletal muscle from young mice. *The Journal of Physiology*, 404, 71–82.

Brooks, S. & Faulkner, J. A. (1994a). Skeletal muscle weakness in old age: underlying mechanisms. *Medicine and science in sports and exercise,* 4, 432-439.

Brooks, S. & Faulkner, J. A. (1994b). Isometric, shortening and lengthening contractions of muscle fiber segments from adult and old mice. *The American Journal of Physiology,* 267, C507-13.

Brooks, S. & Faulkner, J. A. (1996). The magnitude of initial injury induced by stretches of maximally activated muscle fibres of mice and rats increases in old age. *The Journal of Physiology*, 479, 2, 573-580.

Brown, M. & Hasser, E. M. (1996). Complexity of age-related change in skeletal muscle. *J. Gerontol. A. Biol. Sci. Med. Sci.* 51, 2, B117-B123.

Cavagna, G. (1993). Effect of temperature and velocity of streching on stress relaxation of contracting frog muscle fibres. *Journal of Physiology,* 462, 161–173.

Chan, S., & Head, S. I. (2010). Age- and Gender-Related Changes in Contractile Properties of Non-Atrophied EDL Muscle. *PloS One*, 5(8), 20–22.

D'Antona, G., Pellegrino, M. A., Adami, R., Rossi, R., Carlizzi, C. N., Canepari, M., Bottinelli, R. (2003). The effect of ageing and immobilization on structure and function of human skeletal muscle fibres. *The Journal of Physiology*, 552(Pt 2), 499–511.

Degens, H., Turek, Z., Hoofd, L., van't Hof, M. A., & Binkhorst, R. A. (1993a). Capillarisation and fibre types in hypertrophied m. plantaris in rats of various ages. *Respiration Physiology*, 94(2), 217–226.

Degens, H., Turek, Z., Binkhorst, L.A. (1993b). Compensatory hypertrophy and training effects on the functioning of ageing rat M. plantaris. *Mechanisms of Ageing and Development,* 66(3), 299-311.

Degens, H., Hoofd, L., & Binkhorst, R. A. (1995). Specific force of the rat plantaris muscle changes with age, but not with overload. *Mechanisms of Ageing and Development*, *78*, 215–219.

Degens, H., Yu, F., Li, X., & Larsson, L. (1998). Effects of age and gender on shortening velocity and myosin isoforms in single rat muscle. *Acta Physiologica Scandinavica,* 163, 33–40.

Degens, H. & Alway, S. (2003). Skeletal muscle function and hypertrophy are diminished in old age. *Muscle & nerve,* 27, 339-347.

Degens, H. & Larsson, L. (2007). Application of skinned single muscle fibres to determine myofilament function in ageing and disease. *Journal of musculoskeletal & neuronal interactions, 1, 56-61.*

Degens, H., Bosutti, A., Gilliver, S., Slevin, M., van Heijst, A., Wust, R. (2010). Changes in contractile properties of skinned single rat soleus and diaphragm fibres after chronic hypoxia. *European Journal of Physiology,* 460, 863-873.

Frontera, W. R., Suh, D., Krivickas, L. S., Hughes, V. a, Goldstein, R., & Roubenoff, R. (2000). Skeletal muscle fiber quality in older men and women. *American Journal of Physiology. Cell Physiology*, *279*(3), C611–8.

Gilliver, S. F., Degens, H., Rittweger, J., Sargeant, a J., & Jones, D. a. (2009). Variation in the determinants of power of chemically skinned human muscle fibres. *Experimental Physiology*, *94*(10), 1070–8.

Gilliver, S. F., Jones, D. a, Rittweger, J., & Degens, H. (2010a). Effects of oxidation on the power of chemically skinned rat soleus fibres. *Journal of Musculoskeletal & Neuronal Interactions*, *10*(4), 267–73.

Gilliver, S. F., Degens, H., Rittweger, J., & Jones, D. A. (2010b). Effects of submaximal activation on the determinants of power of chemically skinned rat soleus fibres. *Experimental Physiology*, *96*(2), 171–8.

Goodpaster, B. H., Park, S. W., Harris, T. B., Kritchevsky, S. B., Nevitt, M., Schwartz, A. V. (2006). The Loss of Skeletal Muscle Strength, Mass, and Quality in Older Adults : The Health, Aging and Body Composition Study. *Journal of Gerontology*, *61*(10), 1059–1064.

Hook, P., Sriramoju, V., Larsson, L. (2001). Effects of aging on actin sliding speed on myosin from single skeletal muscle cells from mice, rats and humans. *American Journal of Physiology,* 280, C782-C788.

Hortobágyi, T., Zheng, D., Weidner, M., Lambert, N. J., Westbrook, S., & Houmard, J. A. (1995). The influence of aging on muscle strength and muscle fiber characteristics with special reference to eccentric strength. *The Journals of Gerontology. Series A, Biological Sciences and Medical Sciences*, *50*(6), B399–406.

Larsson, L., & Moss, R. L. (1993). Maximum velocity of shortening in relation to myosin isoform composition in single fibres from human skeletal muscles. *Journal of Physiology*, *472*, 595–614.

Larsson, L., Li, X., Yu, F., & Degens, H. (1997a). Age-related changes in contractile properties and expression of myosin isoforms in single skeletal muscle cells. *Muscle & Nerve. Supplement*, S74–8.

Larsson, L., Li, X., & Frontera, W. R. (1997b). Effects of aging on shortening velocity and myosin isoform composition in single human skeletal muscle cells. *The American Journal of Physiology*, *272*(2 Pt 1), C638–49.

Linari, M., Bottinelli, R., Pellegrino, M. A., Reconditi, M., Reggiani, C., & Lombardi, V. (2003). The mechanism of the force response to stretch in human skinned muscle fibres with different myosin isoforms. *The Journal of Physiology*, *554*(Pt 2), 335–52.

Lindle, R. S., Metter, E. J., Lynch, N. A., Fleg, J. L., Fozard, J. L., Tobin, J., Hurley, B. F. (1997). Age and gender comparisons of muscle strength in 654 women and men aged 20-93 yr. *Journal of Applied Physiology (Bethesda, Md. : 1985)*, *83*(5), 1581–7.

Lombardi, V., & Piazzesi, G. (1990). The contractile response during steady lengthening of stimulated frog muscle fibres. *Journal of Physiology*, *431*, 141–171.

Ochala, J., Dorer, D. J., Frontera, W. R., & Krivickas, L. S. (2006). Single skeletal muscle fiber behavior after a quick stretch in young and older men: a possible explanation of the relative preservation of eccentric force in old age. *European Journal of Physiology*, 452(4), 464–70.

Ochala, J., Frontera, W. R., Dorer, D. J., Van Hoecke, J., & Krivickas, L. S. (2007). Single skeletal muscle fiber elastic and contractile characteristics in young and older men. *The Journals of Gerontology. Series A, Biological Sciences and Medical Sciences*, *62*(4), 375–81.

Phillips, S. K., Bruce, S. A., & Woledge, R. C. (1991). In mice, muscle weakness due to age is absent during stretching. *Journal of Physiology,* 437, 63–70.

Phillips, S. K., Wiseman, R. W., Woledge, R. C., & Kushmerick, M. J. (1993). Neither phosphorus metabolite levels nor myosin isoforms can explain the weakness in aged mouse muscle. *Journal of Physiology,* 463, 157–167.

Power, G. a, Rice, C. L., & Vandervoort, A. A. (2012). Increased residual force enhancement in older adults is associated with a maintenance of eccentric strength. *PloS One*, *7*(10).

Roig, M., Macintyre, D. L., Eng, J. J., Narici, M. V, Maganaris, C. N., & Reid, W. D. (2010). Preservation of eccentric strength in older adults: Evidence, mechanisms and implications for training and rehabilitation. *Experimental Gerontology*, *45*(6), 400–9.

Stienen, G. J., Versteeg, P. G., Papp, Z., & Elzinga, G. (1992). Mechanical properties of skinned rabbit psoas and soleus muscle fibres during lengthening : effects of phosphate and Ca^{2+}. *Journal of Physiology* 451*,* 503-523.

Thompson, L. V, & Brown, M. (1999). Age-related changes in contractile properties of single skeletal fibers from the soleus muscle. *Journal of Applied Physiology*, *86*, 881–886.

Trappe, S., Gallagher, P., Harber, M., Carrithers, J., Fluckey, J., & Trappe, T. (2003). Single muscle fibre contractile properties in young and old men and women. *The Journal of Physiology*, *552*(Pt 1), 47–58.

Vandervoort, A. A., Kramer, J. F., & Wharram, E. R. (1990). Eccentric knee strength of elderly females. *Journal of Gerontology*, *45*(4), B125–8.

CHAPTER 5

Does the force response to inorganic phosphate after a ramp stretch differ between young and old mouse soleus fibres?

5.1 Abstract

Age-related changes in contractile properties are of considerable interest, but relatively little is known about the response of young or old muscle to stretch. Particularly, the decay of force may give information about the kinetics of the various cross bridge states. As discussed in the previous chapter, the stress relaxation (SR) after the *Fpeak* was faster the older the muscle and it was one of the aims of this chapter to evaluate 1) whether addition of phosphate shows a reversion of that pattern and 2) whether this effect is more obvious in old muscle by a larger shift in the stress relaxation contributions. The contributions A1 and A2 were studied in single permeabilised soleus muscle fibres from adult (10 months), middle-aged (18 months) and old (32 months) mice in the absence (0 mM) or presence (5 and 15 mM) of inorganic phosphate (Pi) in the activating solution at 15ºC. Fibres were stretched for 5% of their length at 0.0625; 0.25 and 1 fibre length per second, and A1 and A2 determined. With no added Pi, SR of the older fibres was faster than that of the 10 months fibres at all three speeds of stretch (*$p<0.05$)* and faster than the 18 months at 0.25 and 1 (fl/s). There were no significant differences in force enhancement. Adding Pi slowed SR at 5 and 15 mM, reducing the fast A2 component significantly more in the old than in the adult fibres. This reduction became more obvious at the fastest stretch, where SR of the oldest fibres became almost identical to that of the 18 months and A2 was 52% for both ages and different than the 42% of A2 for the youngest group. The two components of SR may represent differences in the detachment rate of two cross bridge intermediates and the fact that added Pi increases the slow and decreases the fast component, suggests that A1 and A2 represent, respectively, cross bridge states before and after the release of Pi. This further suggests that the release of Pi from the actomyosin complex is somewhat faster in old muscle compared to the young, giving rise to faster SR and a greater proportion of the A2 component, evident when the muscle is stretched.

5.2 Introduction

When skeletal muscle is actively contracting the cyclic binding of myosin heads to actin filaments produces force, with ATP hydrolysis releasing ADP and inorganic phosphate (Pi). Several studies (Potma et al., 1995; Wang & Kawai, 1997; Tesi et al., 2000; 2002) have reported that increased levels of Pi depress isometric force *(Fo)* in skinned muscle fibres but have no effect on the maximum shortening velocity *(Vmax)* (Elzinga et al., 1989; Widrick, 2002). On the other hand, it is known that the ability to resist stretch is better preserved than is isometric force in the presence of high concentrations of inorganic phosphate (Elzinga et al., 1989, Stienen et al., 1992; Iwamoto, 1995). A decrease in isometric force is a well-established feature of old age (Brooks & Faulkner, 1994) and is, in part, due to muscle fibre loss and atrophy, but there is also a decrease in the isometric force per cross-sectional area, or, specific strength (*Po)* (Degens et al., 1995; Morse et al., 2005). Interestingly, however, there are several studies in human and mouse muscle (Phillips et al., 1991; Hortobágyi et al., 1995; Ochala et al., 2006; Brooks & Faulkner, 1988) which show that while isometric force is reduced or little affected, the ability to resist stretch is maintained, a feature that is analogous to the action of phosphate on young muscle. If this were the case then old muscle would be expected to have a larger complement of cross bridges in the low force state, tentatively identified in Chapter 2 as A1, or the A.M.ADP.Pi intermediate. The idea that the impaired contractile function of old muscle may be a consequence of higher levels of inorganic phosphate was explored by Phillips et al. in 1993 who compared the free Pi of young and old mouse muscle using NMR spectroscopy but did not find a difference. It remains possible, however, that young and old muscle may have different sensitivities to Pi. In the previous chapter it was shown that the response to stretch varied with age of the mice although not quite as reported by others. Peak force at the end of stretch showed a tendency to increase with age up to 18 months, but in the oldest group, 32 months, the peak force was lower, rather than higher, than in any other group. In addition, there was a tendency for the stress relaxation to become significantly faster on the 18 and 32 months mice when compared to the 10 months mice, which was interpreted as an increase in the proportion of cross bridges in the high force A2 state, suggested to be the intermediate after the release of Pi. If this were the case then adding Pi might reverse this trend and make the older muscles more similar to the young.

5.3 Materials and methods

5.3.1 Samples

For this study, the soleus muscles from two 10-month-old gtf2ird1, two 10-month-old wild type, three 18-month-old gtf2ird2 and two 32-month-old C57BL6 mice were used and obtained as explained previously in Chapter 3.

5.3.2 Solutions

The solutions have been described previously (Degens & Larsson, 2007; Gilliver et al., 2009) and in Chapter 4. The activating solution contained no added (0 mM), 5 (mM) or 15 (mM) of inorganic phosphate (Pi) by addition of KH_2PO_4 and maintenance of the ionic strength by reduction of KCl.

5.3.3 Preparation of single fibres

The methods to obtain the single fibres from the muscle have been described (Larsson & Moss, 2003; Gilliver et al., 2010) and are also explained in Chapter 4.

5.3.4 Protocols

Once the single fibre was obtained, mounted on the permeabilised-fibre test system the fibre was transferred from the relaxing solution to either the activating solution (pCa 4.5), to pCa 4.5 with 5 mM Pi or to the pCa 4.5 with 15 mM Pi. The order of solutions was randomised to avoid any recursive effect on the results. Once the fibre was in activating solution and isometric force had reached a plateau (Fo) the fibre was subjected to a sequence of isotonic shortening steps to determine the force-velocity relationship (Botinelli et al, 1996) and as explained previously in Chapter 4. Provided *Fo* had not dropped more than 10% or the sarcomere length (Lo) had changed more than 0.1 µm, the fibre was subjected to ramp and hold contractions of 5% Lo at three speeds, 0.0625 (fl/s), 0.25 (fl/s) and 1 (fl/s). After each of the 3 isovelocity stretch ramps, the fibre was held at the new length for 1 second to be then shortened back to Lo. Once the different lengthening speeds were finished, the fibre was returned to the relaxing solution.

5.3.5 Data analysis

Data points obtained from the end of the stretch ramp were fitted to a double exponential using a non-linear least squares regression (Solver, Microsoft Excel). The equation for the double exponential:

$$A1*e^{-kd1*t} + A2*e^{-kd2*t} + C$$

contains five variables A1, A2, kd1, kd2 and C. The term t is time. kd1 and kd2 are the rate constants of the first and second exponential, respectively. A1 is the contribution of the first exponential to the total while A2 is the contribution of the second exponential. Constant C is defined as the asymptote of the force after the stress relaxation, *Fafter,* which is larger than the isometric value before the stretch. The results are presented as means ± SE (standard error) and differences between groups were analysed by repeated measurements ANOVA in SPSS (IBM) with age as between-subjects factor and concentration of inorganic phosphate in solution as the within-subjects factor. If there was a significant age effect or significant concentration, Bonferroni corrected *post-hoc* tests were done to locate the difference. A two-way ANOVA was conducted to examine the interaction between age*concentration effects. Main effects and interactions were considered significant when $p<0.05$.

5.4 Results

Figures 5.1 and 5.2 show the effects of age and Pi on *Fo* and *Po*, respectively, in 31 fibres of 10-month-old mice; 28 fibres of 18-month-old mice and 21 of 32-month-old mice. A total of 5 single fibres were rejected under exclusion criteria. The isometric force was decreased by 41%, 29% and 40% for the adult, middle-age and old fibres, respectively, in presence of 5 mM added Pi compared to the activating solution without addition of Pi (*p<0.05)*. In the presence of 15 mM added Pi, *Fo* was reduced even further by 56%, 50% and 58% (*p<0.05)* for each of the age-groups.

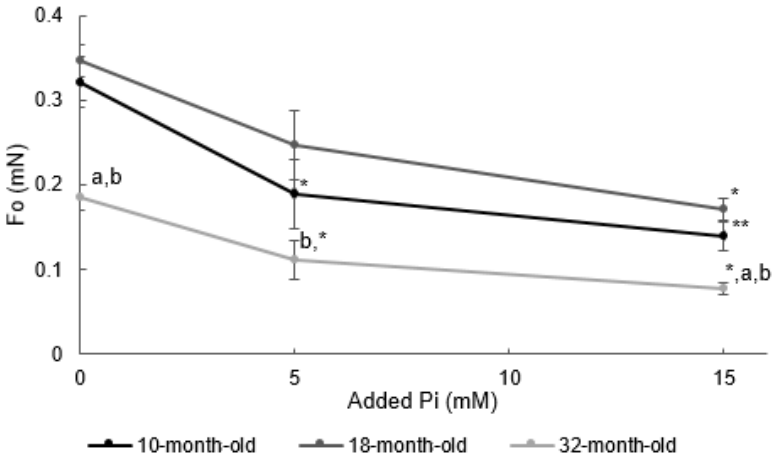

Figure 5.1: *The effect of age (10-, 18- and 32 month-old mice) and Pi (no added, 5 and 15 mM Pi) on the maximal isometric force (Fo) of single soleus fibres. Data are mean ± SE; *: significantly different from no added Pi, **: significantly different from no added and 5 mM Pi. a: significantly different from 10 months, b: significantly different from 18 months.*

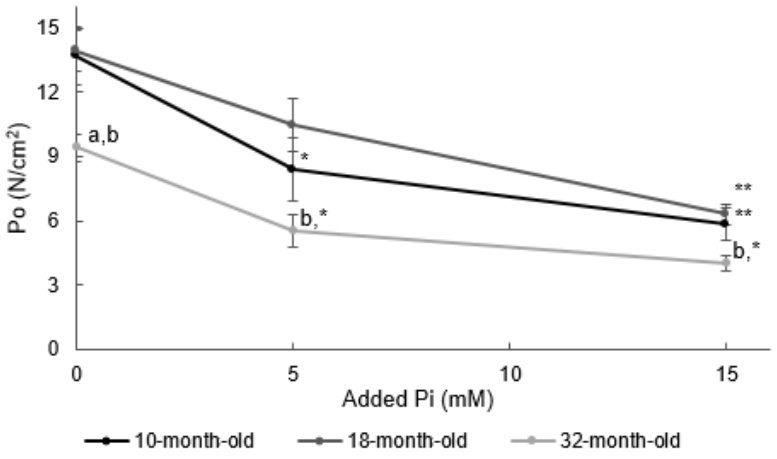

Figure 5.2: *The effect of age (10-, 18- and 32 month-old mice) and Pi (0, 5 and 15 mM Pi) on specific force (Po) of single soleus fibres. Data are mean ± SE. *: significantly different from no added Pi, **: significantly different from no added and 5 mM Pi. a: significantly different from 10 months, b: significantly different from 18 months.*

Furthermore, the decrease in specific force was 39%, 29% and 41% in 5 mM Pi (*p<0.05)* and 57%, 55% and 57% in 15 mM Pi (*p<0.05)* for the 10-, 18- and 32-month-old, respectively. The interaction between Pi and age had a significant effect (*p<0.05)* on *Po.* Vmax, however, was not affected by different [Pi], but was lower in the oldest group compared to the youngest (Table 5.1), while the curvature of the force-velocity curvature showed no significant changes with age or [Pi] (Table 5.2).

Vmax (fl/s)	10 months (n=31)	18 months (n=28)	32 months (n=21)
0 mM Pi	0.49±0.04	0.36±0.05	0.31±0.03[ab]
5 mM Pi	0.47±0.03	0.32±0.05 [a]	0.29±0.04 [a]
15 mM Pi	0.4±0.02	0.28±0.03	0.24±0.04 [a]

Table 5.1: *mean values and SE for the Vmax at different concentrations of Pi from three age-groups.*

a: significantly different from 10-month-old; b: significantly different from 18-month-old. (n=number of single fibres)

a/Po	10 months (n=31)	18 months (n=28)	32 months (n=21)
0 mM Pi	0.23±0.01	0.26±0.01	0.28±0.01
5mM Pi	0.28±0.01	0.29±0.02	0.30±0.02
15 mM Pi	0.26±0.01	0.28±0.02	0.29±0.01

Table 5.2: *mean values and SE for the force-velocity curvature (a/Po) at different concentrations of Pi from three age-groups. (n=number of single fibres)*

The lengthening contractions were performed at three different velocities, 0.0625, 0.25 and 1 (fl/s) for all the fibres from the three age-groups in different concentrations of Pi. During those stretches, the effects of [Pi] and ageing were assessed for every single fibre at each speed. The effects of stretching speeds were not evaluated here, since that analysis has been already done in Chapter 2. The means ± SE of the absolute force at the end of the ramp, *Fpeak,* are shown in Figures 5.3a, c and e. To be able to compare the response between fibres, *Fpeak* was normalized to the isometric force before the stretch and expressed as *Fpeak/Fo*. The normalized *Fpeak* means ± SE are shown in Figure 5.3b, d and f.

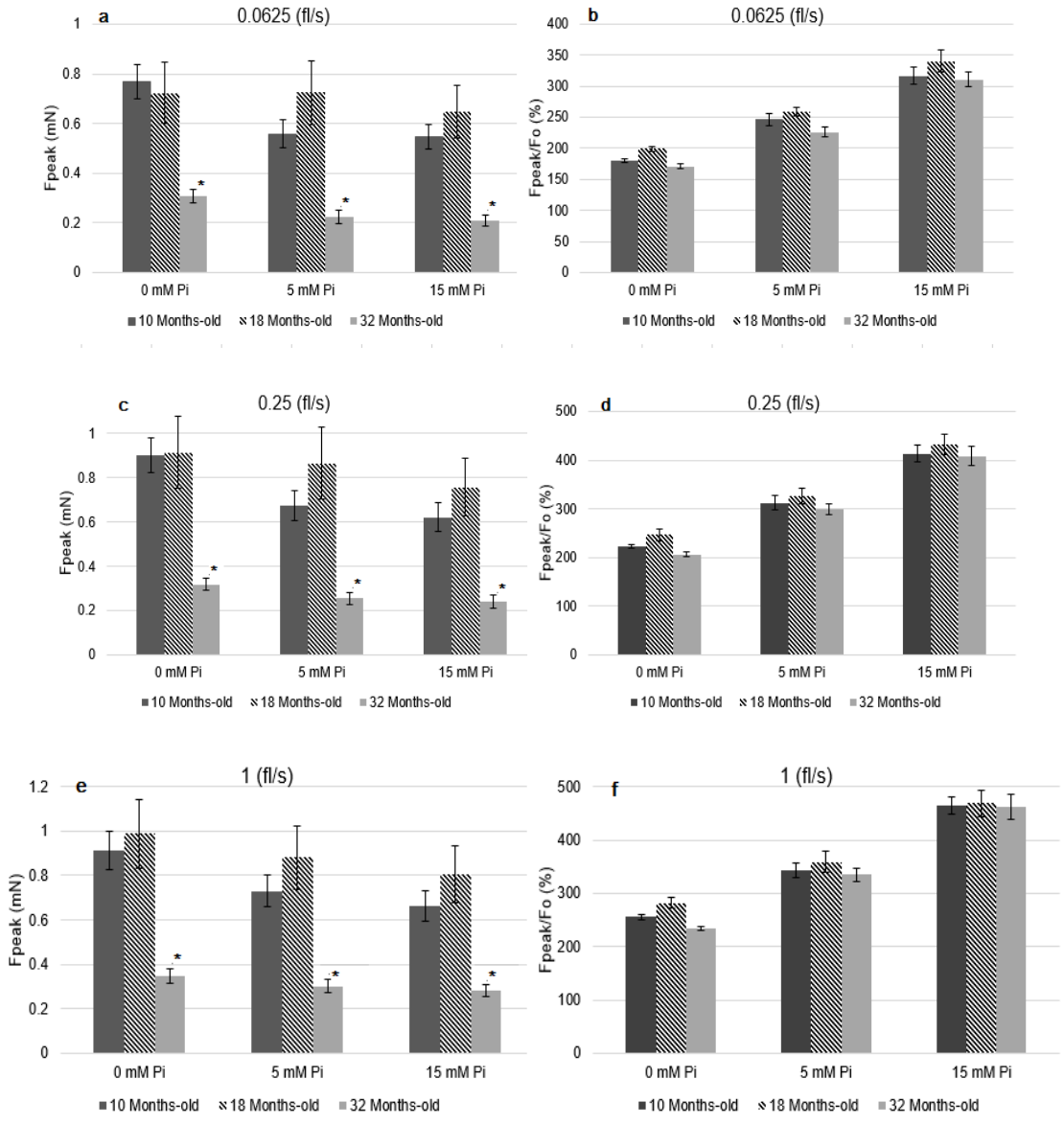

Figure 5.3: *The effects of age (10-, 18- and 32-month-old) and [Pi] (0, 5 and 15 mM) on the absolute Fpeak (a, c and e) and Fpeak as a percentage of Fo (b, d and f). (a,b) Lengthening speed: 0.0625 (fl/s); (c,d) 0.25 (fl/s); (e,f) 1 (fl/s). *: significantly different from 10- and 18-month-old. (n=number of single fibres; 10 months n=31; 18 months n=28; 32 months n=21)*

According to the data shown in Figure 5.3, the absolute values of *Fpeak* were slightly, but not significantly, higher in almost all cases for the 18-month-old and then decreased (*p<0.05)* to a greater extent for the oldest group. When the peak force was expressed as percentage of the isometric force (graphs b, d and f) those differences did not show up, therefore, the ratio *Fpeak/Fo* showed a similar value between age-groups with increasing phosphate and this behaviour was more obvious the faster the stretch. To determine the impact of age and different [Pi] on stress relaxation, the SR curves were analysed keeping the rate constants kd1 and kd2 as the values found for the 10-month-old mice in pCa 4.5 for each velocity of stretch and the data fitted by allowing A1, A2 and C to change. However, they were allowed to vary with the rate of stretch, since kd2 is dependent of the speed of stretch. Using these kd1 and kd2 values to fit the stretch relaxation, the contributions of each exponential curve, A1 (for the slow component) and A2 (for the fast component) were determined. Table 5.3a, b and c present the rate constants at each lengthening speed, as well as the effect of age and [Pi] on the proportions A1 and A2.

	kd1=2.7±0.1 (s^{-1}); kd2=18.2±0.7 (s^{-1})					
	10 month-old (n=31)		**18 month-old (n=28)**		**32 month-old (n=21)**	
0.0625 (fl/s)	**A1 (%)**	**A2 (%)**	**A1 (%)**	**A2 (%)**	**A1 (%)**	**A2 (%)**
0 mM Pi	64±2	36±2	58±2	42±2	52±3^{a}	48±3^{a}
5 mM Pi	77±2*	23±2*	70±2*	30±2 *	58±3*^{a}	42±3*^{a}
15 mM Pi	80±2*	20±2*	73±2*^{a}	27±2*^{a}	71±2**^{a}	29±2**^{a}

Table 5.3a: *means of kd1, kd2, A1 and A2 and their SE from different ages at different [Pi] at a stretch speed of 0.0625 (fl/s). *: significantly different from no added Pi; **: significantly different from 5 mM Pi; a: significantly different from 10 month-old. (n=number of single fibres)*

	kd1=3.4+0.2 (s^{-1}); kd2=38.5+0.9 (s^{-1})					
	10 month-old (n=31)		**18 month-old (n=28)**		**32 month-old (n=21)**	
0.25 (fl/s)	**A1 (%)**	**A2 (%)**	**A1 (%)**	**A2 (%)**	**A1 (%)**	**A2 (%)**
0 mM Pi	56±1	44±1	48±3^{a}	52±3^{a}	35±2^{ab}	65±2^{ab}
5mM Pi	68±2*	32±2 *	56±2*^{a}	44±2*^{a}	48±2*^{ab}	52±2*^{ab}
15 mM Pi	73±2**	27±2**	60±2**^{a}	40±2**^{a}	58±1**^{a}	42±1**^{a}

Table 5.3b: *means of kd1, kd2, A1 and A2 and their SE from different ages at different [Pi] at a stretch speed of 0.25 (fl/s). *: significantly different from no added Pi; **: significantly different from 5 mM Pi; a: significantly different from 10 month-old.; b: significantly different from 18 month-old. (n=number of single fibres)*

	kd1=3.8+0.4 (s^{-1}); kd2=81.4+2.1 (s^{-1})					
	10 month-old (n=31)		18 month-old (n=28)		32 month-old (n=21)	
1 (fl/s)	A1 (%)	A2 (%)	A1 (%)	A2 (%)	A1 (%)	A2 (%)
0 mM Pi	45±1	55±1	36±3 [a]	64±3 [a]	26±1 [ab]	74±1 [ab]
5mM Pi	54±2*	46±2*	44±2*[a]	56±2*[a]	39±1*[a]	61±1*[a]
15 mM Pi	58±2**	42±2**	48±2*[a]	52±2*[a]	48±1**[a]	52±1**[a]

Table 5.3c: *means of kd1, kd2, A1 and A2 and their SE from different ages at different [Pi] at a stretch speed of 1 (fl/s). *: significantly different from no added Pi; **: significantly different from 5 mM added Pi; a: significantly different from 10 month-old.; b: significantly different from 18 month-old. (n=number of single fibres)*

In Figures 5.4a, b and c, the mean stress relaxation curves from young, adult and old muscle has been plotted for the fastest lengthening speed (1 fl/s) with no Pi, 5mM and 15 mM Pi.

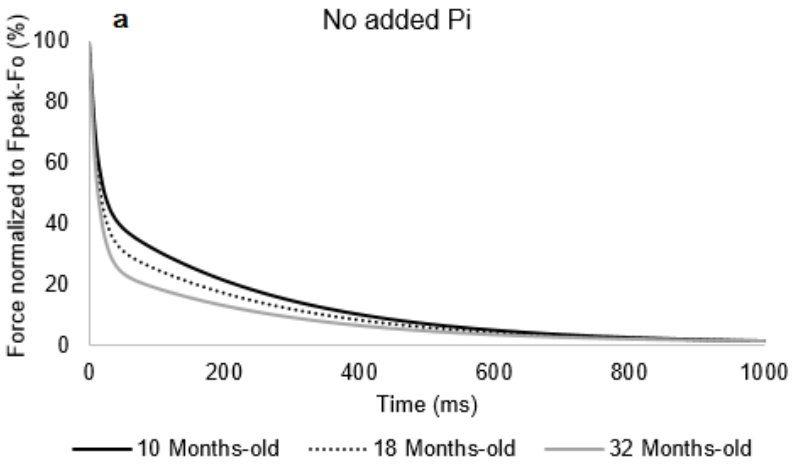

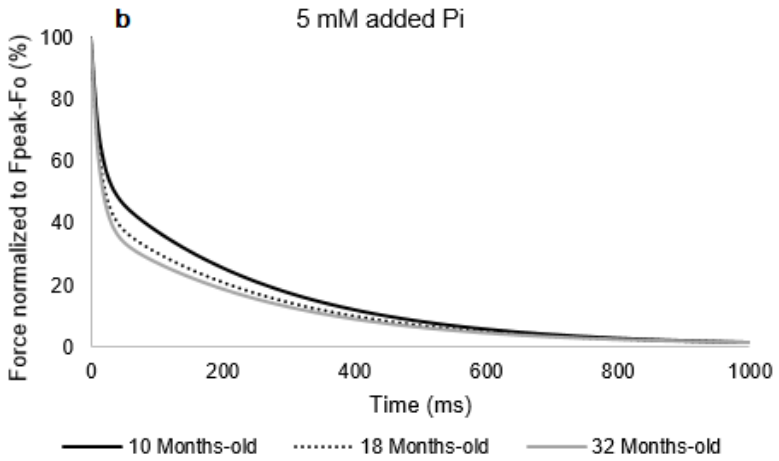

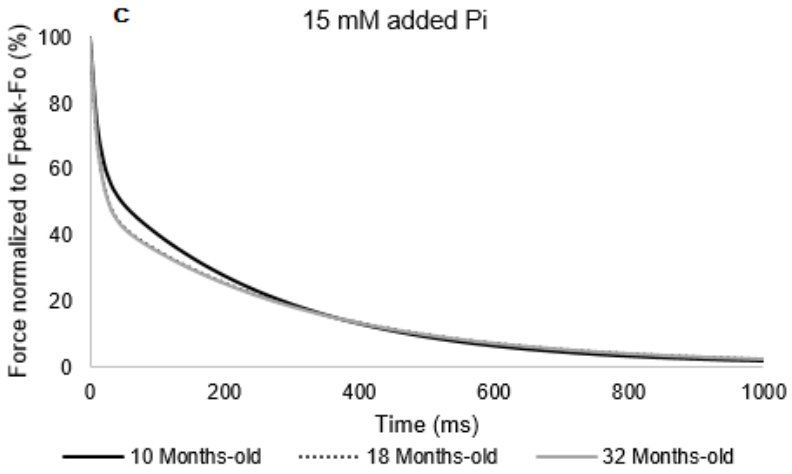

Figure 5.4: *Effect of age (10-, 18 and 32-month-old) and Pi (a) No added Pi; (b) 5 mM Pi; (c) 15 mM Pi on the stress relaxation at a lengthening speed of 1 (fl/s). Mean curves for each age. The 18- and 32-month-old curves are superimposed in (c), when [Pi] is 15 mM. (n=number of single fibres; 10 months n=31; 18 months n=28; 32 months n=21)*

It is notable that the stress relaxation from the oldest fibres that was faster in absence of Pi (5.4a), became slower (5.4b) with 5 mM Pi until appearing virtually superimposed to the stress relaxation of the 18-month-old fibres (5.4c) in the presence of 15 mM Pi. The stress relaxation overlap is a result of a decreased A2 contribution of the oldest fibres for increasing [Pi] compared to the 10-month-old. The A2 contribution of the oldest fibres decreased for increasing [Pi] compared to the 10 month-old.

Figure 5.5 shows the effects of age and different concentration of Pi on the proportions A1 and A2 from the stress relaxation at different velocities. The significant differences of A1 and A2 between ages and [Pi] were displayed in Table 5.3a, b and c and show, basically, that the increased proportion of A2 (and faster SR) for older fibres with no added Pi compared to the young and adult fibres, became less marked with increasing of Pi. Looking at the tendency lines drawn in Figure 5.5 connecting a given [Pi] for different age-groups, the increasing phosphate somehow 'balances' the values of A1 (and A2) until they became similar between the 18- and 32-month-old fibres, and this was more obvious the faster the stretch. At each speed of stretch and no addition of Pi, the 32 months fibres showed a faster stress relaxation than the 10 ($p<0.05$) and 18 ($p<0.05$) months fibres. With 15 mM Pi, although the A2 proportion was still increased ($p<0.05$) in the 32 months compared to the 10 months fibres, it was low enough to become similar than that of the 18 months fibres. This similar proportions are more obvious in Figures 5.5b and c along the lines connecting the 15 mM Pi.

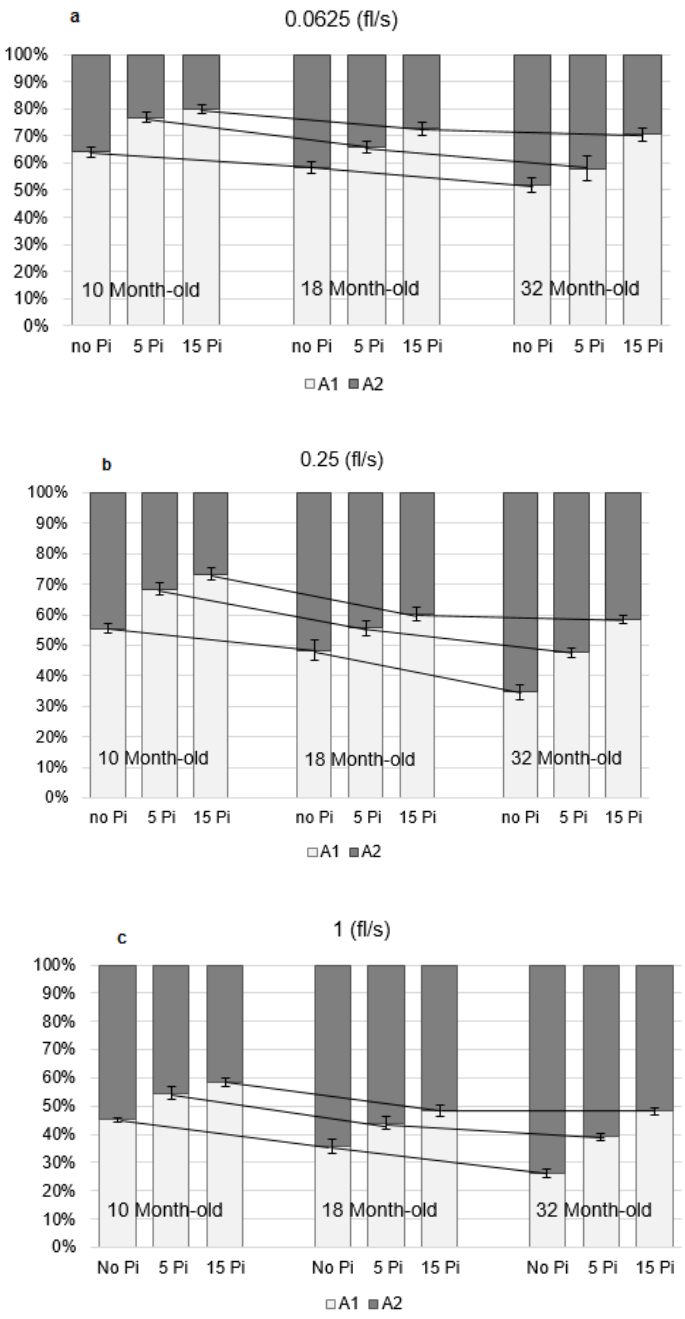

Figure 5.5: *Effects of age (10-, 18- and 32-month-old) and [Pi] (no added, 5 and 15 mM) on contributions A1 and A2 of the stress relaxation. The tendency lines show how the contributions varied between age-groups for a given [Pi]. (a) at 0.0625 (fl/s); (b) at 0.25 (fl/s); (c) at 1 (fl/s). (n=number of single fibres; 10 months n=31; 18 months n=28; 32 months n=21)*

5.5 Discussion

5.5.1 Contractile properties during shortening and isometric contractions

The effects of inorganic phosphate on the contractile properties of adult (10-month-old) mouse soleus muscle fibres were studied and presented in Chapter 3. Here, the study of contractile properties was expanded to middle-aged (18-month-old) and old (32-month-old) mouse soleus muscle fibres. These results show that the older muscle did not have a different sensitivity to inorganic phosphate during isometric and concentric contractions.

5.5.2 Contractile properties during stretches

One of the purposes of the work presented in this chapter was to compare the effect of added Pi on the stretch response of muscles of different ages. Although there were no significant differences on the Fpeak normalized to the Fo between age-groups at different [Pi], the interesting feature that is noticeable in the 15 mM added Pi columns compared to the no added Pi of Figures 5.3b, d and f is a first hint about a different behaviour of the old muscle in phosphate compared to adult and middle-aged. The second purpose of this work was to test the idea that the larger proportion of the A2 component during stretch seen with the 18- and 32-month-old muscles in Chapter 4, could be reversed by the addition of Pi. In the absence of inorganic phosphate, and as discussed in the previous Chapter 4, stress relaxation was fastest in the oldest fibres. However, this behaviour changed with addition of phosphate (See Figure 5.4) with a shift in the contributions (A1 and A2) of the oldest fibres at the higher concentration of Pi, to a similar level to those on the middle-aged muscle (18-month-old fibres). Since the contributions have been considered as different populations of cross bridges, the shift towards A1 in old muscle would mean that the populations changed from fast detaching cross bridges to slow detaching cross bridges in the presence of Pi to a greater extent than those of the other age-groups. This is reflected by the same stress relaxation on old muscle in presence of phosphate as that of younger muscle (18-month-old) as shown in Figure 5.4c**.** In the cross bridge ATPase cycle shown in Figure 1.4 in Chapter 1, in which force production is believed to occur before the release of Pi from the actomyosin complex, it would seem as if the increased proportion of A2 corresponds to cross bridge states after reaction 5 and thus in the 32 months fibres it would appear that the equilibrium of reaction 5 is set to the right compared with the younger fibres. Added Pi slows or reverses reaction 5 leading to an accumulation of AM'.ADP.Pi which in turn slows or reverses reaction 4.

Conclusions

The changes in contractile properties of old muscle in presence of phosphate were similar to those of adult muscle presented in Chapter 3. The decrease in *Fo* and *Po* did not show a different sensitivity of old muscle to phosphate compared to younger samples. The maximum velocity of shortening as well as the curvature of the force velocity relationship was not affected by Pi. Added Pi reduced the proportion of A2 in the older muscles decreasing the rate of stress relaxation so that it was similar to that of younger fibres. This tends to confirm that older muscles have slightly different kinetics regulating the proportions of the cross bridge intermediate states leading to a larger proportion of force states.

References

Bottinelli, R., Canepari, M., Pellegrino, M. A, & Reggiani, C. (1996). Force-velocity properties of human skeletal muscle fibres: myosin heavy chain isoform and temperature dependence. *The Journal of Physiology*, *495 (Pt 2*, 573–86)

Brooks, S. & Faulkner, J. A. (1994). Skeletal muscle weakness in old age: underlying mechanisms. *Medicine and science in sports and exercise,* 4, 432-439.

Degens, H., Hoofd, L., & Binkhorst, R. A. (1995). Specific force of the rat plantaris muscle changes with age, but not with overload. *Mechanisms of Ageing and Development*, *78*, 215–219.

Degens, H., Yu, F., Li, X., & Larsson, L. (1998). Effects of age and gender on shortening velocity and myosin isoforms in single rat muscle. *Acta Physiologica Scandinavica,* 163, 33–40.

Degens, H., & Larsson, L. (2007). Application of skinned single muscle fibres to determine myofilament function in ageing and disease. *Journal of Musculoskeletal & Neuronal Interactions*, *7*(1), 56–61.

Elzinga, G., Stienen, G. J., & Versteeg, P. G. A. (1989). Effect of inorganic phosphate on length responses to changes in load in skinned rabbit psoas muscle, *Journal of Physiology*, 415, 132P.

Gilliver, S. F., Degens, H., Rittweger, J., Sargeant, a J., & Jones, D. a. (2009). Variation in the determinants of power of chemically skinned human muscle fibres. *Experimental Physiology*, *94*(10), 1070–8.

Gilliver, S. F., Jones, D. a, Rittweger, J., & Degens, H. (2010). Effects of oxidation on the power of chemically skinned rat soleus fibres. *Journal of Musculoskeletal & Neuronal Interactions*, *10*(4), 267–73.

Hortobágyi, T., Zheng, D., Weidner, M., Lambert, N. J., Westbrook, S., & Houmard, J. A. (1995). The influence of aging on muscle strength and muscle fiber characteristics with special reference to eccentric strength. *The Journals of*

Gerontology. Series A, Biological Sciences and Medical Sciences, *50*(6), B399–406.

Iwamoto, H. (1995). Strain sensitivity and turnover rate of low force cross-bridges in contracting skeletal muscle fibers in the presence of phosphate. *Biophysical Journal*, *68*(1), 243–50.

Larsson, L., & Moss, R. L. (1993). Maximum velocity of shortening in relation to myosin isoform composition in single fibres from human skeletal muscles. *Journal of Physiology*, *472*, 595–614.

Larsson, L., Li, X., & Frontera, W. R. (1997). Effects of aging on shortening velocity and myosin isoform composition in single human skeletal muscle cells. *The American Journal of Physiology*, *272*(2 Pt 1), C638–49.

Lindle, R. S., Metter, E. J., Lynch, N. A., Fleg, J. L., Fozard, J. L., Tobin, J., Hurley, B. F. (1997). Age and gender comparisons of muscle strength in 654 women and men aged 20-93 yr. *Journal of Applied Physiology (Bethesda, Md. : 1985)*, *83*(5), 1581–7.

Morse, C. I., Thom, J. M., Reeves, N. D., Birch, K. M., & Narici, M. V. (2005). In vivo physiological cross-sectional area and specific force are reduced in the gastrocnemius of elderly men. *Journal of Applied Physiology (Bethesda, Md. : 1985)*, *99*(3), 1050–5.

Ochala, J., Dorer, D. J., Frontera, W. R., & Krivickas, L. S. (2006). Single skeletal muscle fiber behavior after a quick stretch in young and older men: a possible explanation of the relative preservation of eccentric force in old age. *European Journal of Physiology*, 452(4), 464–70.

Phillips, S. K., Bruce, S. A., & Woledge, R. C. (1991). In mice, muscle weakness due to age is absent during stretching. *Journal of Physiology,* 437, 63–70.

Phillips, S. K., Wiseman, R. W., Woledge, R. C., & Kushmerick, M. J. (1993). Neither phosphorus metabolite levels nor myosin isoforms can explain the weakness in aged mouse muscle. *Journal of Physiology,* 463, 157–167.

Potma, E. J., van Graas, I. A., & Stienen, G. J. (1995). Influence of inorganic phosphate and pH on ATP utilization in fast and slow skeletal muscle fibers. *Biophysical Journal*, *69*(6), 2580–9.

Stienen, G. J., Versteeg, P. G., Papp, Z., & Elzinga, G. (1992). Mechanical properties of skinned rabbit psoas and soleus muscle fibres during lengthening : effects of phosphate and Ca^{2+}. *Journal of Physiology* 451*,* 503-523.

Tesi, C., Colomo, F., Nencini, S., Piroddi, N., & Poggesi, C. (2000). The effect of inorganic phosphate on force generation in single myofibrils from rabbit skeletal muscle. *Biophysical Journal*, *78*(6), 3081–3092.

Tesi, C., Colomo, F., Piroddi, N., & Poggesi, C. (2002). Characterization of the cross-bridge force-generating step using inorganic phosphate and BDM in myofibrils from rabbit skeletal muscles. *The Journal of Physiology*, *541*(Pt 1), 187–99.

Wang, G., & Kawai, M. (1997). Force generation and phosphate release steps in skinned rabbit soleus slow-twitch muscle fibers. *Biophysical Journal*, *73*(2), 878–894.

Widrick, J. J. (2002). Effect of P-i on unloaded shortening velocity of slow and fast mammalian muscle fibers. *American Journal of Physiology - Cell Physiology*, *282*(4), C647–C653.

CHAPTER 6

General Discussion

6.1 Introduction

The work described in this thesis was stimulated by concern for the well documented decline in muscle function that is a feature of old age. Whilst many aspects of this decline can be explained in terms of reductions in muscle mass as a result of fibre atrophy and loss, there are also changes in contractile function that are not fully understood. In particular, there are reports that the force sustained by older muscle during stretch is better maintained than is the force of isometric and shortening contractions. The evidence that any such preservation of function is due to changes in the intrinsic properties of muscle fibres is limited and the first objective of the present study was to examine the response to stretch, across the age span, using a single fibre preparation which avoids many of the complications inherent in studies of whole muscle preparations, such as differing tendon properties or fibre type composition. The reported changes in response to stretch of old muscle is similar to the changes in contractile characteristics seen in young muscle in the presence of increased levels of inorganic phosphate (Pi). While it has been shown that older muscles do not have higher Pi levels compared to young there remains the possibility that older muscle may respond differently to inorganic phosphate. The second major objective of this study was, therefore, to compare the contractile responses of young and old muscle to added Pi.

The work presented here had a number of objectives that can be summarised by chapter:

- Chapter 2: To characterise the contractile characteristics of isolated and permeabilised single fibres from adult mouse soleus; more specifically, the response to isovelocity ramp stretches.
- Chapter 3: To study the effects of added inorganic phosphate in different concentrations to the activating solution on the force response with particular emphasis on ramp stretches.
- Chapter 4: To determine the changes in contractile characteristics across the age span, again, with particular interest in the response to stretch.
- Chapter 5: The final study was concerned to determine the extent to which the response to added phosphate varied with age.

6.2 Force curve characteristics as a result of lengthening contractions

The work presented Chapter 2 aimed to characterise the force response during and after a ramp stretch at different velocities of stretch.

6.2.1 Peak force

Despite the wide range of species, stimulus and speeds used along previous studies, what all have in common is that the *Fpeak* was reported to be higher than the isometric force while the muscle is active (Abbott & Aubert, 1952; Getz et al., 1998; De Ruiter et al., 2000; Linari et al., 2003), as it has been shown here in chapter two where the peak force at the end of the ramp stretch was between 1.8 and 2.6 times the value of isometric force and tended to plateau for the fastest speed of stretch. In the present study the stretch used has been an isovelocity ramp of different speeds; 0.0625 (fl/s), 0.25 (fl/s) and 1 (fl/s). The peak force (*Fpeak*) was found to be dependent on the lengthening speed, tending to level out at 2.6 Fo very much as seen in previous studies (Sugi, 1972; Edman et al., 1978; Pinniger et al., 2006).

6.2.2 Stress relaxation

At the end of the ramp stretch the force decayed away towards, but not reaching the isometric force achieved before the start of the stretch. This aspect of the stretch response has received relatively little attention with the exception of, first, Colomo et al. (1989) and later Cavagna (1993), the latter calling the phenomenon ‘stress relaxation’. The SR has been found to be best described when fitted to the sum of two exponential functions and a constant. This approach has been used in the work described in Chapter 2 and then in subsequent Chapters.

The fitting process involves optimising values for 5 variables, the two rate constants kd1 and kd2, the corresponding proportions of the SR, A1 and A2 and the constant value C. Even if unfeasible negative values are excluded there is no unique solution so that, for instance, a faster SR could be fitted by increasing the proportion of A2 or by increasing the rate constant kd2 or decreasing kd1, or any combination of these changes. Consequently all that can be reported is that a certain combinations of these variables is consistent with the observed contractile changes, but this does not provide an absolute proof. In practice it was found impossible to fit the SR curves obtained at the three velocities of stretch using the same rate constants kd1 and kd2 as would be expected if the rates of detachment were strain dependent. Consequently the best fit was obtained independently allowing all the constants to vary for each of the three stretch velocities for the 10 months fibres in the absence of added Pi. These values

for kd1 and kd2 were then kept constant and just A1, A2 and C allowed to change when fitting SR curves for fibres of different ages so that, essentially, the values reported are all relative to those for 10 months fibres. The conclusions that the proportions of A1 and A2 change with age and added Pi are consistent with the observed contractile responses but the possibility cannot be excluded that changes with age and Pi could also be explained by changes in the rate constants, while A1 and A2 remained constant.

Cavagna, in 1993, suggested that the faster rate constant represented the detachment of cross bridges while the slow component was due to the relaxation of a non-contractile series compliant element in the muscle. This was based on the observation that the fast component was sensitive to velocity of stretch, as would be expected of crossbridges, while the slow component was not. What this compliant component might be is not clear. Titin is the obvious candidate but this seems a more likely candidate to explain the force enhancement (Herzog, 2014) since it is known to be length dependent and more evident in fibres at longer sarcomere lengths (see below). In favour of A1 representing a crossbridge state is the fact that the quantity or proportion changes with age but more importantly increases in the presence of Pi. It is unlikely that a simple series compliance would increase in quantity with the addition of Pi, while such behaviour is entirely in keeping with a shift in crossbridge intermediate states towards the Pi bound state, as originally suggested by Stienen et al. (1992).

6.2.3 Residual force enhancement

In all the experiments reported here there was an additional force remaining after the stress relaxation, which was higher than the isometric force before the stretch. This has been called residual force enhancement (FE) and has been studied by several authors (Abbott & Aubert, 1952; Edman et al., 1982; Rassier et al., 2003; Herzog, 2014). Although the underlying nature of this phenomenon are still unclear, it is established that FE is dependent on the length of the stretch and independent of the velocity of stretch, and as shown here in Chapter 2 (section 2.3.2.3). These characteristics are well explained by the presence of the structural protein titin in the muscle fibre (Herzog, 2014).

6.3 Effects of inorganic phosphate on the force response of young muscle

It has been demonstrated by de Ruiter et al. (2000) that fatigue alters the force response to stretch and this may be due to increased intracellular levels of inorganic

phosphate accumulating during fatiguing contractions (Allen & Westerblad, 2001). Inorganic phosphate is one of the products of ATP hydrolysis, together with ADP, that is released during the cyclic interaction of the actin and myosin. According to the Scheme 1 presented in the Introduction (section 1.3), the production of force occurs before the release of Pi (Kawai & Halvorson, 1991; Tesi et al., 2000; Caremani et al., 2008). Several studies have shown how the addition of different concentrations of Pi decrease the isometric force (Potma et al., 1995; Tesi et al., 2000) but had no effects on the maximum velocity of shortening (Osterman & Arner, 1995; Widrick, 2002). The decrease in isometric force with addition of phosphate is said to be due to a decrease in the number of attached cross bridges, while the force per cross bridge remains the same (Caremani et al., 2008). The key feature of this model is that there are no low force crossbridges.

6.3.1 Effects of inorganic phosphate on stretch response

Stienen et al. in 1992, found that the force during isovelocity lengthening contractions at different speeds, was higher in the presence of 15 mM Pi than in the absence of phosphate when normalised to the isometric value. This finding was also observed in the work presented here; the *Fpeak/Fo* was increased with increasing [Pi] at all three lengthening velocities mostly due to a decrease in *Fo* while the additional force generated during the stretch was similar with or without Pi. Stienen explained this in terms of the added Pi shifting the cross bridge states and increasing the proportion of low force cross bridges which, while generating little or no force, were nevertheless attached and would produce force when stretched. It is logical to associate the force-producing state with cross bridges that have released Pi (AM.ADP) and the low- or non-force-producing states with ones that retain Pi (AM'.ADP.Pi) but if the AM'.ADP.Pi state generates full force then the low force state must be the preceding state, A-M.ADP.Pi (see section 1.3). This implies that reaction 4 in the scheme is readily reversible when AM'.ADP.Pi accumulates in the presence of added Pi. This model fits the data presented here but is clearly in conflict with the model of Caremani et al. (2008) which suggests that all attached cross bridges develop force. This is not the only problem with the Caremani model since Woledge et al. (2009) pointed out that the idea that all attached cross bridges generate the same force is difficult to reconcile with temperature jump experiments. The transition A-M.ADP.Pi to AM'.ADP.Pi in reaction 4 is thought to be endothermic and the rapid development of force when a fibre is transferred from cold to warm implies that cross bridges are attached but not generating force in the cold. Linari et al. (2000) propose that during a stretch the strain on the first myosin head brings the second head into a position where it can attach to the actin filament and the additional force is then due to the combination of the two

heads. Thus, force during a stretch might be expected to be about twice that of an isometric contraction and this is generally the case. *Fpeak* was between 150 and 250% *Fo* at the different velocities of stretch in the absence of added Pi (Figure 5.3). If, as implied by Caremani et al. (2008), the reduction in isometric force in the presence of Pi was due to a decrease in the number of attached cross bridges, then the maximum force during stretch should still be about twice the isometric force. This, however, was not the case as *Fpeak* was between 300 and 400% *Fo* at the different velocities of stretch (Fig 5.4).

6.3.2 Effects of inorganic phosphate on the residual force enhancement

The absolute values of the force enhancement was not affected by the presence of different concentrations of inorganic phosphate. When the FE was normalised to the isometric force before the stretch, it increased with increasing Pi, but this simply reflected the decrease in *Fo* with added Pi. This observation is in agreement with the idea that the force enhancement is not cross bridge related, but related to a structural protein, titin.

6.4 Effects of ageing on the force response to stretch

Age-related changes in contractile properties of muscle during isometric and shortening contractions have been widely studied but there is not much literature concerning the effects of ageing on the force response to eccentric contractions. The results presented in Chapter 4 show changes in isometric force, specific force and shortening velocity which reflect growing and maturational stages over the ages of 3, 10 and 18 months while the changes between 18 and 32 months represent true ageing. These changes are very similar to those reported in the literature and are reviewed in Chapter 4.

6.4.1 Force exerted during lengthening contractions: ageing effects.

There is a general belief that the force exerted by muscle whilst being stretched is better maintained with age than that of isometric or shortening contractions, based on the work of several authors (Vandervoort et al., 1990; Phillips et al., 1991; Brooks & Faulkner, 1994; Hortobágyi et al., 1995) investigating either human or mouse muscle. However, this is not a universal conclusion as Lindle et al., in 1997 studied a large human population and determined that the eccentric force was no better maintained with age than the isometric or concentric force. The results presented in Chapter 4 support the findings of Lindle et al rather than those of the earlier studies. In addition to differences in the kinetics of cross bridge function as discussed in section 6.3, there

are a number of other factors that may affect the response to stretch and could account for some of the discrepancies between the present finding and those of previous studies. These include different proportions of connective tissue or changes in compliance of connective tissue and tendons, differences in temperature and differences in fibre type composition. Of these various possibilities, changes in fibre type composition may be the best explanation of the relative preservation of force during stretch seen in the whole muscle preparations of Vandervoort et al. (1990); Phillips et al. (1991); Brooks & Faulkner (1994); Hortobágyi et al. (1995). Linari et al. in 2003, testing fast and slow human fibres, showed that the slow fibres generate relatively low isometric force but similar forces to fast fibres when stretched. Consequently the ratio *Fpeak/Fo* was greater for slow fibres in much the same way as reported for whole muscle preparations. An increase in the proportion of slow fibres is a well-documented change that occurs with muscle ageing (Chan & Head, 2010). There are two other studies of ageing that used single fibre preparations at the same temperature as in the present study. Ochala et al. (2006) examined both type I and IIa human fibres and used a step increase, as opposed to the ramp stretch used here. The authors make reference to "age- related preservation of the tension increments" but the data in the two tables quite clearly show no preservation of force in either fibre type. The only significant difference between young and old was in the time of T3, the secondary rise in force after the initial drop following the step. The biological significance of this is far from clear. Brooks & Faulkner (1994) used rat EDL single fibres (12- and 27-month-old) at 15ºC and reported that the force during stretch was better maintained relative to isometric force in the older animals. Whether there are differences between fast and slow muscle with respect to ageing is a topic that might reward further investigation.

6.4.2 Effects of ageing on the stress relaxation

When studying the stress relaxation in fibres of different age-groups there was, in reality, very little difference in the relaxation curves. There was, however, a trend for relaxation to become somewhat faster with age, being particularly noticeable in the oldest groups, 18 and 32 months. This phenomenon was more obvious at the faster stretches. Analysing the SR curves as double exponentials and making the assumption that the rate constants for a given velocity of stretch were the same at all ages, there was a shift in the proportions of A1 and A2, with a significantly greater proportion of the faster A2 component in the older fibres. The A1 component is suggested to be the low force state which nevertheless sustains a normal force during stretch and thus a high *Fpeak/Fo*. It follows that if A2 is increased, as in the 32 months fibres then the *Fpeak/Fo* would be expected to be reduced and indeed, compared with

the 18 months fibres, the oldest fibres did show a trend for a lower *Fpeak/Fo* (Figure 4.6).

6.5 Effects of phosphate on the response to stretch of old muscle

One of the aims of Chapter 5 was to study how the presence of phosphate would affect the muscle force response of different ages, thus, expanding the work presented in Chapter 3. The original reason for being interested in the relationship between age and the effect of Pi on stretch was the similarity between the reported preservation of the eccentric force in older muscles and the effect of added Pi, both increasing *Fpeak/Fo*. In the event, the present study has found no such preservation of eccentric force with the oldest muscle fibres, in fact a trend in the opposite direction was observed, with a decrease in *Fpeak/Fo* and somewhat faster SR in the oldest fibres. Nevertheless there is some interest in determining the effect of Pi on ageing muscle since it was suggested in Chapter 5 that in the oldest muscle there was an increased proportion of the faster A2 component and if this were the case then adding Pi would be expected to reverse this effect.

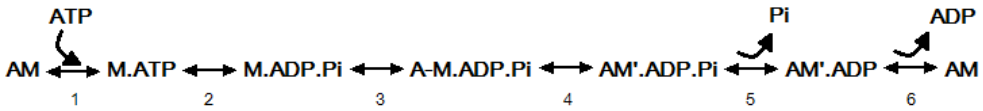

Figure 6.1: Scheme of cross bridge ATPase cycle

The value of *Fpeak/Fo* in the absence of added Pi was lower in the 32 months fibres compared with the 18 months fibres but with the addition of Pi the values became similar (Fig 5.3). Likewise there was a greater proportion of A2 in the oldest fibres but in the presence of added Pi the proportions of A1 and A2 became similar to those of the younger fibres (Fig 5.5). This result confirms the suggestion that the oldest fibres have a different content of cross bridge intermediates compared with young fibres, the implication being that they contain a higher proportion of the high force states and different equilibrium states of either reactions 4 or 5 in the reaction scheme discussed in Chapter 1. If it were reaction 4 then young and old muscle might show differences in the temperature dependence of force since reaction 4 is thought to be endothermic in the forward direction. Having a higher proportion of cross bridges in the high force state clearly does not explain the lower specific force of the older fibres but is consistent

with the lower *Fpeak/Fo*. It is difficult to see any functional consequences of this shift in crossbridge intermediate states.

6.6 Summary

In summary, the work described in this thesis has added weight to the original suggestion by Stienen et al. (1992) that during a ramp stretch the additional force is the result of stretching low force cross bridges and the proportion of these is increased in the presence of added Pi. The unique contribution of the present work is to quantify these effects by determining the proportions of A1 and A2 by analysis of the stress relaxation curves. Further work remains to be done to reconcile these conclusions with those of Caremani et al. (2008), possibly by making detailed measurements of stiffness during a stretch and SR, which take into account the compliance of the thick and thin filaments. The other aspect of this thesis concerns the response of older muscle to stretch and here the conclusions contradict much of the published literature. However, there are no other comparable studies using the same fibre types and temperature and future work might investigate the behaviour of fast fibres to repeat the study of Brooks & Faulkner (1994) and use higher temperatures as in the work of Phillips et al. (1991).

References

Abbott, B. C., & Aubert, X. M. (1952). The force exerted by active striated muscle during and after change of length. *Journal of Physiology*, *117*, 77–86.

Allen, D. G., & Westerblad, H. (2001). Role of phosphate and calcium stores in muscle fatigue. *The Journal of Physiology*, *536*(Pt 3), 657–65.

Brooks, S. V, & Faulkner, J. A. (1994). Isometric, shortening and lengthening contractions of muscle fiber segments from adult and old mice. *The American Journal of Physiology*, *267*, C507–13.

Caremani, M., Dantzig, J., Goldman, Y. E., Lombardi, V., & Linari, M. (2008). Effect of inorganic phosphate on the force and number of myosin cross-bridges during the isometric contraction of permeabilized muscle fibers from rabbit psoas. *Biophysical Journal*, *95*(12), 5798–808.

Cavagna, G. (1993). Effect of temperature and velocity of streching on stress relaxation of contracting frog muscle fibres. *Journal of Physiology*, *462*, 161–173.

Chan, S., & Head, S. I. (2010). Age- and Gender-Related Changes in Contractile Properties of Non-Atrophied EDL Muscle. *PloS One*, *5*(8), 20–22.

Colomo, F., Lombardi, V., Menchetti, G., & Piazzesi, G. (1989). The recovery of isometric tension after steady lengthening in tetanized fibres isolated from frog muscle. *Journal of Physiology*, *415*, 130P.

D'Antona, G., Pellegrino, M. A., Carlizzi, C. N., & Bottinelli, R. (2007). Deterioration of contractile properties of muscle fibres in elderly subjects is modulated by the level of physical activity. *European Journal of Applied Physiology*, *100*(5), 603–611.

Edman, K. a, Elzinga, G., & Noble, M. I. (1978). Enhancement of mechanical performance by stretch during tetanic contractions of vertebrate skeletal muscle fibres. *The Journal of Physiology*, *281*, 139–155.

Edman, K. a, Elzinga, G., & Noble, M. I. (1982). Residual force enhancement after stretch of contracting frog single muscle fibers. *The Journal of General Physiology*, *80*(5), 769–784.

Getz, E. B., Cooke, R., & Lehman, S. L. (1998). Phase transition in force during ramp stretches of skeletal muscle. *Biophysical Journal*, *75*(6), 2971–2983.

Herzog, W. (2014). The role of titin in eccentric muscle contraction. *The Journal of Experimental Biology*, *217*(Pt 16), 2825–33.

Hortobágyi, T., Zheng, D., Weidner, M., Lambert, N. J., Westbrook, S., & Houmard, J. A. (1995). The influence of aging on muscle strength and muscle fiber characteristics with special reference to eccentric strength. *The Journals of Gerontology. Series A, Biological Sciences and Medical Sciences*, *50*(6), B399–406.

Kawai, M., & Halvorson, H. R. (1991). Two step mechanism of phosphate release and the mechanism of force generation in chemically skinned fibers of rabbit psoas muscle. *Biophysical Journal*, *59*(February), 329–342.

Linari, M., Bottinelli, R., Pellegrino, M. A., Reconditi, M., Reggiani, C., & Lombardi, V. (2003). The mechanism of the force response to stretch in human skinned muscle fibres with different myosin isoforms. *The Journal of Physiology*, *554*(Pt 2), 335–52.

Lindle, R. S., Metter, E. J., Lynch, N. A., Fleg, J. L., Fozard, J. L., Tobin, J., … Hurley, B. F. (1997). Age and gender comparisons of muscle strength in 654 women and men aged 20-93 yr. *Journal of Applied Physiology (Bethesda, Md. : 1985)*, *83*(5), 1581–7.

Ochala, J., Dorer, D. J., Frontera, W. R., & Krivickas, L. S. (2006). Single skeletal muscle fiber behavior after a quick stretch in young and older men: a possible explanation of the relative preservation of eccentric force in old age. *Pflügers Archiv : European Journal of Physiology*, *452*(4), 464–70.

Osterman, a, & Arner, a. (1995). Effects of inorganic phosphate on cross-bridge kinetics at different activation levels in skinned guinea-pig smooth muscle. *The Journal of Physiology*, *484 Pt 2*(1995), 369–83.

Phillips, S. K., Bruce, S. A., & Woledge, R. C. (1991). In mice, muscle weakness due to age is absent during stretching. *Journal of Physiology*, *437*, 63–70.

Pinniger, G. J., Ranatunga, K. W., & Offer, G. W. (2006). Crossbridge and non-crossbridge contributions to tension in lengthening rat muscle: force-induced reversal of the power stroke. *The Journal of Physiology*, *573*(Pt 3), 627–43.

Potma, E. J., van Graas, I. A., & Stienen, G. J. (1995). Influence of inorganic phosphate and pH on ATP utilization in fast and slow skeletal muscle fibers. *Biophysical Journal*, *69*(6), 2580–9

Rassier, D. E., Herzog, W., Wakeling, J., & Syme, D. a. (2003). Stretch-induced, steady-state force enhancement in single skeletal muscle fibers exceeds the isometric force at optimum fiber length. *Journal of Biomechanics*, *36*(9), 1309–1316.

Stienen, G. J., Versteeg, P. G., Papp, Z., & Elzinga, G. (1992). Mechanical properties of skinned rabbit psoas and soleus muscle fibres during lengthening : effects of phosphate and Ca^{2+}. *Journal of Physiology*, *451*, 503–523.

Sugi, H. (1972). Tension changes during and after stretch in frog muscle fibres. *Journal of Physiology*, 237–253.

Tesi, C., Colomo, F., Nencini, S., Piroddi, N., & Poggesi, C. (2000). The effect of inorganic phosphate on force generation in single myofibrils from rabbit skeletal muscle. *Biophysical Journal*, *78*(6), 3081–3092.

Vandervoort, a a, Kramer, J. F., & Wharram, E. R. (1990). Eccentric knee strength of elderly females. *Journal of Gerontology*, *45*(4), B125–8. Retrieved from

Widrick, J. J. (2002). Effect of P-i on unloaded shortening velocity of slow and fast mammalian muscle fibers. *Amer.J.Physiol Cell Physiol*, *282*(4), C647–C653.

Woledge, R. C., Barclay, C. J., & Curtin, N. a. (2009). Temperature change as a probe of muscle crossbridge kinetics: a review and discussion. *Proceedings. Biological Sciences / The Royal Society*, *276*(1668), 2685–95.

APPENDIX A

Hysteresis in muscle

A.1 Abstract

This paper presents an introduction to hysteresis from a broad range of scientific disciplines and demonstrates a variety of forms including clockwise, counter clockwise, butterfly, pinched and kiss-and-go, respectively. For the first time, as far as the authors are aware, kiss-and-go hysteresis is demonstrated in single fibre muscle when subjected to both, lengthening and shortening periodic contractions. The hysteresis observed in the experiments is of two forms. Without any relaxation at the end of lengthening or shortening, the hysteresis loop is a convex clockwise loop, whereas a concave clockwise hysteresis loop (labelled as kiss-and-go) is formed when the muscle is relaxed at the end of lengthening and shortening. Future research will focus on finding other types of hysteresis and investigating critical slowing down in muscle.

A.2 Introduction

In 1885, Sir James Alfred Ewing first coined the term hysteresis whilst showing the persistent effects on ferric metals exposed temporarily to magnetic fields (Ewing, 1885). The irreversibility of the magnetisation and demagnetisation processes makes these hysteretic devices useful as magnetic memory, and indeed, the magnetic memory characteristics of chromium and iron oxides has led to the continued development of magnetic storage media used to store computer data as well as audio and video signals (Piramanayagam & Chong, 2011). Hysteresis is the time-based dependence of a system's output based on present and past outputs. In some applications, the input-output diagram is the same at every frequency. Such systems have *rate independent hysteresis*. However, in most systems the dynamic response changes with the input frequency giving distinct diagrams for different frequencies of excitation. Therefore, these systems have *rate dependent hysteresis* (Muller & Xu, 1991). As muscle tires with repeated use it is not surprising to find that hysteresis in muscle is rate dependent. The two essential ingredients for hysteresis are nonlinearity and feedback. Hysteresis is not a new phenomenon, indeed it abounds throughout the realms of science. Hysteresis has its foundations in physics, in elasticity (Muller & Xu, 1991), in ferroelectric and ferromagnetic materials (Smith et al., 2006; Damjanovic, 2005) and Lynch et al. have demonstrated hysteresis in a wide range of nonlinear optical resonators and microfiber ring resonators (Lynch & Steele, 2011; Lynch et al., 2015). In electric circuits, Borresen and Lynch (2002), have demonstrated hysteresis in Chua's electrical circuit for the first time. In mechanical engineering, hysteresis is possible between multiple stable limit cycles (Lynch & Christopher, 1999) when investigating surge in jet engines and wing rock phenomena in modern aircraft. In

chemical kinetics, simple models of Hopf bifurcation in a Brusselator model and hysteresis in an autocatalytic chemical reaction are demonstrated (Lynch, 2011). In economics, hysteresis is present in inflation-unemployment models (Ball, 2009). In biology, there is hysteresis in blood cell population dynamics (Lynch, 2005) and neuronal networks (Lynch & Bandar, 2005), and hysteresis is present in cell biology (Pomenering et al., 2003), genetics (Kramer & Fussenegger, 2005), immunology (Das et al., 2009), angiogenesis and haematopoiesis (Lynch & Borresen, 2015) and Noori (2014), covers more general examples of hysteresis phenomena in biology. Many nonlinear dynamical systems display hysteresis when some form of feedback mechanism is present. When modeling systems mathematically, bifurcation diagrams are plotted in order to display the hysteresis phenomena using packages such as MATLAB^{R} , Maple^{TM} and Mathematica^{R} (Lynch, 2014, 2010, 2007). The second iterative method is adopted where a parameter is varied and the solution to the previous iterate is used as the initial condition for the next iterate. In this case, there is a history associated with the process and only one point is plotted for each value of the parameter. For example, most of the bifurcation diagrams plotted in this section were plotted using the second iterative method. The system has to have at least two stable steady states which could be fixed points, critical points or stable limit cycles. The different forms of hysteresis will now be illustrated by means of example.

A.2.1 Biological hysteresis

A.2.1.1 Agar gel

For most biologists, if not all, agar is a well-known gelling agent in solid media used commonly in microbiology. It is defined as a hydrophilic colloid that contains two major fractions, agarose, which is the gelling fraction, and the non-gelling fraction agaropectin. Agar is found as the supporting structure of the cell walls in a certain species of algae and the interest for this study is the characteristic “gelation hysteresis“, as shown in Figure 1, between the melting and setting temperature. Typically, agar gels at temperatures between 32º and 45º when cooled, depending on the used seaweed, and needs to be heated above 90º to melt and form a good solution (Armisen & Galatas, 1987; Lahaye & Rochas, 1991).

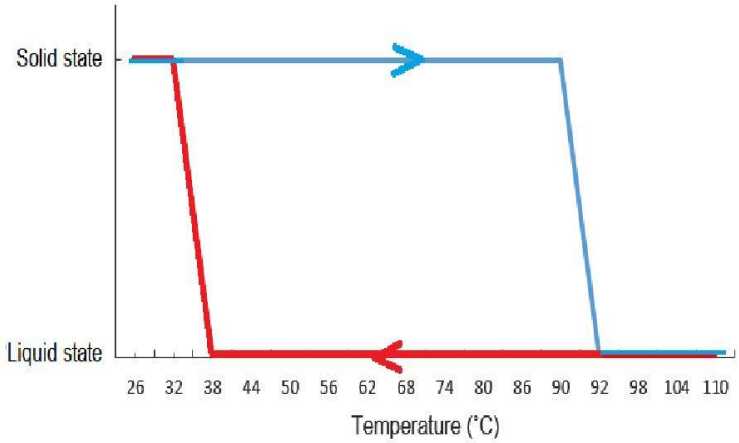

***Figure A.1**. Clockwise hysteresis cycle between the melting and setting temperatures, 32º and 90º, respectively, of the agar gel. Whether the agar is solid or liquid at a certain temperature between the melting and gelling states will depend on the previous state of the substance.*

A.2.2 Mechanical hysteresis

A.2.2.1 The preloaded two-bar linkage mechanism

Historically, muscle has been modeled using springs and dashpots and so this section includes those type of models. Drincic and Berstein (2011), analysed the dynamics of a two-bar linkage mechanism with joints P, Q and R, preloaded by a stiffness k, as shown in Figure A.2. A periodic force F is applied at Q, where the two bars are joined by a frictionless pin. The angle θ denotes the counter clockwise angle the left bar makes with the horizontal, q denotes the distance between P and R, and x is the distance between the joint Q and the horizontal dashed line shown in Figure 2.

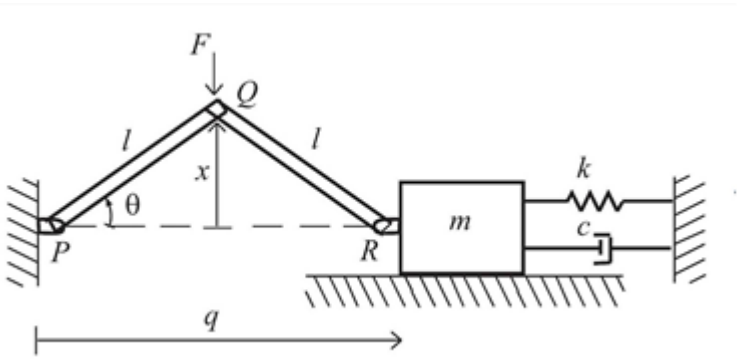

***Figure A.2:** The preloaded two-bar linkage with a periodic force F acting at the joint Q. As the point Q moves vertically up and down, the mass m moves horizontally left and right.*

Then,

$$x = l \sin \theta \quad \text{(A.1)}$$

$$q = 2l \cos \theta \quad \text{(A.2)}$$

$$F = \sin(\omega t) \tag{A.3}$$

The equations of dynamics for the preloaded two-bar linkage are given by

$$\left(\left(2ml^2 + \frac{9}{8}m_{bar}l^2\right)\sin^2\theta + \frac{5}{24}m_{bar}l^2\right)\ddot{\theta} + \left(\left(2ml^2 + \frac{9}{8}m_{bar}l^2\right)\sin\theta\cos\theta\,\dot{\theta}^2\right.$$
$$\left. + 2cl^2\sin^2\theta\,\dot{\theta} + 2kl2\,(\cos\theta 0 - \cos\theta)\sin\theta = \frac{-l\cos\theta}{2}F, \right. \tag{A.4}$$

And the dynamics in terms of the displacement q, using equations A.1 to A.4 is given by

$$\left(\left(m + \frac{9}{16}m_{bar}\right)(4l^2 - q^2) + \frac{5}{12}m_{bar}l^2\right)(4l^2 - q^2)\ddot{q} + \frac{5}{12}m_{bar}l^2q\dot{q}^2$$
$$+ c\dot{q}(4l^2 - q^2)^2 + k(q - q_0)(4l^2 - q^2)^2 = \frac{1}{2}q\,(4l^2 - q^2)^{3/2}F \tag{A.5}$$

Equations (A.4) and (A.5) represent the linkage dynamics under a periodic external force F. As in (Drincic & Bernstein, 2011), take parameter values k = 1 (N/m), m = 1 (kg), c = 1 (Ns/m), m_{bar} = 0.5 (kg) and l = 1 (m). Figure A.3 shows the hysteresis loop for the vertical force F, measured in Newtons, against the vertical displacement x, measured in metres. This figure demonstrates a clockwise hysteresis loop. Note the ringing at either end of the hysteresis loop where the steady state oscillates before settling on to a stable critical point. This ringing phenomenon is a standard feature with hysteresis loops. Note also that the area bounded by the hysteresis loop represents the energy dissipated in one cycle and is proportional to the frequency of stimulation.

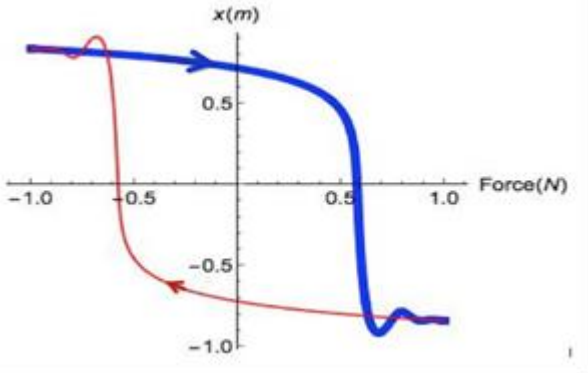

Figure A.3: *Input-output clockwise hysteresis loop between F and x at ω=0.05 radians per second. The area of the loop is the energy dissipated in a complete cycle and is proportional to the frequency of stimulation. The lower the frequency, the lower the dissipated energy, thus, the smaller the area of the loop. Note the ringing at the ends of the hysteresis loop, a common occurrence in hysteresis. The parameters used are k = 1 (N/m), m = 1 (kg), c = 1 (Ns/m), mbar = 0.5 (kg), l = 1 (m) and F = sin (ωt). As with other hysteresis loops shown in this section, the blue curve represents ramp up, in this case F decreases from F = 1 to F = -1.*

Figure A.4 shows the hysteresis loop for the vertical force F, measured in Newtons, against the horizontal displacement q. This hysteresis loop has been labeled a butterfly hysteresis.

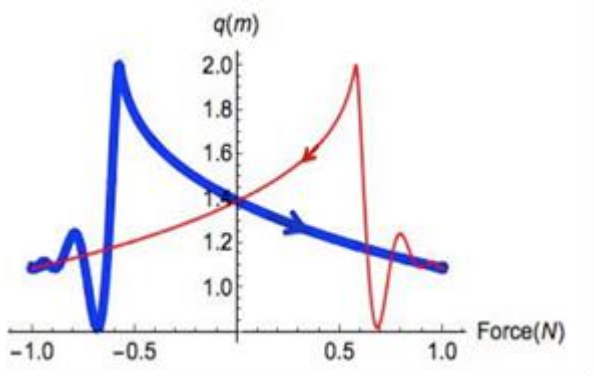

Figure A.4: *Input-output map between the vertical force, F, and the horizontal displacement q, given by equation (A.5) at a low frequency ω=0.05 (rad/s). Note the ringing at the ends of the hysteresis loop. The parameters used are k = 1 (N/m), m = 1 (kg), c = 1 (Ns/m), mbar = 0.5 (kg), l = 1 (m) and F = sin (ωt).*

A.2.2.2. The periodically forced nonlinear pendulum

The Duffing equation can be used to model different physical systems. Here it is used to model a pendulum that is periodically driven and it has a nonlinear restoring force (Lynch, 2014). A diagram of this system is presented in Figure A.5. The equation modelling this system is given by

$$\ddot{x} + k\dot{x} + (x^3 - x) = \Gamma\cos(\omega t) \qquad \text{(A.6)}$$

Where k is a damping coefficient, $\dot{x}$ is the speed of the mass, Γ is the amplitude of force vibration and ω is the frequency of the driving force. Consider the Poincaré map of system (A.6) as the amplitude Γ varies when k and ω are fixed. The radius of the limit cycle on the Poincaré section is given by r.

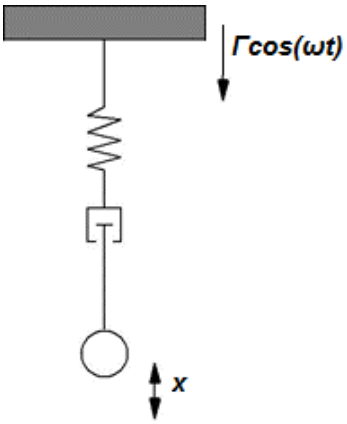

Figure A.5: *Periodically forced pendulum with a cubic spring. The driving force is given by F = Γcos(ωt) and x represents the displacement from equilibrium.*

Figure A.6 shows the hysteresis loop for a nonlinear pendulum when k = 0.1, ω = 1.25 and the forcing amplitude is ramped up from Γ = 0 to Γ = 0.12 and then ramped back down again. There is a clockwise hysteresis loop and the steady states in this case are both stable limit cycles. The examples illustrating wing rock and surge in jet engines (Lynch & Christopher, 1999) also involve multiple steady states made up of stable limit cycles.

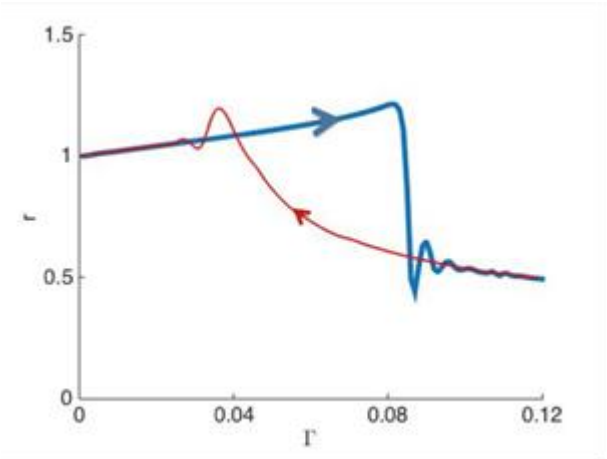

Figure A.6: *Plot of Γ vs r for the nonlinear pendulum. Note the ringing at the ends of the hysteresis loop. The steady states in this case are stable limit cycles. The parameters used in this case were k = 0.1, ω = 1.25 (rad/s), where Γ is linearly ramped up from Γ = 0 to Γ = 0.12, and then ramped back down again.*

Chaotic phenomena in human-like reaching movements using a two-link arm mechanism driven by six muscles is described by Rahatabad et al. (2011), where bifurcation maps, Lyapunov exponents and power spectra are employed to detect the chaos. In 1994, Webber and Zbilut applied recurrence plot strategies to assess physiological states such as respiration and muscle fatigue dynamically. The methodology is applicable to any rhythmical system including chemical, electrical, hormonal, neural and mechanical, and provides a nonlinear diagnostic tool in

assessing physiological systems and states. Chaos and chaos control in cardiac muscle has been extensively investigated, see (Weiss et al., 1999; Gauthier et al., 2002), in terms of heart rate variability and arrhythmic mortality, and practical applications of chaos theory to the modulation of human ageing were proposed by Kyriatzis et al. in 2003. A simple example of a system displaying hysteresis affected by chaos is now described.

A.2.3 Optical hysteresis and chaos

Optical hysteresis, or optical bistability, as it is sometimes known, was first proposed by Szoke et al. in 1969. There has been an immense amount of interest in it regarding its potential applications in high-speed all-optical signal processing, all-optical computing and more recently, optical sensing (Lynch & Steele, 2011). For optical hysteresis, nonlinearity is provided by the medium as a refractive (or dispersive) or absorptive nonlinearity, or both. The feedback is introduced through mirrors or fibre loops. A block diagram of the Simple Fibre Ring (SFR) resonator is shown in Figure A.7.

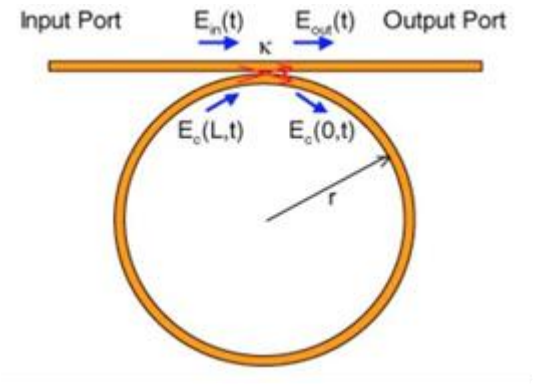

Figure A.7: *A schematic of the SFR resonator. The electric fields entering and leavind the fibre ring are indicated. The parameter k represents the power-splitting ratio at the coupler and L is the length of the fibre loop.*

Three different forms of hysteresis, namely, clockwise, counter-clockwise and butterfly, are all displayed in one system when modelling a homogeneously broadened two-level atomic system in a ring cavity within and without the rotating wave approximation (Lynch et al., 2015). By considering the famous Maxwell-Bloch and Maxwell-Debye equations, Ikeda (Ikeda, 1979; Ikeda et al., 1980) theoretically investigated a nonlinear absorbing medium containing two-level atoms situated in a bulk ring cavity. He was able to demonstrate that optical circuits exhibiting optical hysteresis could also contain

temporal instabilities, or chaos. Subject to certain constraints Ikeda was able to demonstrate that the complicated delay differential equations could be approximated by a much simpler discrete complex system (Lynch, 2014). What's more, this simple system also accurately models the SFR (Lynch et al., 1998). The iterative equation is given by

$$E_{n+1} = A + B\,E_n\,e^{-i|En|^2}, \qquad \text{(A.7)}$$

Where $A = i\sqrt{1-k}E_{in}$, $B = \sqrt{k}$ and E_j is the electric field amplitude at the j_{th} circulation around the fibre loop. A bifurcation diagram for system (A.7) is shown in Figure A.8, where a counter-clockwise loop is clearly visible. Note that, to the right of the hysteresis loop is a period doubling cascade to chaos. As the parameter $B = \sqrt{k}$ increases, and more light is allowed to circulate in the fibre loop, the chaos shifts to the left and swamps the hysteresis loop, which should be avoided for applications.

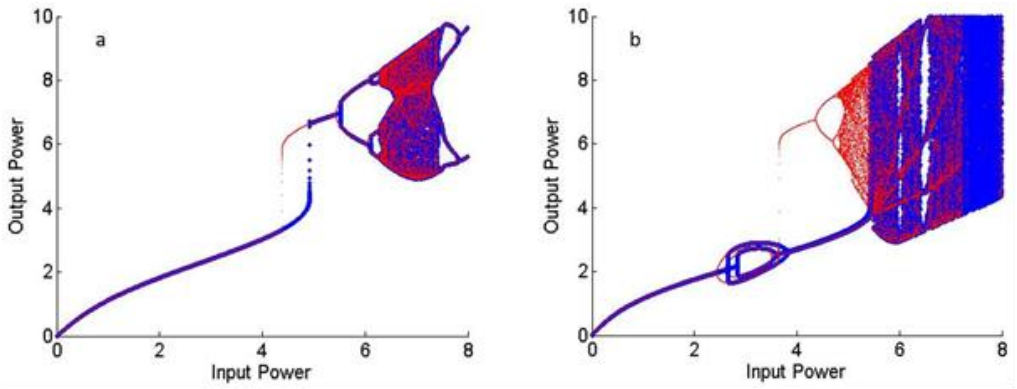

Figure A.8: *Bifurcation diagram of the SFR resonator, the power $|A|^2$ was ramped up from 0 (Wm^{-2}) to 8 (Wm^{-2}), and back down again. (a) When B = 0.15, the isolated counter-clockwise hysteresis loop (bistable region) is followed by a region of period-doubling to chaos. (b) When B = 0.24, instabilities encroach upon the hysteresis cycle at both ends.*

A.2.4 Memristors and pinched hysteresis

Professor Leon Chua is widely acknowledged as the father of nonlinear circuit theory. For many decades it was believed that there are three fundamental electronic components, the resistor, the inductor and the capacitor, and many biological systems, such as the famous Hodgkin-Huxley system used to model the giant squid axon (Hodgkin & Huxley, 1952), were simulated using these components. It is now known that there is another fundamental circuit element, and its sub-elements (Qingjiang et al., 2014), called the memristor. Chua (1971), used mathematics to prove the existence of the fourth nonlinear fundamental nonlinear element which relates flux and charge

and he gave the name to this component. In 1976, Chua and Kang discovered that a memristor displays a pinched hysteresis, which is shown in Figure A.9. It is now understood that memristors have been around for hundreds of millions of years as they existed in plants and early life forms (Prodromakis et al., 2012). More recently, Chua (2013) was able to correct a mistake in the Hodgkin-Huxley equations by introducing a memristor term into their equations. The next section is concerned with hysteresis in muscle where a kiss-and-go phenomena is observed for the first time.

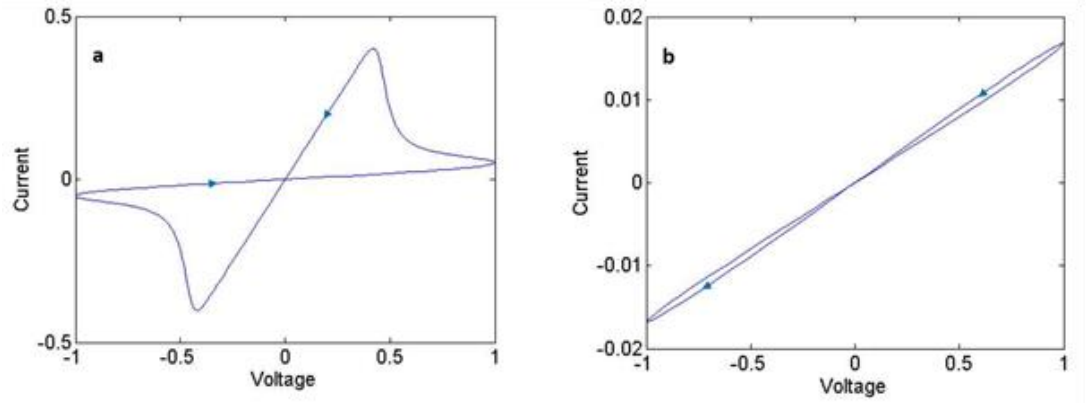

Figure A.9: *Pinched hysteresis of a memristor in the I − V plane. (a) For low frequencies there is a definite pinched hysteresis. (b) As the frequency gets higher, the pinched hysteresis degenerates and the memristor acts like a linear resistor. For more details see (Lynch, 2014).*

A.3 Materials and methods

A.3.1 Muscle samples

Soleus muscles were dissected from 18-month-old (adult male, gtf2ird2) mice. The animals were humanely killed using approved schedule 1 methods (cervical dislocation) for other research projects approved by the local Animal Ethics Research Committee of the University of Manchester. This is in accord with the generally accepted guideline of reducing animal numbers to a minimum in biomedical research. The right soleus muscle was rapidly excised, weigh and immersed in glycerol/relax solution at 4º for 24 hours. It was then treated with increasing concentrations of sucrose (Degens et al., 2010), which acts as an effective cryoprotectant, preventing damage of the contractile properties of the fibres. After sucrose-treatment, muscles were frozen in liquid nitrogen and stored at -80º for later use.

A.3.2 Solutions

The composition of the solutions have been described previously (Larsson & Moss, 1993; Giliver et al., 2009; Degens et al., 2010). The relaxing solution contained (mM): MgATP, 4.5; free Mg^{2+}, 1; imidazole, 10; EGTA, 2 and KCl, 100 and the pH was adjusted to 7.0 using KOH. The Glycerol/relax was the same as relaxing solution containing 50% (v/v) glycerol. The pCa (-log[free Ca^{2+}]) of the activating solution was 4.5 and contained: MgATP, 5.3; free Mg^{2+}, 1; imidazole, 20; EGTA, 7; creatine phosphate, 19.6; KCl, 64 with pH 7.0.

A.3.3 Preparation of single fibres

The procedures for preparing single fibres have been described previously (Degens et al., 2010; Gilliver et al., 2011). Briefly, fibre bundles were taken from the -80º storage, thawed and treated with decreasing concentrations of sucrose and stored in glycerol/relax at -20º for use within a month. The day of experiments, a small bundle was cut from the muscle and immersed in relaxing solution containing 1% Triton X-100 for 20 minutes to permeabilise the membranes and sarcoplasmic reticulum. After this, single fibres were teased from one end of the bundle and mounted in a permeabilised-fibre test system (400 Aurora Scientific Inc. Ontario, Canada). With the fibre mounted and immersed in relaxing solution, it was tied with nylon thread to fine insect pins attached to a force transducer (Aurora, 403) and a lever motor arm (Aurora, 312). The sarcomere length (sl) of the resting fibre was set at 2.6µm and checked along the length of the fibre. Fibre length (lo) was determined and checked at regular intervals thereafter. Fibre diameter was measured at three places along the length of the fibre while submerged in relaxing solution and the cross-sectional area calculated assuming the fibre to have a circular cross-section (Gilliver et al., 2010). All experiments were carried out at 15º.

A.3.4 Methods

Fibres were transferred from the relaxing to the activating solution (pCa 4.5). When the isometric force (*Fo*) reached a plateau, the fibre was subjected to length changes following a bipolar triangle input with an amplitude of 5% at a frequency of 0.25(s^{-1}). A set of five fibres, one at a time, was used for this type of protocol. Then, another set of 20 fibres, one at a time, was subjected to the same wave with an extra resting time between the positive and negative half. The amplitudes for this second type of input were 3% or 5% of lo at different frequencies starting from f=0.125 (s^{-1}) up to 1.25(s^{-1}).

Examples of the length change inputs and their corresponding force outputs are shown in Figure A.10, where *Fo* and lo are the initial values of force and length respectively. The positive half of the input wave corresponded to stretches of either 3% or 5% of lo after which the fibre was returned to lo. On the other hand, the negative half corresponded to shortening contractions of the fibre, by the same percentages.

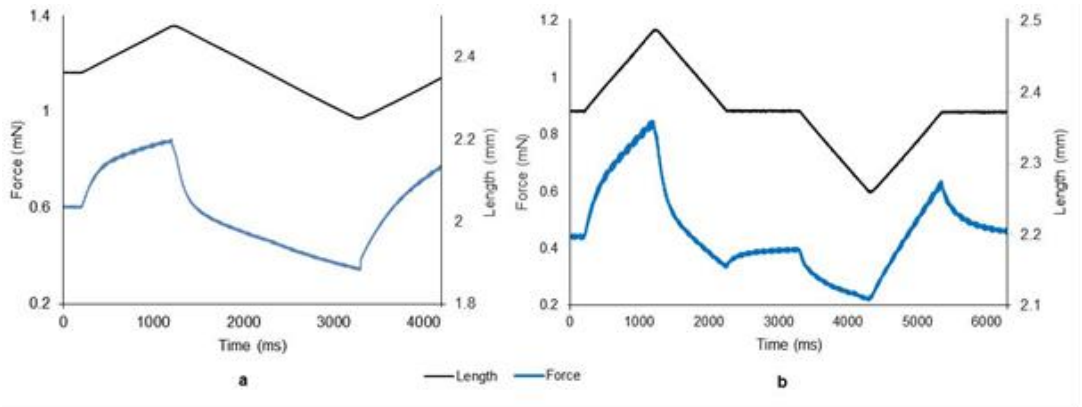

Figure A.10: *Force response (blue curve) to a change in the fibre length (black curve). In case a, there is no rest between stretch and contraction, while in case b there are short rest periods. The amplitude of the length change in both examples is 5% of lo, and the frequency is f=0.25(s^{-1}) for a and f =0.167(s^{-1}) for b.*

A.3 Results

A.3.1 Force response to a 5%lo length change

In this section, the force-length relationship is plotted for a set of trials. It must be noted that in all the figures to follow, the origin of coordinates is where *F=Fo* and l=lo. The absolute values of these variables are different between fibres, therefore the origin is indicated in each figure. The response that appears in Figure A.11 is a clockwise hysteresis loop representing the force-length relationship to one period of the bipolar triangle input shown in Figure A.10(a). Similar hysteresis loops were obtained with other fibres when there is no rest period.

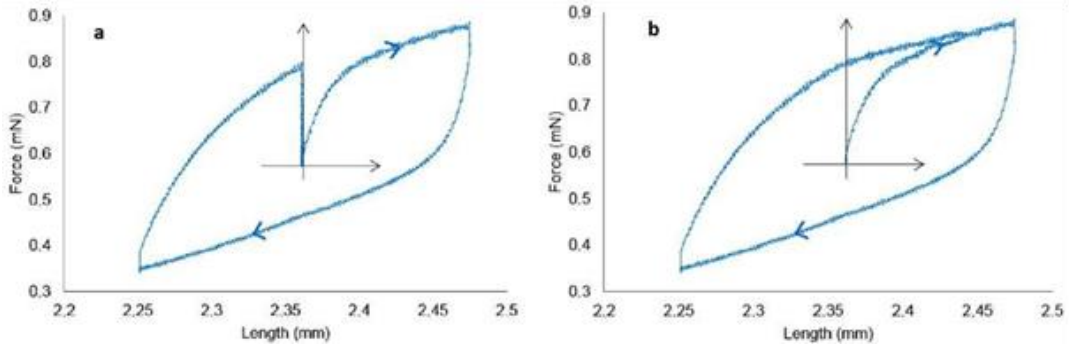

Figure A.11: *(a) Force-length relationship corresponding to Figure 10a. The curve is a hysteresis loop for only one period of the input and for this fiber the origin is where Fo=0.58 (mN) and lo=2.36 (mm). (b) A convex clockwise hysteresis loop develops when there is no relaxation at the end of lengthening and shortening.*

When a relaxation time after each half wave was added, the response showed a concave hysteresis loop, as shown in Figure A.12.

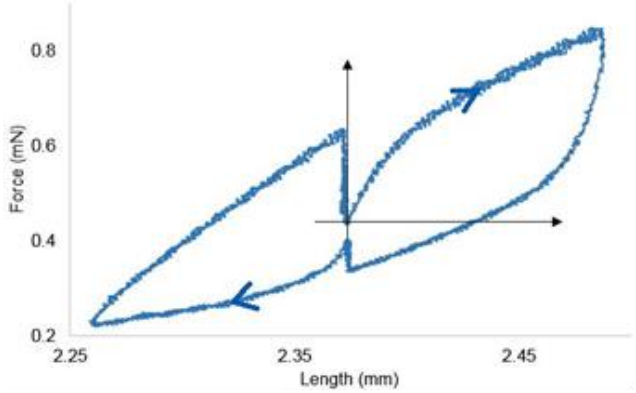

Figure A.12: *Force-length relationship corresponding to Figure A.10b. The curve consists of two loops that resemble those of kiss-and-go hysteresis (a concave clockwise hysteresis loop). The loops tend to touch one another at the origin, where Fo=0.45 (mN) and lo=2.37 (mm) in this example.*

These loops resemble those of kiss-and-go hysteresis (Volkov et al., 2014), which tend to touch each other at the center. The arrows indicate the clockwise direction of the loops. For the rest of the figures, the force response is normalized as a percentage of *Fo* and a relaxation is imposed at the end of each lengthening and shortening interval. Similar figures to those shown in this paper can be plotted when there is no relaxation at the end of lengthening and shortening but the overall effect is the same in both cases. In Figure A.13, force vs length is plotted for two different fibres (a and b), stimulated at the same frequency. The response of another two single fibres (Figures A.14a and A.14b) was obtained at a higher frequency of stimulation than that used in Figure 13. All these four fibres had a length change of 5% lo. Only the first period of

the force response is shown in each case.

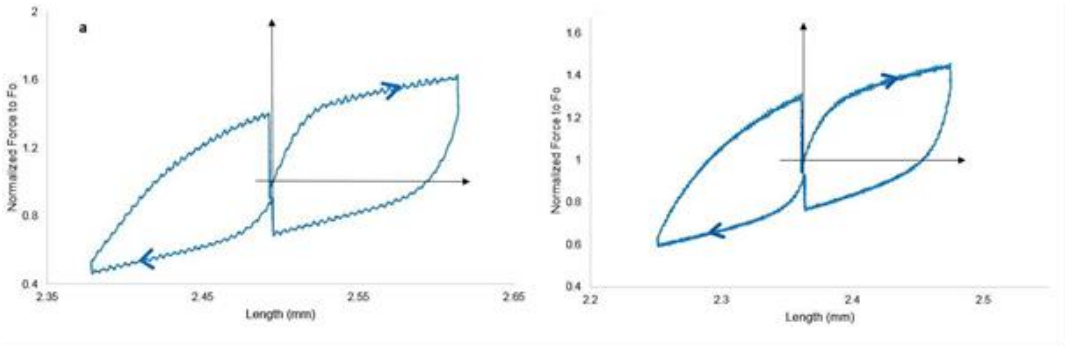

Figure A.13: *Normalized force vs length for two different fibres a and b. The input frequency for both examples was f =0.125 (s^{-1}). The force produced by the fibres reached different percentages of Fo.*

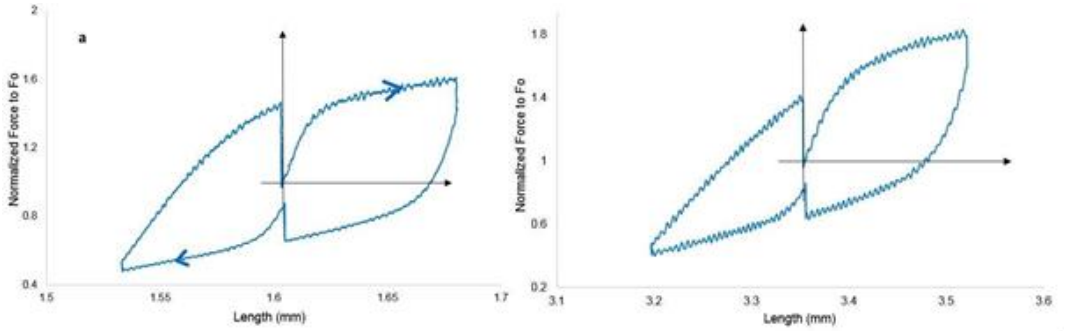

Figure A.14: *Normalized force vs length for two different fibres. The input frequency was double that used to produce Figure 13, f =0.25 (s^{-1}).*

The amount of force produced is different between the fibres even when it is normalized to *Fo*, as is shown in Figures A.13 and A.14. However, the response pattern is similar, and therefore reproducible, between the fibres presented here.

A.4.2 Force response to a 3% lo length change

Examples of single fibres' force response to a length change of 3% lo are shown in Figures A.15 and A.16, where the input frequency was f =0.25 (s^{-1}). In Figure A.15, two periods of the output are plotted while in Figure 16, four periods of the force-length relationship are shown. A similar behaviour was observed in all fibres, and in some cases (see below Figure A.15b), the force response did not appear overlapped during the positive semi-periods. Both cycles of the force-length relationship appear overlapped in Figure A.15a, while in Figure A.15b the response to the positive semi-period (or right loop) appears as two loops not completely overlapped.

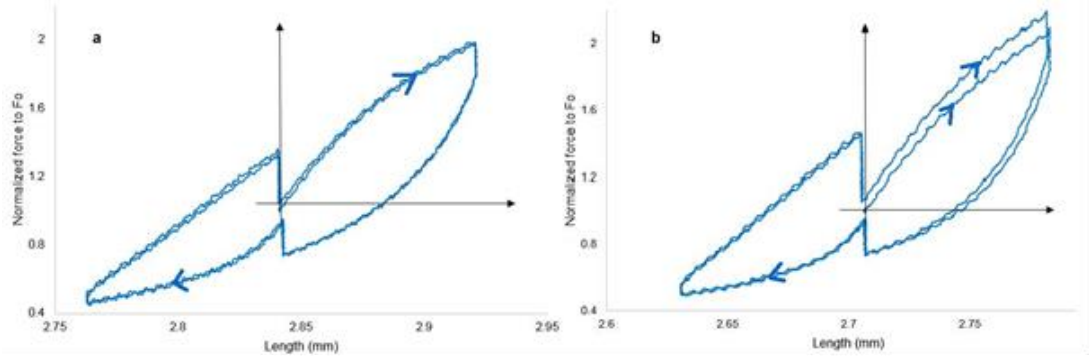

Figure A.15: *Two cycles of length change and its normalized force response for two different fibres a and b with f = 0.25 (s^{-1}).*

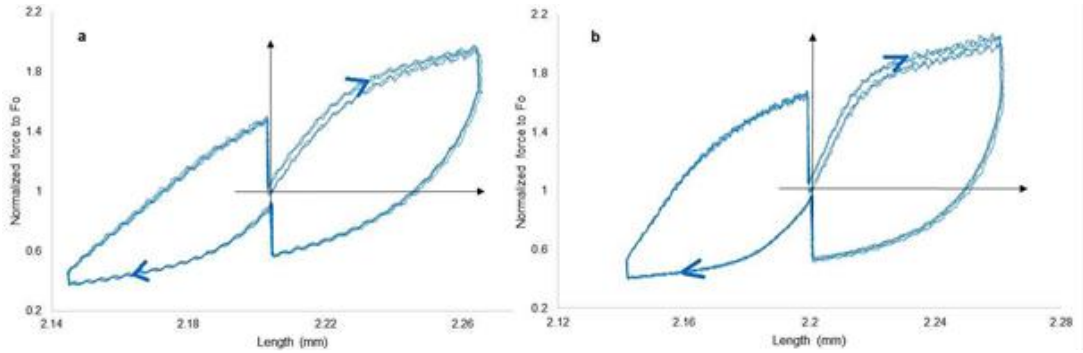

Figure A.16: *Four cycles of normalized force vs length, for two different fibres a and b with f = 0.25 (s^{-1}).*

A.4.3 Force response of a single fibre to different input frequencies

In these experiments, the single muscle fibres were subjected to an input that varied its frequency from f =0.125 (s^{-1}) to 0.625 (s^{-1}) to 1.25 (s^{-1}). The objective of these experiments was to look at the shape of the force response (loops) from the same fibre when the input frequency had a two or ten-fold variation.

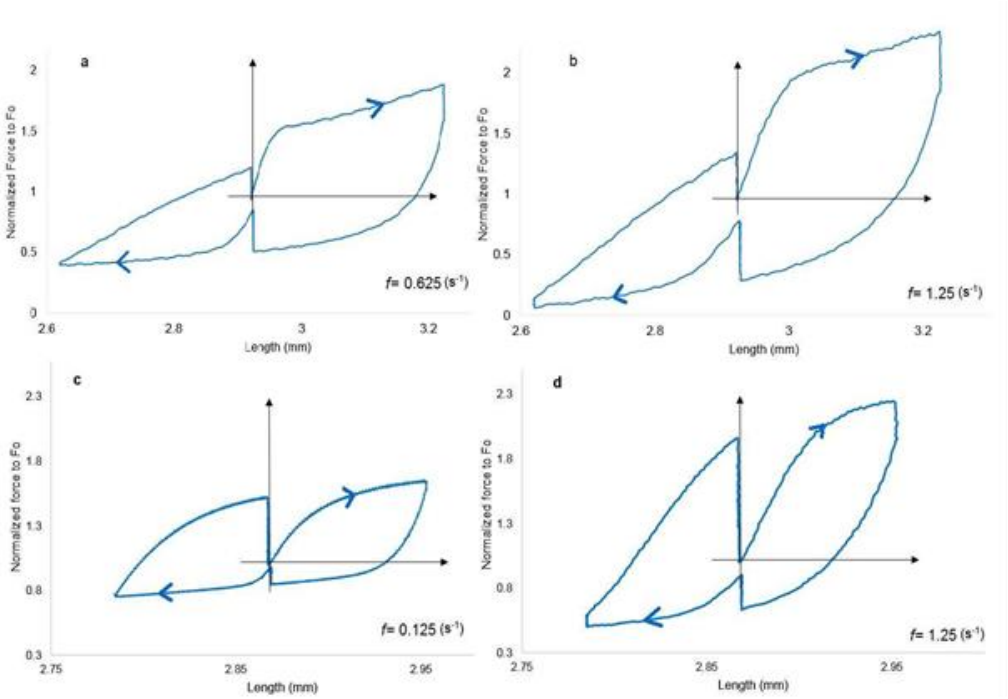

Figure A.17: *Normalized force vs length for two single fibres.* ***a*** *A single fibre subjected to a low frequency input, f = 0.625 (s^{-1}). The energy dissipated in this case was 3.98×10^{-7} (J).* ***b****, the same fibre as used in* ***a*** *with f = 1.25 (s^{-1}). The energy dissipated in this case was 5.88 × 10^{-7} (J).* ***c*** *A single fibre subjected to a low frequency input, f = 0.125 (s^{-1}). The energy dissipated in this case was 8.45 × 10^{-}8 (J).* ***d*** *The same fibre as used in* ***c*** *with f = 1.25 (s^{-1}). The energy dissipated in this case was 1.29 × 10^{-7} (J). The amplitude change was 3% of lo in all cases.*

Figure A.17a shows the hysteresis loops of a fibre subjected to a low frequency input, while the curve in Figure A.17b shows the hysteresis loops of the same fibre for a two-fold increase of the input frequency (high frequency). For the second fibre, the curve in Figure A.17c shows the loops at a low frequency and the curve in Figure A.17d displays the hysteresis after a ten-fold increase in frequency. In both cases, the areas of the loops (equivalent to energy dissipated) increased with an increase of the input frequencies.

A.5 Discussion

The muscle force response to a periodic length change has been observed for different amplitude and frequency values of the input. Without relaxation, the force-length relationship consisted of a convex hysteresis loop for a bipolar triangle input. However, when a relaxation time was added at the end of each semi-period, the muscle fibres were able to return to their isometric state giving two characteristic hysteresis loops that have been reproducible in different experiments. The curves presented in Figures A.12 to A.17 show one loop on the right of lo representing the change in force when

the fibre is lengthened and back to the initial length. Another loop is on the left of lo and represents the force change when the muscle fibre is shortened and returned to the initial fibre length. Although the loops are not completely closed, they are visibly separated. The behaviour of this force-length relationship could be considered as ”kiss-and-go” loops, as defined by (Volkov et al., 2014), where the branches do not self-cross, but tend to touch each other at the origin of the coordinates system, i.e. where l=lo and *F=Fo* for the curves in this study. This characteristic has been present in all the results regardless of the amplitude or frequency of the stimulation. In this study, two different amplitudes of the length change were evaluated, 5 and 3%lo. The observed force response as a %Fo was independent of the amplitude. In Figures A.15 and A.16 are shown two and four response cycles, respectively. The hysteresis loops on the right of Figures A.15b, A.16a and A.16b do not appear completely overlapped for the whole duration of the experiment. Particularly, in Figure A.15b, the force produced in the second cycle (at the end of the stretch) was higher than that one in the first cycle, given that the force starting point for the second cycle was somehow higher than that from the start of the first period. This occurs as a result of muscle fibre stretching and being brought back to lo where it did not relax completely to *Fo* after a complete period of length change, but to a higher force value. Despite the force production differing between different single fibres, the force vs length relationship consisted of two hysteresis loops that tend to touch each other at the origin of the coordinate system. When the muscle single fibre was subjected to different input frequencies, the area of the loops increased as did the stimulation frequency by two or ten-fold (Figure A.15). The change in response when the input frequency changed means that this system has rate dependent hysteresis. In conclusion, when a muscle single fibre is considered as a mechanical system and submitted to a periodic input, the force vs length relationship showed hysteresis loops and the system was rate-dependent. These loops were reproducible along the experiments and the hysteresis observed in this study is not a pinched hysteresis, but is labelled here as kiss-and-go. Future research is expected to concentrate on other forms of hysteresis in muscle, and another potential avenue of research is in critical slowing down in muscle, where the return time of a disturbance back to a stable steady-state increases close to a bifurcation, see (Bardy et al., 1999) and (Alherbey et al., 2014), for example.

References

Alherbey, R.A., Nejad, L.A.M., Lynch, S. and Hassan, S.S. (2014). Critical slowing down in biological bistable models. *International Journal of Pure and Applied Mathematics*, 93, 581–602.

Armisen, R. and Galatas, F. (1987). Production, properties and uses of agar. FAO, 137–148.

Ball, L.M. (2009) Hysteresis in Unemployment: Old and New Evidence. *US National Bureau of Economic Research (NBER)*, Working Paper No. 14818.

Bardy, B.G., Oullier, O., Bootsma, R.J., Stoffregen, T.A. (1999). Dynamics of human postural transitions. *Journal of Experimental Psychology-Human Perception and Performance*, 28, 499–514.

Borresen, J. and Lynch, S. (2002). Further investigation of hysteresis in Chua's circuit. *International Journal of Bifurcation and Chaos*. 12, 129–134.

Chua, L.O. (1971). Memristor-missing circuit element. *IEEE Transactions on Circuit Theory* CT18, 507– 519.

Chua, L.O., and Kang, S.M. (1976). Memristive devices and systems. *Proceedings of the IEEE* 64, 209–223.

Chua, L.O. (2013). Memristor, Hodgkin-Huxley and the edge of chaos. *Nanotechnology* 24, 383001.

Chua, L.O. (2014). If its pinched its a memristor. *Semiconductor Science and Technology*, 29, 104001.

Damjanovic, D. (2005). Hysteresis in piezoelectric and ferroelectric materials. The Science of Hysteresis 3, eds. Mayergoyz, I and Bertotti, G., (Elsevier), 337–465.

Das, J., Ho M., Zikherman, J., Govern, C., Yang, M., Weiss, A, Chakraborty, A.K., Roose, J.P. (2009). Digital Signaling and Hysteresis Characterize Ras Activation in Lymphoid Cells. *Cell,* 136, 337351.

Degens, H., Bosutti, A., Gilliver, S.F., Slevin, M., Van Heijst, A. and Wust, R.C.I. (2010). Changes in con-tractile properties of skinned single rat soleus and diaphragm fibres after chronic hypoxia. *European Journal of Physiology*, 460, 863–873.

Drincic, B. and Bernstein, D.S. (2011). Why are some hysteresis loops shaped like a butterfly? *Automatica*, 47, 2658–2664.

Ewing, J.W. (1885). Experimental researches in magnetism. *Transactions of the Royal Society of London* 176, 523640.

Gauthier, D.J., Hall, G.M., Oliver, R.A., Dixon-Tulloch, E.G., Wolf, P.D., Bahar, S. (2002). Progress to-ward controlling in vivo fibrillating sheep atria using a nonlinear-dynamics-based closed-loop feedback method. Chaos 12, 952-961.

Gilliver, S.F., Degens, H., Rittweger, J., Sargeant, J. and Jones, D.A. (2009). Variation in the determinants of power of chemically skinned human muscle fibres. *Experimental Physiology*, 94, 1070–1078.

Gilliver, S.F., Jones, D.A., Rittweger, J. and Degens, H. (2010). Effects of oxidation on the power of chemically skinned rat soleus fibres. *Journal of Musculoskeletal and Neuronal Interactions*, 10, 267– 273.

Gilliver, S.F., Degens, H., Rittweger, J. and Jones, D.A. (2011). Effects of submaximal activation on the determinants of power of chemically skinned rat soleus fibres. *Experimental Physiology*, 96, 171–178.

Hodgkin, A.L. and Huxley, A.F. (1952). A qualitative description of membrane current and its application to conduction and excitation in nerve. *Journal of Physiology* 117, 500–544.

Ikeda, K. (1979). Multiple-valued stationary state and its instability of the transmitted light by a ring cavity system. *Opt. Comm*. 30, 257261.

Ikeda, K., Daido, H. and Akimoto, A. (1980). Optical turbulence: chaotic behaviour of transmitted light from a ring cavity. *Phys. Rev. Lett*. 45, 709712.

Kramer, B.P., Fussenegger, M. (2005). Hysteresis in a synthetic mammalian gene network. *Proceeding of the National Academy of Sciences USA*, 102, 9517–9522.

Kyriatzis M. (2003). Practical applications of chaos theory to the modulation of human ageing: nature prefers chaos to regularity. *Biogerontology*, 4, 7590.

Lahaye, M. and Rochas, C. (1991). Chemical structure and physico-chemical properties of agar. *Hydrobiologia,* 221, 137–148.

Larsson,L. and Moss, R. L. (1993). Maximum velocity of shortening in relation to myosin isoform composition in single fibres from human skeletal muscles. *Journal of Physiology*, 472, 595–614

Lynch, S., Steele, A.L. and Hoad, J.E. (1998). Stability analysis of nonlinear optical resonators*. Chaos, Solitons and Fractals*, 9, 935–946.

Lynch, S. and Christopher, C.J. (1999). Limit cycles in highly non-linear differential equations. *Journal of Sound and Vibration,* 224 505–517.

Lynch, S. (2005). Analysis of a blood cell population model. *International Journal of Bifurcation and Chaos*, 15, 2311–2316.

Lynch, S. and Bandar, Z. (2005). Bistable neuromodules. *Nonlinear Anal Theory, Meth. & Appl.* 63, 669–677.

Lynch, S. (2007). Dynamical Systems with Applications using Mathematica, Springer, New York.

Lynch, S. (2010) Dynamical Systems with Applications using Maple 2nd ed., Springer, New York.

Lynch, S. and Steele, A.L. (2011). Nonlinear optical fibre resonators with applications in electrical engineering and computing. Applications of Nonlinear Dynamics and Chaos in Engineering eds. Banerjee, S., Mitra, M. and Rondoni, L. (Springer) 1, 65–84.

Lynch, S. (2011). MATLAB programming for engineers and scientists. Applications of Nonlinear Dynamics and Chaos in Engineering. eds. Banerjee, S., Mitra, M. and Rondoni, L., (Springer) 1, 3–35.

Lynch, S. (2014). Dynamical Systems with Applications using MATLAB 2nd ed., (Springer International Publishing).

Lynch, S., Alharbey, R.A., Hassan, S.S. and Batarfi, H.A. (2015). Delayed-dynamical bistability within and without rotating wave approximation. *Journal of Nonlinear Optical Physics and Materials,* 24, 1550037.

Lynch, S., Borresen, J. (2015). Oscillations, feedback and bifurcations in mathematical models of angio-genesis and haematopoiesis. Handbook of Vascular Biology Techniques, eds. Slevin M, McDowell G, Cao Y, Kitajewski J., (Springer, New York), 373–390.

Mayergoyz, I.D. (2003). Mathematical Models of Hysteresis and Their Applications. Academic Press Series in Electromagnetism, (Elsevier).

Muller, I. and Xu, H. (1991). On the pseudo-elastic hysteresis. *Acta Metallurgica et Materialia*, 39, 263– 271.

Noori, H.R. (2014). Hysteresis Phenomena in Biology, (Springer Berlin Heidelberg).

Piramanayagam, S.N. and Chong, T.C. (2011). Developments in Data Storage: Materials Perspective, (Wiley-IEEE Press).

Pomerening, J.R., Sontag, E.D., Ferrell, J.E. (2003). Building a cell cycle oscillator: hysteresis and bistability in the activation of Cdc2. *Nature Cell Biology*, 5, 346251.

Prodromakis, T., Toumazou, C. and Chua, L.O. (2012). Two centuries of memristors. *Nat. Mater.* 11, 478–481.

Qingjiang, L., Khiat, A. et al. (2014). Memory Impedance in TiO2 based Metal-Insulator-Metal Devices. *Scientific Reports*, 4, Article number: 4522.

Rahatabad, F.N., Fallah, A., Jafari, A.H. (2011). A study of chaotic phenomena in human-like reaching movements. *International Journal of Bifurcation and Chaos* 21, 3293-3303.

Smith, R.C., Seelecke, S., Dapino, M., et al. (2006). A unified framework for modeling hysteresis in ferroic materials. *Journal of the mechanics and physics of solids*, 54, 46–85.

Szoke, A., Daneu, V., Goldhar, J. and Kirnit, N.A. (1969). Bistable optical element and its applications. *Appl. Phys. Lett*. 15, 376.

Volkov, A.G., Tucket, C., Reedus, J., Volkova, M. I., Markin, V.S. and Chua, L.O. (2014). Memristors in plants. *Plant Signaling and Behavior*, 9, 18.

Webber C.L. and Zbilut J.P. (1994). Dynamical assessment of physiological systems and states using recurrence plot strategies*. Journal of Applied Physiology*, 76, 965-973.

Weiss, J.N., Garfinkel, A., Karagueuzian, H.S., Qu, Z.L., Chen, P.S. (1999). Chaos and the transition to ventricular fibrillation - A new approach to antiarrhythmic drug evaluation. *Circulation*, 99, 2819-2826.

APPENDIX B

ID mouse	Age (months)	Gender	Genotype	#SF in Chapter 2	#SF in Chapter 3	#SF in Chapter 4	#SF in Chapter 5	#SF in Appendix A
1	3	Male	C57BL6			11		
2	3	Male	C57BL6			12		
3	3	Male	C57BL6			9		
4	10	Female	Gtf2ird	13				
5	10	Female	Gtf2ird	9				
6	10	Female	Gtf2ird	6				
7	10	Female	Gtf2ird		9			
8	10	Female	Gtf2ird		10			
9	10	Female	Gtf2ird			7		
10	10	Female	Gtf2ird			8		
11	10	Female	Gtf2ird			7		
12	10	Female	Gtf2ird				9	
13	10	Female	Gtf2ird				7	
14	10	Female	Wild type	10				
15	10	Female	Wild type	10				
16	10	Female	Wild type	7				
17	10	Female	Wild type	6				
18	10	Female	Wild type		8			
19	10	Female	Wild type		10			
20	10	Female	Wild type			8		
21	10	Female	Wild type			8		
22	10	Female	Wild type				8	
23	10	Female	Wild type				7	
24	18	Male	Gtf2ird			7		
25	18	Male	Gtf2ird			5		
26	18	Male	Gtf2ird			6		
27	18	Male	Gtf2ird			7		5
28	18	Male	Gtf2ird			7		6
29	18	Male	Gtf2ird				8	5
30	18	Male	Gtf2ird				9	4
31	18	Male	Gtf2ird				11	5
32	32	Male	C57BL6			15		
33	32	Male	C57BL6			11	8	
34	32	Male	C57BL6				13	

Table B.1: *Characteristics of the mice used in the different experiments and number of single fibres (#SF) used from each mouse in Chapters 2-5 and data shown in Appendix A.*